Online ISSN : 2249-4626
Print ISSN : 0975-5896
DOI : 10.17406/GJSFR

Global Journal

of Science Frontier Research: A

Physics and Space Science

Issue of Rotating Galaxies

Features of Nuclear Interaction

Highlights

Vavilov-Cherenkov Radiation

Model of an Atom without Quarks

Discovering Thoughts, Inventing Future

VOLUME 23 ISSUE 8 VERSION 1.0

Global Journal of Science Frontier Research: A
Physics & Space Science

Global Journal of Science Frontier Research: A
Physics & Space Science

Volume 23 Issue 8 (Ver. 1.0)

Open Association of Research Society

Incorporation No.: 0423089
License No.: 42125/022010/1186
Registration No.: 430374
Import-Export Code: 1109007027
Employer Identification Number (EIN):
USA Tax ID: 98-0673427

Global Journals Inc.

*(A Delaware USA Incorporation with "Good Standing"; **Reg. Number: 0423089**)*

Sponsors: *Open Association of Research Society*
Open Scientific Standards

Publisher's Headquarters office

Global Journals® Headquarters
945th Concord Streets,
Framingham Massachusetts Pin: 01701,
United States of America
USA Toll Free: +001-888-839-7392
USA Toll Free Fax: +001-888-839-7392

Offset Typesetting

Global Journals Incorporated
2nd, Lansdowne, Lansdowne Rd., Croydon-Surrey,
Pin: CR9 2ER, United Kingdom

Packaging & Continental Dispatching

Global Journals Pvt Ltd
E-3130 Sudama Nagar, Near Gopur Square,
Indore, M.P., Pin:452009, India

Find a correspondence nodal officer near you

To find nodal officer of your country, please email us at *local@globaljournals.org*

eContacts

Press Inquiries: *press@globaljournals.org*
Investor Inquiries: *investors@globaljournals.org*
Technical Support: *technology@globaljournals.org*
Media & Releases: *media@globaljournals.org*

Pricing (Excluding Air Parcel Charges):

Yearly Subscription (Personal & Institutional)
250 USD (B/W) & 350 USD (Color)

Editorial Board

Global Journal of Science Frontier Research

Contents of the Issue

Global Journal of Science Frontier Research: A
Physics and Space Science
Volume 23 Issue 8 Version 1.0 Year 2023
Type: Double Blind Peer Reviewed Interenational Research Journal
Publisher: Global Journals
Online ISSN: 2249-4626 & Print ISSN: 0975-5896

Axions in a Dispersed Medium: Light Scattering, Vavilov-Cherenkov Radiation

By Ogluzdin V. E.

Introduction- What happens to photons of laser radiation whose energy differs from the energy of the inter-level electronic transitions of atoms of the substance under study. According to Bohr and Einstein, the traditional scheme of interaction between radiation and matter includes the following processes: 1) resonant absorption of radiation, 2) spontaneous radiation, 3) resonant stimulated radiation. In the absence of resonance between the pumping frequency and the frequencies of electronic transitions in atoms alloying a dispersed medium, the interaction of radiation and matter is carried out due to the annihilation of pairs of pump radiation photons, the birth of axions and their subsequent decay into new photons whose energy differs from the energy of the pump photons. If in atomic vapors in the resonant case one photon is required for the transition of an electron from the ground level S to the excited P, then in the non-resonant case such a transition is possible due to the annihilation of a pair of photons.

GJSFR-A Classification: *LCC: QC406-413*

AXIONSINADISPERSEDMEDIUMLIGHTSCATTERINGVAVILOVCHERENKOVRADIATION

Strictly as per the compliance and regulations of:

Axions in a Dispersed Medium: Light Scattering, Vavilov-Cherenkov Radiation

Ogluzdin V. E.

I. Introduction

What happens to photons of laser radiation whose energy differs from the energy of the inter-level electronic transitions of atoms of the substance under study. According to Bohr and Einstein, the traditional scheme of interaction between radiation and matter includes the following processes: 1) resonant absorption of radiation, 2) spontaneous radiation, 3) resonant stimulated radiation. In the absence of resonance between the pumping frequency and the frequencies of electronic transitions in atoms alloying a dispersed medium, the interaction of radiation and matter is carried out due to the annihilation of pairs of pump radiation photons, the birth of axions and their subsequent decay into new photons whose energy differs from the energy of the pump photons. If in atomic vapors in the resonant case one photon is required for the transition of an electron from the ground level S to the excited P, then in the non-resonant case such a transition is possible due to the annihilation of a pair of photons.

II. Axions in A Dispersed Medium

First of all, we should recall the definition of a dispersed medium (DM). In DM, the doping (alloying) phase in the form of small formations is distributed in the main volume of the continuous phase. Continuous phase DM - glass, liquid, air, vacuum. The second is the doping component DM, weighted in the volume of the continuous phase: these are atoms, molecules or nanoparticles of an element alloying the medium. Air, water, organic liquids, atomic vapors of alkali metals in a vacuum cuvette are also DM. When a laser beam propagates in DM, its spectral and angular characteristics change.

The aim of the work is to analyze the processes accompanying the propagation of a laser beam in DM in the absence of resonance between the pumping frequency and the frequencies of electronic transitions. The high density of photons in the laser beam and the high intensity of the electromagnetic field of the atomic nuclei of the element selected for DM doping cause the possibility of annihilation of photon pairs, which leads to the birth of axions. Their decay determines the features of the spectral and angular structures of radiation at the exit from the medium.

Author: Federal Research Center A. M. Prokhorov Institute of General Physics of the Russian Academy of Science, Moscow, Russia.
e-mail: ogluzdin@kapella.gpi.ru

What happens to the photons of laser radiation in DM? What do we have at the output of DM? How does the radiation spectrum change?

Only in a vacuum does the propagation of light radiation obey the laws of wave optics. In this case, laminar collisionless movement of photons in the beam occurs. In the case of propagation of light radiation in the DM, due to the interaction of the photons of the beam with the electron shell of the atomic nuclei of the atoms alloying the medium and the atoms of the medium itself, the laminar motion of the photons is disrupted, the velocity of the photons meeting the electron shell of the atoms alloying the medium slows down. This circumstance leads to interphoton collisions, interphoton interaction, annihilation of photon pairs with the birth of axions in the strong field of the atomic nucleus [1].

According to the works [2] of the American physicist Primakov (HENRY PRIMAKOFF), annihilation (fusion) of two quanta (photons) in the electro-magnetic field of the atomic nucleus can lead to the birth of the axion - A•. Leaving the atom, the axion decays into two new quanta (photons) – the forward and reverse Primakov effects:

$$h\nu + h\nu = \mathrm{A}\bullet = h\nu_{ij} + h\nu_{0j} \qquad (1)$$

where:
$h\nu$ is the energy of quanta (photons) of light radiation used to pump DM,
ν is the frequency of this radiation.

Just note that the Primakov effect may be direct or reverse. In the second case, when you turn off the field of the atomic nucleus decays of the axion to two photons.

$h\nu_{ij}$ - is the energy of quanta (photons) of radiation from one of the many components of the broadened spectrum of radiation scattered by the medium, or one of the many components of the photoluminescence spectrum, or one of the many components of the angular spectrum of radiation at the output of the investigated DM, (determined by the difference between the energy of the virtual level - i and the energy of atomic level j; The energy of the virtual level is equal to the sum of the energies of two pump photons. The energy of the virtual level – i can be greater or less than the

Global Journal of Science Frontier Research (A) Volume XXIII Issue VIII Version I Year 2023

energy of the electronic levels of the doping element under study.

$h\nu_{0j}$ - is the energy of the quanta absorbed by the medium; the energy of this quantum is equal to the energy of the electron transition from the ground level to the excited one .The number of levels j in the spectrum of the atom of the element under study is infinite.

What determines the energy of the virtual level? The energy of the virtual level - $i$can be greater or less than the energy of the electronic levels of the alloying element under study.

Since the birth of the axion and its existence presupposes the presence of strong electromagnetic fields, in our case, the fields of the atomic nucleus, neither Rayleigh scattering on solid particles nor Mandelstam—Brillouin scattering by condensed media (solids and liquids) as a result of its interaction with the intrinsic elastic vibrations of these media will be considered by us. We will also not take into account the scattering of light by fluctuations in the density of the medium (small local deviations of the density from its average value), with which, as is commonly believed in the wave model, the scattering process is associated.

a) *Forced electron raman scattering (EFRS) in atomic potassium vapors*

It was experimentally possible to register the process of annihilation of photonic pairs and the decay of axions in the case of almost resonant interaction of laser radiation with atomic potassium vapor in the frequency range, where the normal dispersion and where the refractive index is greater than one. These conditions in atomic potassium correspond to the electronic transition $4S_{1/2}$-$4P_{3/2}$(Fig.1). We will consider a region of the spectrum where interphoton interaction is possible, annihilation of photon pairs, the birth of axions and their decay are possible.

As a rule, the energy of laser-pumped photons does not coincide with the inter-level energy interval of any of the electronic transitions of both the alloying atom and the atoms and molecules of the doped medium. A frequency-tunable parametric light generator (PLG) was used as a pumping laser in [3], which made it possible to study changes in the frequency and angular structure of the spectrum at the output of the cuvette in atomic pairs of cadmium in the frequency range of the main doublet. The radiation power of PLG was 50...500 kW with a pulse duration of 10...15 ns. The temperature of potassium vapors in the cuvette was maintained in the range of 250...300°C. The radiation spectrum at the outlet of the cuvette was recorded on a spectrograph with a dispersion of 6 A°/mm. Recall the frequencies corresponding to potassium doublet lines: low-frequency doublet line $4S_{1/2}$-$4P_{1/2}$: ν_{02} = 12989 cm^{-1}, high-frequency doublet line $4S_{1/2}$-$4P_{3/2}$: ν_{01} = 13046 cm^{-1}. This experiment is described in detail in [3-5].

In the first spectrogram (Fig. 1a), the pump radiation frequency is $\nu \approx 13020$ cm^{-1}, less than the transition frequency $4S_{1/2}$-$4P_{3/2}$. In this case, with a shift to the low-frequency region of the spectrum relative to the pumping frequency -ν, a resonant electron forced raman scattering (EFRS) line is recorded at the output of the cuvette, the frequency of which is indicated by ν_3:

$$\nu_3 = 2\nu - \nu_{01}. \quad (2)$$

Calculated according to the ratio (2), the frequency value ν_3 coincides with the experimental value.

The energy of photons of radiation at the frequency $\nu_3$can be obtained from the ratio:

$$h\nu_3 = 2h\nu - h\nu_{01} . \quad (3)$$

In relation (3) there is a term $2h\nu$, indicating the addition of two pump radiation photons (annihilation of which in the field of the atomic nucleus leads to the appearance of an axion - the Primakov effect). In the field of the same atomic nucleus, in an elementary act, an axion whose energy is equal to $2h\nu$, decays into two photons (quanta) – the reverse Primakov effect.

Laser radiation (frequency $\nu \approx 13020$ cm^{-1}) transfers electrons from the ground level $4S_{1/2}$to the virtual one, the energy of which is determined by the value E = 2 $h\nu$ with the formation of an axion. The energy of the virtual level in the atom is counted from the main level. When the axion decays, the electron transitions from the virtual level 2 $h\nu$to the level $4P_{3/2}$.

The radiation line of the pump – ν at the outlet of the cuvette is widened. The question of broadening the laser radiation lines in a dispersed medium was considered in [1]. The broadening of the lines is associated with the annihilation of photon pairs, the appearance of axions and their decay. Accordingly, with the pump – ν radiation line at the output of the cuvette, the EFRS - ν_3 line is also widened, which follows from the ratio (2).

In the spectrogram (Fig. 1a), in addition to the pump – ν radiation and the radiation at the frequency of ν_3, there is a complex spectral structure in the anti-stokes region of the spectrum relative to the pump (from νtoν_{as}), reflecting the change in the divergence (angular spectrum) of radiation at the output of the cuvette.

The features of the spectrum associated with the change in the angular spectrum of radiation at the output of the cuvette at the frequencies ν, ν_3, ν_{as}, we will consider in the next section.

Global Journal of Science Frontier Research (A) Volume XXIII Issue VIII Version I Year 2023

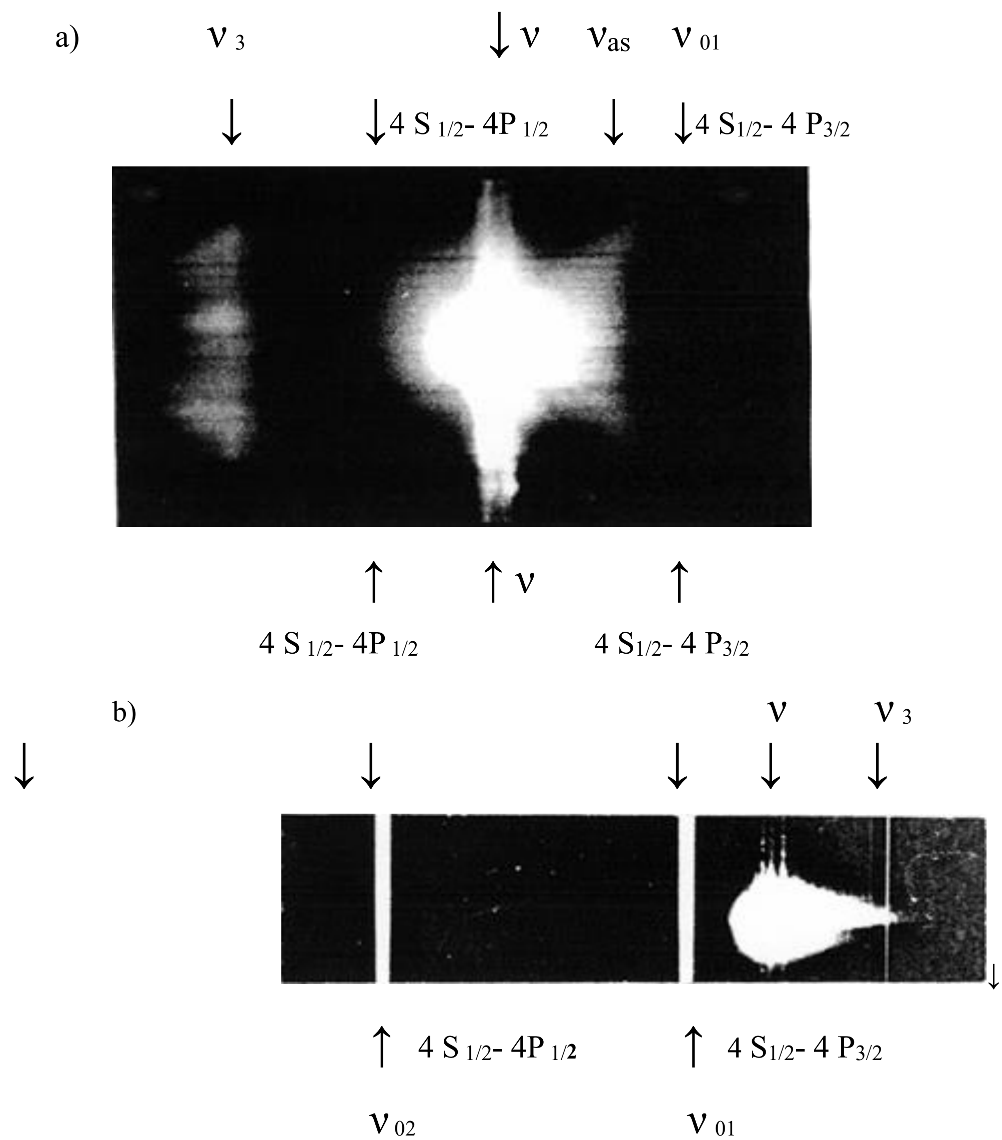

Fig. 1: Spectrograms illustrating the role of axions in the propagation of laser radiation pulses through a cuvette with potassium vapor in the frequency range of the main doublet 4 $S_{1/2}$- 4 $P_{1/2,\ 3/2}$. ν is the frequency of laser radiation; ν_{01} is the frequency of the transition line $4S_{1/2}$–$4P_{3/2}$ (13046 cm^{-1}); ν_{02} is the frequency of the transition line 4 $S_{1/2}$- 4 $P_{1/2}$, (12986 cm^{-1}); ν_3 is the frequency of the forced electron raman scattering line.

$\nu_3 = 2\nu - \nu_{01}$ (the value of 2ν reflects the process of annihilation of two photons with the formation of an axion, during the decay of which photons appear at the frequency ν_3). The reference lines of the doublet ν_{02}, ν_{01} on the spectrogram 1 b) were obtained using a spectral lamp. In the second spectrogram (Fig. 1b), the pump radiation frequency $\nu \approx$ 13070 cm^{-1} is shifted to the anti-Stokes region relative to the frequency of the transition line $4S_{1/2}$-$4P_{3/2}$. In this case, we have a broadening of the frequency spectrum. On a spectrogram with a shift to the high-frequency region of the spectrum relative to the pumping frequency -ν, a weak line of resonant electron forced raman scattering (EFRS) is also recorded at the output of the cuvette, the frequency of which is indicated by ν_3.

Thus, the EFRS process observed at small detunings of the pump frequency from the resonant transition frequency in potassium vapor during the absorption of two photons in an elementary act with the formation of an axion is accompanied by the transfer of electrons from the main level $4S_{1/2}$ to the level $4P_{3/2}$. What distinguishes an almost resonant process from a resonant one. In the case of resonant pumping, the transfer of an electron from the $4S_{1/2}$ level to the $4P_{3/2}$level is carried out due to single-photon absorption.

b) *The structure of the angular spectrum of the laser beam, behind the output window of the cuvette with atomic potassium vapor*

When considering the angular spectrum of the laser beam at the output of the cuvette, in the frequency range close to the frequency of the resonant transition, self-action processes (self-focusing, self-focusing) take place [3,5], which do not imply a change in the structure of the frequency spectrum of laser radiation at the output of the medium. The results of the observation of these processes are presented in [6,7]. The effects of self-action are associated with an uneven, Gaussian distribution of the radiation intensity over the cross-section of the laser beam. Near the frequency of the resonant transition, the refractive index of the medium (in our case of atomic potassium vapors) in the electromagnetic field of the laser beam depends on the intensity distribution over the cross-section of the beam. This circumstance explains the change in the wavefront of the beam, leading either to self-focusing ($\nu<\nu_{01}$) or to self-focusing ($\nu>\nu_{01}$).

Let us turn once again to the spectrograms presented in Fig. 1. The optical scheme of their registration is constructed in such a way that frequencies are recorded on the spectrograms outside the output window of the cell in the horizontal direction relative to the axis of the laser beam, and in the vertical direction the radiation propagating at an angle to the axis of the laser beam is recorded. To do this, a lens was installed between the output window of the cuvette and the slit of the spectrograph, displaying the output window of the cuvette on the slit of the spectrograph. The slit displays the diameter of the base of the cone of light radiation resting on the exit window of the cuvette. Such an optical scheme makes it possible to register the frequency spectrum of the cone components of radiation scattered in potassium vapor at an angle to the optical axis.

Consider the features of the angular spectrum of radiation at the output of the cuvette in the case when the radiation frequency of the pump is $v< v_{01}$. In this case, the structure of the angular spectrum at the frequencies v , v_3, as well as in the frequency range between v and v_{as} is recorded on the spectrogram.

First of all, we note (Fig.1a) that at the frequency v outside the output window of the cell, the central spot corresponds to the initial direction of propagation of the laser beam. The radiation shifted up and down relative to the optical axis of the frequency v at the same angle indicates that a divergent cone of radiation is formed in the cuvette, the base of which is the output window of the cuvette.

In the considered region of the spectrum, the refractive index is greater than one. In such an environment, the speed of photons outside the laser beam is equal to the phase speed of light at the frequency $v = c / n$. When a laser beam propagates in atomic potassium vapors, first of all, the populations of the 4*S* and 4*P* levels align on the beam axis, which changes the refractive index. Under these conditions, it is equal to one. Therefore, along the beam axis, both photons and axions can propagate at the speed of light - c. According to the definition, the propagation of particles (in our case axions) at the speed of light in a medium where photons move at the phase speed of light is accompanied by Vavilov-Cherenkov radiation. Two spots shifted up and down at the same angle indicate the birth of such radiation in a cuvette with potassium vapors.

Let's return to Fig.1a. At the frequency ν_3 we have a similar picture – a central spot and components scattered at an angle up and down. According to relation (2), their appearance is caused by the process of three-photon electron scattering, which repeats the structure of the radiation spectrum at the frequency v for the frequency v_3.

Finally, we need to explain the structure of the angular spectrum in the frequency range from v to vas. In [8] this structure was called "mustache". It is interesting because there are no pump photons on the beam axis near the frequency v_{as}. In [6], it was proposed to use nonlinear polarization to interpret this structure.. The absence of pump radiation photons on the optical axis does not exclude the presence of axions there – particles propagating in the medium at the speed of light and responsible for the Vavilov-Cherenkov radiation cone. This interpretation of the nature of the "mustache" strictly corresponds to the definition of Vavilov-Cherenkov radiation, according to which it is the beam of particles (axions), moving at the speed of light that, causes this radiation.

c) *Propagation of laser radiation in transparent media (air, water); heating of the medium*

In the case of propagation of laser beams in transparent media (air, water), light scattering occurs, which can be explained by the decay of axions in the electromagnetic fields of nitrogen, oxygen and hydrogen atoms. Let us analyze the case of the propagation of a light beam in a medium, considered in [9]. "Let's assume that we illuminate a transparent medium in complete darkness, for example, clean water, with an intense laser beam. Even if the medium does not contain any impurity particles, the trajectory of the beam in the medium may become slightly noticeable even when observed in directions that do not lie in the plane of incidence…We must... reveal... the origin of this weakly scattered light in all directions, which is superimposed on a more intense unidirectional beam." The authors [9] believe that fluctuations in the density of the medium (in this case, water) are responsible for the scattering of light in all directions. However, this explanation is not enough, part of the energy of the laser beam is spent on heating water. Scattering by density fluctuations does not lead to heating of water.

In our opinion, it is natural to assume that when axions decay into two photons at a frequency v_{ij}, radiation scattering occurs in all directions (angle 4 π steradian). It is possible to explain the heating of the medium, which is associated with the process of non-radiative relaxation to the ground level of electrons trapped at the excited level when the medium absorbs the second quantum of the decayed axion in accordance with the ratio (1).It can also be assumed that similar processes occur in the earth's atmosphere under the influence of solar radiation; solar photons annihilate in the earth's atmosphere with the formation of axions, the decay of which is associated with the heating of the atmosphere and possibly photons at frequencies v_{ij} contribute to the blue color of the sky.

Let's add a few remarks to the question of what role axions play in laser technology. We found out that in the absence of resonance between the pump radiation frequency and electronic transitions in the medium, the axion decay involves the transfer of thermal energy to the medium and its heating due to the process of non-radiative relaxation. Therefore, cooling systems are used for heat removal in solid-state lasers, and active medium pumping systems are used in dye lasers.

The process of scattering radiation in all directions (angle 4 π steradian) in [10] was used to illuminate the laser mirror with the reversal of the wave front. Such a laser works in the presence of phase in homogeneities in the resonator.

III. Conclusion

According to Bohr and Einstein, the traditional scheme of interaction between radiation and matter includes the following processes: 1) resonant absorption of radiation, 2) spontaneous radiation, 3) resonant stimulated radiation. In the absence of resonance between the pumping frequency and the frequencies of electronic transitions in atoms alloying a dispersed medium, the interaction of radiation and matter is carried out due to the annihilation of pairs of pump radiation photons, the birth of axions and their subsequent decay into new photons whose energy differs from the energy of the pump photons. Let's list the processes for which the use of the axiope model seems natural. This is the scattering of light in dispersed media, including scattering in air by a solid angle equal to 4 π steradian. This is resonant forced raman scattering of electrons (EFRS). The decay of the axion into two quanta, whose energy differs from the energy of the pump radiation photons, explains the heating of the medium by the incident pump radiation. This is also the photoluminescence process considered in [11].

Finally, an axion is a particle generating a cone of Cherenkov-Vavilov radiation under specially created experimental conditions.

References Références Referencias

1. Ogluzdin V. E. The Role of [Axions in the Formation of Frequncy and Angular Spectra of Laser Radiation Propagatedina Dispersion Medium *Journal of Applied Spectroscopy*, 2023, Vol. 89, No. 6, January, (Russian Original 2022, Vol. 89, No. 6, November–December).
2. Primakoff H. Photo-Production of Neutral Mesons in Nuclear Electric Fields and the Mean Life of the Neutral Mesons. *Phyz. Rev.*1951, 81, 86-89.
3. S. A. Akhmanov, A. I. Kovrigin, and S. A. Maksimov, V. E. Ogluzdin. Pis'maZh. Éksp. Teor. Fiz., 1972, 15, 186–191.
4. Anikin V. I., Kryuchkov S. V., Ogluzdin V. E. Resonant electron forsedraman scattering in potassium vapor. Dispersion near the main doublet and the influence of four-photon processes. *Kvantovaja Electron.* 1974, 1, 1991-1998.
5. Ogluzdin V.E. *Investigation of the processes of propagation of coherent radiation pulses in resonant media with inverted and non-inverted populations.* PhD thesis It is protected in the council in K-053 the specialty Kvantovaja Electron at the Moscow State University named after M.V. Lomonosov. 1980, 05.23
6. Ogluzdin V.E. Vavilov- Cherenkov effect under condition of near resonant interaction of intence light beams with atomic potassium vapor.*Zh.Eksp. Teor. Phyz.*1980, 79 361-367.
7. Ogluzdin V.E. Photons traveling at the speed of light in two-level atomic medium as source of Cherenkov radiation cones. *Physics-Uspekhi*. 2004, 47, 829-832.
8. Yu. M. Kirin, S. G. Rautian, A. M. Semenov, and B. M. Chernobrod, Pis'maZh. Éksp. Teor. Fiz.,1970,11, 340 ().
9. Bohren C.F., Huffman D.R. *Absorption and Scattering of Light by Small Particles.* A Willey-Interscience Publication, John Willey &Sons Inc, New York•Chichester•Brisbane•Toronto•Singa-pore, 1983.
10. Bagan A A, Gerasimov V B, Golyanov AV, Ogluzdin V. E *Kvatovaya Electronika* 1990 17 *№1,* 21-24
11. Ogluzdin V.E. The Role of Axions in the Formation of the Photoluminescence Spectrum in Dispersive Media. *Foundations.* 2022, 2, 184-198, https//doi.org/10.3390/foundations2010011.

This page is intentionally left blank

Global Journal of Science Frontier Research: A
Physics and Space Science
Volume 23 Issue 8 Version 1.0 Year 2023
Type: Double Blind Peer Reviewed Interenational Research Journal
Publisher: Global Journals
Online ISSN: 2249-4626 & Print ISSN: 0975-5896

Model of an Atom without Quarks and Features of Nuclear Interaction

By Stanislav Konstantinov
Herzen State Pedagogical University

Abstract- The article proposes Lev Sapogin's unitary model of the atom and atomic nucleus without quarks and flavors. Based on the table of Dmitry Mendeleev, where the first cell was occupied by the ether (physical vacuum), which in the monstrous gravitational, electric and magnetic fields of black holes is polarized, generating particles and antiparticles, I presented the possible assembly of atoms of chemical elements from elementary particles using a very fast plasma centrifuge a quasar.

Keywords: *dark matter; baryonic matter; black hole; quasar; electron; positron; positronium; atom; quark.*

GJSFR-A Classification: *PACS: 04.20.-q, 04.50.-h, 06.20.Jr*

MODELOFANATOMWITHOUTQUARKSANDFEATURESOFNUCLEARINTERACTION

Strictly as per the compliance and regulations of:

Model of an Atom without Quarks and Features of Nuclear Interaction

Stanislav Konstantinov

Abstract- The article proposes Lev Sapogin's unitary model of the atom and atomic nucleus without quarks and flavors. Based on the table of Dmitry Mendeleev, where the first cell was occupied by the ether (physical vacuum), which in the monstrous gravitational, electric and magnetic fields of black holes is polarized, generating particles and antiparticles, I presented the possible assembly of atoms of chemical elements from elementary particles using a very fast plasma centrifuge a quasar.

Keywords: dark matter; baryonic matter; black hole; quasar; electron; positron; positronium; atom; quark.

PACS: 01.10.Fv, 04.50.-h, 12.10.Kt, 95.36. + X, 98.80.-k

I. Introduction

Dear reader, in the proposed article, the concepts familiar to you are debunked: the orbits of electrons in an atom, the regular Rutherford-Bohr planetary model of the atom, two types of quarks that form the nucleus of an atom and six flavors of quarks along with six flavors of leptons and many other concepts received in the Standard Model status of physical concepts. In the quark model of the American physicist M. Gell-Mann, one quark should have a positive electrical charge of 2/3 of the charge of the electron, and the other quark should have a negative charge of 1/3. Professor M. Gell-Mann called this charge difference between quarks flavors. New experiments and modeling of the behavior of black holes - these factories of baryonic and dark matter - have made it possible to discover the accurate physical picture of the structure of matter. It turned out that when describing the design of the atomic nucleus, guided by the principle of “Okaama’s razor” and cutting off all unnecessary things, including hypothetical quarks and all the perfumery of aromas, one can obtain an actual model of the atomic nucleus. I want to remind you of the words of A. de Saint-Exupery: “Truth is not at all something that can be convincingly proven it is something that makes everything simpler and clearer.”

II. Atom Model

The atomic model proposed by Professor Lev Sapogin [1] does not contradict the latest new ideas about the internal structure of atoms. Unitary quantum theory makes it possible to explain the strange behavior of electrons in an atom when the electron orbitals of the p- and d-states of the bit look like figure eights with nodal points in the atomic nucleus (Fig. 1) [2].

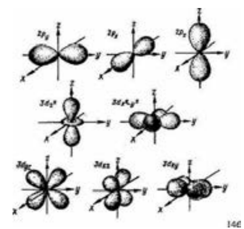

Figure 1: Forms of electron clouds for different states of electrons in atoms

Since the areas allowed by quantum mechanics for an electron to reside in them are only the internal regions of these orbitals to get from one half-branch of the “eight” to the opposite, the electron must jump through the nucleus of the atom. This allows us to take a new look at the mechanism of the mysterious K-capture of an electron in an atom. Electron capture, as is known, consists in the fact that the nuclei of atoms of some isotopes of chemical elements, in some mysterious way, sometimes capture an electron from the inner (K- or L-) electron shell of the atom. Physicists have long been tormented by the question of how such a capture occurs if the electron in an atom, according to existing concepts, is very far (on nuclear scales) from the nucleus. But if an electron constantly tunnels through the nucleus of an atom, then everything becomes clear. In Lev Sapogin's model, electrons inside an atom do not fly in orbits, as in Rutherford's model, but are a standing electromagnetic wave that does not have an orbit and coordinates, but has a certain frequency and amplitude. A similar conclusion follows from the law of formation of the spectra of the hydrogen atom corresponding to the stationary energy levels of the electron. The law of spectroscopy does not have a component corresponding to the orbital motion of the electron, which means the absence of orbital motion of the electron in the atom. Therefore, to describe the behavior of electrons in an atom, the concept of the energy level of an electron in an atom is introduced, instead of the existing concepts of orbit and orbital. This representation of the atom allows for electron tunneling through the atomic nucleus. Lev Sapogin explained tunneling by the fact that the electric charge of an elementary particle is not constant in time, but periodically changes (oscillates) with a monstrously high

Author: Department of Physical Electronics, Herzen State Pedagogical University, Saint Petersburg RSC” Energy”, Russia.
e-mail: konstantinov.s.i@yandex.com

Global Journal of Science Frontier Research (A) Volume XXIII Issue VIII Version I Year 2023

frequency, sometimes increasing to a maximum, sometimes decreasing to zero according to the harmonic law. Therefore, quantum theory operates with time-averaged values of the effective charge of a particle and its mass, which also oscillates in time according to a harmonic law ranging from zero to maximum [2]. To tunnel, the particle must approach the potential barrier in a phase when the amplitude of the wave packet is small, and the particle, in the absence of a charge, overcomes the barrier without "noticing" it. Moreover, at the moment of tunneling, the instantaneous values of the charge and mass of the electron are close to zero and, due to the law of conservation of momentum, at this time the electron must develop a very high speed of movement through the nucleus of the atom. However, if the tunneling process is disrupted, the electron is either captured by the nucleus, or a nonlinear interaction begins, and the particle can be reflected from the barrier. In this case, not the entire electron is captured, but only its electric charge and most of the mass, which are attached to one of the positively charged protons P of the nucleus, which turns into a neutron N, the mass of which is greater than the mass of the proton. But the remainder of the electron in the form of an electron neutrino ν_e flies far beyond the boundaries of the atom. Physicists suggest that in this case a process occurs in the nucleus of the atom:

$$P + e^{"} \longrightarrow N + \nu_e \qquad (1)$$

which, however, has never been observed in experiments on the bombardment of protons by beams of accelerated electrons [1]. This confirms experiments of Andras Kovacs, Valery Zatelepina, and Dmitry Baranov related to the discovery of the nuclear electron and the measurement of its mass [3]. Andras Kovacs, Valery Zatelepina, and Dmitry Baranov measured the mass of a nuclear electron and obtained two values: for ^{58}Ni, the capture measurement gives 1554 keV, and for 1H, it gives 1553 keV. Thus, the average value of the mass of a nuclear electron will be 1553.5 keV. The neutron is made up of a proton and a nuclear electron. The mass of a nuclear electron is 1553.5 keV. As a free particle, the nuclear electron has a short, but not zero, half-life. A nuclear electron is stabilized by binding to one or more protons. The binding energy between a proton and a nuclear electron is 260 keV [3]. Andras Kovacs, Valery Zatelepina, and Dmitry Baranova established the existence of much experimental evidence for the presence of negative elementary charges in nuclei. A possible explanation may be the K-capture of an electron by the nucleus, in which the total positive charge of the nucleus decreases by one (in units of proton charge). Therefore, during K-capture, the nucleus turns into the nucleus of an atom of one of the isotopes of the chemical element that appears in the periodic table before the original chemical element. In the article "The Energy of Our Future," 1931 Nikola Tesla wrote: "The worst of the modern theories is probably the electron theory. Of the four or five theories of atomic structure proposed today, not one is probable. No more than one in a thousand scientists believe that an electron - whatever it may be - can exist only in the ideal vacuum of intermolecular and interstellar space" [4].This statement was brilliantly confirmed by the experiments of Andras Kovacs, Valery Zatelepin, and Dmitry Baranov [3].

III. Quasars - Factories of Baryonic and Dark Matter

In September 2021, Professors Xavier Calmett and Folkert Kuipers from the Department of Physics and Astronomy at the University of Sussex published a report that the structure of black holes is more complex than previously thought, and quantum gravity can lead to pressure black holes on the quantum environment. Xavier Calmett said: "Our finding that Schwarzschild black holes have a pressure as well as a temperature is even more exciting given that it was a total surprise. Hawking's landmark intuition that black holes are not black but have a radiation spectrum similar to that of a black body makes black holes an ideal laboratory to investigate the interplay between quantum mechanics, gravity, and thermodynamics" [5]. At the edge of a black hole, the physical vacuum is in a conditionally stressed state, as a result of which it is polarized in a quantum manner. Nothing of the kind follows from Einstein's General Theory of Relativity. Einstein's general relativity, in general, is incompatible with quantum concepts. Studying the behavior of quantum fields near a black hole, Stephen Hawking predicted that a black hole necessarily radiates particles into outer space and thereby loses mass [6]. This effect is called Hawking radiation (evaporation). Vacuum polarization occurs under the influence of monstrous gravitational and magnetic fields, as a result of which the formation of not only virtual but also real particle-antiparticle pairs is possible. According to Hawking, on the surface of the event horizon, the direction of expansion of the generated particles ceases to be random, i.e., becomes polarized, namely, orthogonal to the surface of the black hole [6]. The existence of stable Hawking radiation - the process of emission of various particles by a black hole - was first proved by specialists from the Israel Institute of Technology [7]. A report of the production of a substance with properties identical to plasma in the vicinity of a black hole also appeared in a joint work of Russian, Japanese and French researchers from the LaPlaz Institute, the National Research Nuclear University MEPhI and the CELIA laboratory of the University of Bordeaux, published in 2020 [8]. Black hole accretion disks were obtained in laboratory conditions. This structure results from the fall of diffuse material with spinning momentum onto a massive central body (accretion) around neutron stars and black holes. Compression of matter, as well as the release of heat due to friction of differentially rotating layers, leads to heating of the accretion disk. Therefore, the accretion disk emits thermal electromagnetic and X-ray radiation. Experiments have shown that the technique developed by an international group makes it possible to create not only quasi-stationary magnetic fields of record magnitude, but also to simulate the state of plasma emerging in them with a high energy density of matter - 10^{18} particles per cm^3. The uniqueness of the experiment is that the parameters of the resulting plasma do not need to be scaled; they correspond to the real parameters of the plasma in the vicinity of the black hole of binary systems like Cygnus X-1 (Fig. 2) [8].

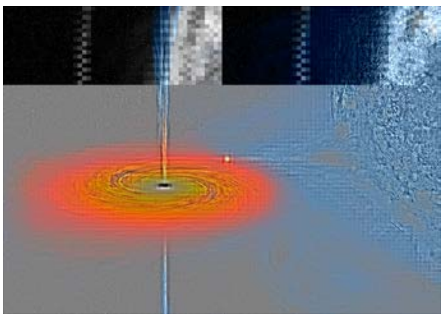

Figure 2: Black water Swan X-1

Later, researchers at the University of Manchester, led by Nobel Prize winner Andre Geim, discovered that inside graphene, it is possible to recreate conditions identical to those in which matter emerges from the vacuum in the vicinity of black holes and other space objects [9]. In laboratory experiments, they reproduced the Schwinger effect using very narrow strips of graphene. In this case, super-powerful electric or magnetic fields will act on the vacuum in such a way that virtual particles and antiparticles forming dipole structures - positronium - will break apart and form very real positrons and electrons [9].

The experiment showed that the technique developed by the international group makes it possible to create quasi-stationary magnetic fields of record magnitude, and to simulate the state of the plasma arising in them with a high energy density of matter and electromagnetic energy. As a result, we get an electron-positron mixture near of the black hole, consisting of approximately equal numbers of negative electrons and positive positrons. In a free state, electrons and positrons annihilate - this is an indisputable fact. However, in the accretion disk, electrons and positrons are not entirely free. They continue to rotate by inertia within the plasma disk at about the speed of light. And it is this speed, or rather the force of inertia, keeps them from direct collisions and complete mutual destruction. At this stage, electrons and positrons form dipole structures - positroniums. Experimentally, such a pair was discovered in 1951 by the German physicist Martin Deutsch (Figure 3) and reliably established by Professor DB Cassidy and his assistant A. P. Mills, Jr. in 2007 [10].

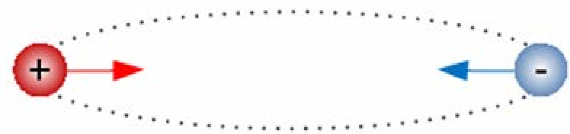

Figure 3: Positronium atom

Positronium has stable, compact states with high binding energies, which can be interpreted as particles and unit cells of the quantum vacuum structure. Positronium has a mass of two electronic, and its energy in the ground state of E = 3727.7763 161411854 eV. In the work of RAS Academician RF Avramenko, it is says that the future opens with a quantum key [11]. Cassidy and Mills calculated that in their experiment, the density of positronium atoms was 10^{15} per cm^3. Calculations show that with an increase in this density by three orders of magnitude, these atoms at a temperature of 15 kelvin will merge into a single quantum system — Bose-Einstein condensate [10]. Now physicists say that instead of studying empty space, they can create a Bose-Einstein condensate. When cooled to just above absolute zero, the atoms slow down enough to overlap and form a high-density cluster of atoms, acting as a single "super-atom". In it, sound particles and photons become audible in a background vacuum. The sound is not produced by the detector, but is heard due to acceleration. The Unruh effect creates a thermal response of an accelerated detector as it moves in a vacuum [12]. In June 2020, a Bose-Einstein condensate was successfully recreated in Earth orbit on the International Space Station (ISS). Only there was it possible to weaken the Earth's gravity and create all the conditions for the emergence of the quantum fifth state of matter within a few seconds, but this was enough for scientists to get the idea that dark matter moves as a single whole [13].

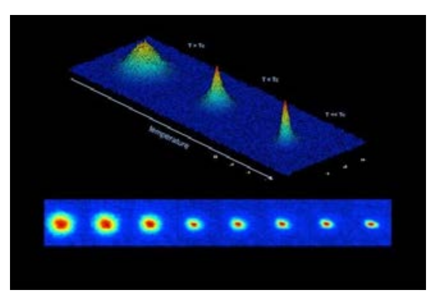

Figure 4: Bose-Einstein condensate (BEC)

Atomic nuclei are born in the plasma of quasars at a density of 10^{18} particles per cm^3, monstrous magnetic fields and pressure. It was precisely this pressure of 10^{35} Pascal that Professor Volker Berkert from the Jefferson Laboratory discovered in the nuclei of protons during experiments by bombarding protons with electrons [14]. An article by astrophysicists from Finland, published on June 1, 2020, states that "the matter inside the most massive stable neutron stars is interpreted as plasma that filled the newborn Universe approximately 20 microseconds after the Big Bang, which cooled to the state of "ordinary" matter and filled the Universe" [15].

However, the massive appearance of neutrons on the outskirts of the plasma disk marks a fundamentally new stage in formation of mother in the infinite Universe, the evolution of which does not require a Big Bang and has no beginning and end. From this moment on, the conveyor for the production of chemical elements begins to operate. Experimental physics has reliably established that a free neutron decays into a proton and an electron in about 15 minutes. Thanks to this, the most common substance in the Universe is born - hydrogen. Hydrogen atoms gradually accumulate around the rotating disk of protoplasm and envelop it in a reasonably dense layer. At some point, the density of the hydrogen blanket reaches a critical value, and the free escape of neutrons from the plasma disk becomes difficult. The next cycle of synthesis of atoms of matter begins. This is the next chemical element of the periodic table - helium. Such processes of wrapping a neutron centrifuge in a gas cushion are repeated for each new chemical element. The further we move along the periodic table, the denser the outer nucleon layer becomes, and the fewer atoms of a new substance are formed at the output. Therefore, in our Universe hydrogen makes up 70% of the total mass of all chemical elements. The described process allows us to understand how the synthesis of all chemical components of the universe proceeds. This is not explosive thermonuclear fusion in the depths of several generations of stars still the careful assembly of atoms of chemical elements from elementary particles using a high-speed plasma centrifuge. Our further task is to understand the principle of the formation of atomic nuclei based on protons and neutrons, which have, respectively, the charge and magnetic moment of the proton, as well as the magnetic moment of the neutron and its lack of charge. The presence of magnetic moments in these particles gives us grounds to assert that they have magnetic poles. The magnetic forces of the opposite poles of the magnetic fields of the proton and neutron are the only forces capable of connecting these particles with each other. The experimentally measured values of the magnetic moments of the proton and neutron are $\mu p = 2.79\mu N$ and $\mu n = -1.91\mu N$, where the magnetic moments are measured in nuclear magnetons, which are approximately 2000 times smaller than the Bohr magneton $\mu B=0.5788\times10^{-14}$MeV/G. The negative value of the neutron magnetic moment is due to the fact that the vector of the neutron magnetic moment μn is directed in the opposite direction from the neutron spin Sn. The directions of the vectors of the proton's magnetic moment μp and its spin Sp coincide. The difference between the magnetic moments of the proton and neutron from the Dirac values indicates that these particles are not point particles, but have a complex internal structure. The proton and neutron are considered as two charge states of one particle - the nucleon. The electrostatic forces of protons are the only forces that limit the proximity of protons in the nucleus. However, the existence of nuclear forces that connect protons and neutrons in the nuclei of atoms has also been experimentally established. If we take into account the enormous magnetic field strength near the center of symmetry of the proton $Hp=8.5074256 \times 10^{14}$ Tesla and assume that it is approximately the same for the neutron, then there is reason to believe that the magnetic forces of the proton and neutron, acting at distances close to their geometric centers, are those forces that are called nuclear. Then we can assume that nuclear forces are actually magnetic forces acting at extremely small distances between the centers of mass of protons and neutrons. The absence of orbital motion of electrons creates the conditions under which each electron must interact with one proton of the atomic nucleus. It follows from this that protons must be located on the surface of the nucleus. Then, to weaken the repulsive forces acting between protons, they must combine with neutrons so that there are necessarily neutrons between the protons. This condition is met if the neutron has six magnetic poles. And then, Professor A.V. Rykov determined the force of elastic deformation inside the nucleon $F = 5.211 \times 10^{26}$ [kg/s²] [16]. It is this enormous force that counters the 10^{35} Pascal pressure force discovered by Burkert inside the core and directed outward. Thus, there is no need for such concepts as gluon plasma inside the nucleus, which glues quarks together and resists internal pressure.

IV. Nuclear Interaction

Vacuum is involved in all fundamental interactions, but if the polarization of the void in electromagnetic interactions is accompanied by the formation of electron-positron pairs with the participation of exchanged virtual photons, then in nuclear interaction the polarization of the quantum vacuum is accompanied by the construction of three unstable π-mesons (π^0, $\pi+$, π-) with the participation of virtual exchange pions and the subsequent creation of short-lived protons and antiprotons. At the same time, the energy spectrum of the birth of new particles and antiparticles changes, which indicates a difference in the structure of the quantum vacuum when it is included in the nuclei of atoms [17]. Professor Anatoly Rykov called the medium of virtual pi-mesons, participating as exchange particles in atomic interactions, the meson ether. Next, I will give an excerpt from Rykov's work [16], published in 2000 but still relevant today: "It is easy to see that the structural element is the mass of the dipole. Multiplying it by $2m_e$, we get $\alpha^{-1}\cdot 2m_e=274.0720\cdot m_e$ a value very close to pion $m_{(+-)}=273.2\cdot m_e$. This coincidence turns out to be significant. If in the previous case the "photon exchange" was reduced to the deformation of the photon ether, then the pion exchange forms the basis of the strong interaction. How do pions deform the ether so that the acting forces during the deformation of the "pion" structure of the ether correspond to intranuclear forces? The existence of three types of "nuclear" pions π^0, $\pi^+\pi^-$ can, apparently, be somehow taken into account in the structure of the meson ether in order, in a similar way to photon exchange, to find a new interpretation of meson exchange in nucleons, eliminating the need for physics to artificially introduce exchange processes using particles. At the moment we have only one "fact" - in the structure of the photonic ether there is a cluster with a mass $274.0720\cdot m_e$ that acts during the photoelectric effect and during electromagnetic interaction and is formed by electron + positron pairs. Pions have an independent "life" and are unique clusters, as if formed from electrons and positrons. A pion π^0 contains an integer *264.2* electron and positron masses plus *0.2* elementary masses. The integer defines the zero charge of the pion π^0. Pions π^+,π^- contain an odd number of *273* electron and positron masses. Nature seems to suggest that π^+ there is π^- one excess positron, and one excess electron. One thing is clear that pions represent a single whole (indivisible quantum systems capable of virtual and real existence in accordance with their short lifetimes). The lack of charge pion masses can be interpreted as a bond mass defect or binding energy $\Delta m_{(+-)}=0.8720\cdot m_e$. For the π^0 pion, two variants of the mass defect can be assumed: $\Delta m_{(0)}=0.2\cdot m_e$, or $\Delta m_{(0)}=9.872\cdot m_e$. The variants can be distinguished by the lifetime of the π^0 pion. Since the π^0 -pion has a lifetime shorter than that of charge pions, the first option should be accepted, that is, $\Delta m_{(0)}=0.2\cdot m_e$. Let us assume that the meson structure of the ether is formed by a triple of pions π^0,π^+,π^-. This is a significant difference from the structure of the ether, which has an electron + positron pair. At the same time, a certain analogy appears to the qualitative "triple" structure of the nucleus - 2 protons and 1 neutron. They must form an elementary quasi-stable structure according to the polarization scheme proton(+) (–neutron–) (+) proton. In fact, a stable structure of 2 protons is organized only with the help of 4 neutrons, the polarization of which, apparently, best suits the stable spatial structure of the nucleus. From the above it follows that pi-mesons and protons can be represented as formed from the only elementary particles - electrons and positrons" [16].

V. Conclusion

Thus, we can conclude that Dmitry Mendeleev reasonably placed ether (physical vacuum) in the first place in the periodic table, which is polarized in the monstrous gravitational, electric and magnetic fields of black holes, generating particles and antiparticles that form atoms. The absence of ether in the periodic table today is a clear indicator of the level of modern science and a gross distortion of Mendeleev's scientific heritage. The second conclusion from the article is the rejection of speculative structures of quarks in the atomic nucleus. Indirect evidence of the existence of quarks in the nucleus is hadronic jets that arise during the inelastic scattering of electrons, muons and neutrinos on a nucleon. However, the interpretation of their nature as a manifestation of the quark structure of nucleons is not as unambiguous as apologists of modern nuclear physics try to present it.

References Références Referencias

1. Leo G. Sapogin and Stanislav Konstantinov. "Rejection of Rutherford's Planetary Model of the Atom, Bohr's Postulates and the Tunnel Effect" // Journal of Physics & Optics Sciences, Volume 3(1): 2-4 (2021).
2. Leo G. Sapogin, Ryabov Yu.A., Boichenko V.A. "The Unitary Quantum Theory and a New Sources of Energy" // Science Publishing Group, USA.(2015)
3. András Kovács, Valery Zatelepin, Dmitry Baranov. The Discovery of the Nuclear Electron and its Mass Measurement, BroadBit Energy Tech. Inleas Laboratory // "МИС-РТ"-2022 Сборник №79-1-4 http://ikar.udm.ru/mis-rt.htm
4. Nikola Tesla The Energy of Our Future // Everyday Science and Mechanics, December (1931).
5. Xavier Calmet et al, "Quantum gravitational corrections to the entropy of a Schwarzschild black hole" // Physical Review D (2021). DOI: 10.1103/PhysRevD.104.066012
6. Stephen Hawking. "From the Big Bang to Black Holes" // New York: Bantam Books, 1988.
7. Ingrid Fadelli , "Researchers observe stationary Hawking radiation in an analog black hole" // Phys.org , FEBRUARY 19, 2021
8. K. F. F. Law, Y. Abe, A. Morace, Y. Arikawa, S. Sakata, S. Lee, et al, "Relativistic magnetic reconnection in laser laboratory for testing an emission mechanism of hard-state black hole system" // Phys. Rev. E 102, 033202 – Published 3 September 2020
9. Alexey Berdyugin, A.K. Geim, et al, "Out-of-equilibrium criticalities in graphene superlattices" // SCIENCE, Vol 375, Issue 6579, (2022), DOI: 10.1126/science.abi8627

10. D. B. Cassidy, A. P. Mills, Jr. “The production of molecular positronium” // Nature. V. 449. (2007) P. 195–197.
11. The future opens with a quantum key. Sat. articles by academician RF Avramenko.-M., "Chemistry", 2000.
12. S. Autti et al., “Fundamental dissipation due to bound fermions in the zero-temperature limit” // Nature Communications volume11, Article number: 4742 (2020).
13. David C. Aveline et al., “Observation of Bose–Einstein condensates in an Earth-orbiting research lab”, Nature volume582, pages193-197 (June 11, 2020).
14. Burkert V.D. and Elouadrhiri L. and Girod F.X., “The pressure inside the proton” Nature, 557:396–399, (2018).
15. Eemeli Annala, and et al., “Evidence for quark-matter cores in massive neutron stars”, Nature Physics, (01 June 2020).
16. A.V. Rykov, “Fundamentals of the theory of ether” // M.: Russian Academy of Sciences, Institute of Physics of the Earth, (2000).
17. Stanislav Konstantinov, “The Role of Vacuum Polarization in the Large Hadron Collider” // Global Journals Inc. (USA) GJSFR-A, Volume 20, Issue 4, Version 1.0, pp 21-27, (2020).

Global Journal of Science Frontier Research: A
Physics and Space Science
Volume 23 Issue 8 Version 1.0 Year 2023
Type: Double Blind Peer Reviewed Interenational Research Journal
Publisher: Global Journals
Online ISSN: 2249-4626 & Print ISSN: 0975-5896

Relativistic Exploration of Dark Matter Effects in Rotating Galaxy, Studied Fluid-Dynamically

By Tsutomu Kambe
Former Professor at University of Tokyo

Abstract- Galactic space is filled with interstellar clouds of neutral gases. Motion of the space-clouds is viewed as a flow of continuous fluid in curved space with gravity. Dynamical motions of the space-fluid of rotating galaxies are investigated by extending Fluid Dynamics to that in the frame of general relativity. Fluid flow field to be extended to that of a relativistic theory is reinforced by the fluid gauge theory equipped with a background (dark) gauge field conditioning the fluid continuity. The Gravity-space Fluid Dynamics thus developed captures main feature of the dark-matter effect as the action of the gauge field on the motion of space fluids. In the present formulation, the stress-energy tensor in the general relativity is revised in order to take account of general nature of stress field by extending the isotropic pressure to an-isotropic stress field.

Keywords: dark-matter-effect – space-cloud – fluid-gauge-field – gravity – relativistic-fluid-dynamics.

GJSFR-A Classification: FOR Code: 020104

Strictly as per the compliance and regulations of:

Relativistic Exploration of Dark Matter Effects in Rotating Galaxy, Studied Fluid-Dynamically

Tsutomu Kambe

ABSTRACT

Galactic space is filled with interstellar clouds of neutral gases. Motion of the space-clouds is viewed as a flow of continuous fluid in curved space with gravity. Dynamical motions of the space-fluid of rotating galaxies are investigated by extending *Fluid Dynamics* to that in the frame of *general relativity*. Fluid flow field to be extended to that of a relativistic theory is reinforced by the *fluid gauge theory* equipped with a background (*dark*) gauge field conditioning the fluid continuity. The *Gravity-space Fluid Dynamics* thus developed captures main feature of the dark-matter effect as the action of the gauge field on the motion of space fluids. In the present formulation, the stress-energy tensor in the general relativity is revised in order to take account of general nature of stress field by extending the isotropic pressure to an-isotropic stress field.

Regarding the dark-matter effect, McGaugh-Lelli-Schombert (2016) found a strong evidence, that shows existence of a functional correlation between the *observed centripetal* radial-acceleration and the *gravitational* acceleration predicted by observed baryon distribution within galaxy. This implies that the dark matter contribution is specified by the baryon distribution. Present theory is consistent with this view and gives an explicit mathematical expression to the acceleration attributed to the dark-matter effect. The effect is created by the action of the gauge field $\boldsymbol{a}$. The gauge field is determined by an equation in which the field $\boldsymbol{a}$ is excited by the current flux defined with product of fluid density ρ and fluid velocity $\boldsymbol{v}$, and the degree of excitation of $\boldsymbol{a}$ is controlled by a field parameter μ_{F}.

Agreement between astronomical data and the data deduced from the theory is excellent.

Keywords: dark-matter-efect – space-cloud – fuid-gauge-feld – gravity – relativistic-fuid-dynamics.

Global Journal of Science Frontier Research (A) Volume XXIII Issue VIII Version I Year 2023

I. Introduction

The cosmological issue of *dark matter effect* is studied with a new approach to spiral galaxies in rotational motion (Fig.1). To that end, it is essential to recognize that, in cosmic space, gas clouds are abundant and free to move under physical fields: gravity field *etc.*

a) *Motion of space clouds viewed as continuous flows*

The emission lines (such as the HI-21 cm line) in cosmic space show abundance of neutral gas clouds in the galactic interstellar space. The neutral gases are captured by the galactic disk via its gravitational field and its spiral arms. Kalberla & Kerp (2009) coined it as *Galactic Atmosphere* over the galactic disk. Concerning the gas clouds moving about cosmic space, their dynamical motions should be described as flows of continuous fluids. Present study is carried out from this view on the basis of the *Fluid Gauge Theory* (Kambe 2021a).

Although stars are very sparse in outer part (halo) of our galaxy, the halo is dominated by invisible matters and actually contains considerable portion of the total mass of the galaxy. Present approach is based on the view that the dark matter effect might be caused by invisible space-fluids, driven by the action of a fluid gauge-field according to *the theory*. The space-fluids are moving at very-high orbital speeds of about $200 \sim 300$ km$\cdot$s^{-1} in the galactic space (Tully & Fisher (1977), Sofue & Rubin (2001), McGaugh et al. (2016)) under interaction with the galactic arms that rotate at high speeds as well. Dynamical mechanism of the interaction of space-fluids with the galactic arms moving at high orbital speeds is the target of the present investigation.

Author: Former Professor at University of Tokyo, Guest Scholar at MIMS, Meiji University, Tokyo, Japan. e-mail: kambe@ruby.dti.ne.jp

Figure 1: A sample spiral galaxy in rotation: NGC 3198 (GALEX image, *NASA*).

It is known that observed rotation curves of galaxies do not match the one expected from the Keplerian law of velocity decreasing as $R^{-1/2}$ with R the distance from the gravity center. At distances away from the center, the stellar orbital motion tends to rotation with almost constant velocity. This hints that certain mechanism is working at halo parts of galaxies more conspicuously.

b) Field description strengthened for rotational one

Present approach takes a new two-sided strategy, namely on the one hand the theory is strengthened by an improved action term of new stress field, on the other hand the dark object might be space-fluids existing abundantly in cosmic space. In fact, its flow field is reinforced by the *fluid gauge theory* equipped with a background (*dark*) gauge field (Kambe 2021a).

According to the theory, the *isotropic* pressure of *Eulerian* system is extended to *an-isotropic* stress fields giving rise to flows of rotational nature inherently. Thus, a new approach is formulated on the basis of the variation principle for a perfect fluid in the presence of gravity.

The present theory reinforces the fluid flow fields with a background (dark) gauge field. The gauge field not only ensures the mass conservation of fluid flows, but also assists the flow field with transition of its stress field σ_{jk}, from the isotropic pressure stress $p\delta_{jk}$ prevailing in quiet states of slow motion to an-isotropic stress field M_{jk} prevailing in turbulent flow states.

In this regard, a past study of acoustics (Kambe 2022) is helpful to understand the transition. In the resonance problem studied by Kundt, increasing the strength of acoustic excitation triggers spontaneous transition of the acoustic field from isotropic to an-isotropic stress field. The an-isotropic rotational field is generated by an invisible gauge field and responsible to formation of the mysterious dust striations studied by Kundt (1866).

c) Fluid Lorentz force

An important feature of the present theory is that it includes a new dark gauge-field a_ν ($\nu = 0, 1, 2, 3$: relativistic 4-components). Incorporation of a *non-gravitational* field a_ν to the gravity field is assured by the *local-flatness theorem* (Schutz 1985) and the *Einstein Equivalence Principle* (Will 1993) in the general relativity. In addition to the gravitational Lagrangian built of metric alone yielding curved gravity space, fluid motions are described by new fluid Lagrangians. Thus new terms are introduced in equations of motion. The new terms are analogous to electromagnetic terms, but derived for neutral fluids here. One particular term to be remarked is the *fluid* Lorentz force, $\boldsymbol{v} \times \boldsymbol{b}$ with $\boldsymbol{v}$ the fluid velocity and $\boldsymbol{b}$ the fluid-magnetic field from a_ν.

d) Twisted connection between physics of galaxy rotation and visible matters

Physics of galaxy rotation is, in general, closely tied to the gravity field of baryonic visible matters. But in the present case, astronomical observations state that mutual relation between them is not straightforward.

Observing celestial objects within a spiral galaxy, their orbital velocities are detected spectroscopically at their respective distances from the galactic center, while the gravitational force is estimated from the data of baryonic visible mass distribution of stars and gases in the galaxy. The gravity forces thus obtained are not sufficient to reproduce the observed velocity curves at outer parts of most galaxies. This raised issues concerning presence of dark matters in most galaxies.

On the other hand, the recent study (McGaugh et al. 2016) proposed a universal behavior, stating that the rotational motion of a disk galaxy is determined entirely by visible matters it contains, even if the disk is filled with unknown dark matters, paradoxically. The last implies a strong *twisted* connection between the visible matters and the physics producing the rotational motion. Possible interpretations given by the authors of McGaugh et al. (2016) are rephrased in the following ways: either (a) *it represents the end product of galaxy formation*, or (b) *it is the result of new dynamical laws rather than dark matter*, or (c) *it represents new physics of a dark sector that leads to the observed coupling.*

Present study takes new double-sided approach both dynamically and physically: namely incorporating a new dynamical field of dark gauge-field and attacking the system with a new physics using an-isotropic stress fields. Therefore, present approach is related to both categories (b) and (c), in addition, with implicitly taking the view (a). The present approach is based on the general-relativistic version of *Fluid Gauge Theory*.

e) HI-21 cm line tells a mystery from cosmic space

Few galaxies exhibit the *Keplerian* law $v_* \propto R^{-1/2}$ for the stellar velocity v_* at large distance R from the galactic center, but the galactic rotation velocities keep high values at large values of R, flat instead of falling. This was recognized as early as 1950s (Sofue & Rubin 2001), and later updated to the *Tully-Fischer* relation (Tully & Fisher 1977): $M_{bar} \propto (v_H)^p$ with $p = 3.5 \sim 4$, for the Hydrogen gas velocity v_H at outer halo part of a galaxy and the total baryonic mass M_{bar} of the galaxy, even in case with substantial dark matter. The Tully-Fisher relation does not show any variation with scale or size of galaxy, remarked by McGaugh (2005).

f) A key relation of galaxy dynamics: McGaugh-Lelli-Schombert observational law

An important mathematical facet has been found for the galaxy dynamics by McGaugh et al. (2016), from statistics of a large set of 153 galaxies with different morphology, masses, sizes and gas fractions. Concerning the radial accelerations A_c (toward the center) of orbiting celestial objects of rotating galaxies, the law says how the centripetal acceleration A_c is related to the absolute value of gravity acceleration A_g.

To get an idea from simple analyses, let us take an axi-symmetric cylindrical coordinate system (Z, R, ϕ) with an axi-symmetric disk plane, defined by $Z = 0$. Consider a typical galaxy rotating around its center $(R = 0, Z = 0)$ with the velocity $(0, 0, V(R))$, keeping steady state circular rotation.

In this circumstance, the observed centripetal acceleration is given by $A_c = V^2(R)/R$. On the other hand, from observed mass density distribution $\rho(R)$ within a galaxy, the gravity potential Φ_g is determined by solving $\nabla^2\Phi_g = 4\pi G\rho$, and the gravity acceleration A_g is given by $A_g = |\partial\Phi_g/\partial R|$ (> 0, for clarity). A fitting curve was found by McGaugh et al. (2016) statistically, as

$$A_c = \mathcal{F}(A_g) \equiv \frac{A_g}{1 - e^{-\sqrt{A_g/A_\dagger}}}, \tag{1}$$

where $A_\dagger \approx 1.20 \times 10^{-10}\,\mathrm{m\,s^{-2}}$. This implies a strong connection between the baryonic gravity acceleration A_g and the physics that generates the observed A_c.

Looking at lower end of A_g value (at halo part), the curve is found to be consistent with the Tully-Fischer relation. In fact, assuming $|A_g/A_\dagger| \ll 1$ and using $A_c \equiv (v_H)^2/R$ and $A_g \propto M_{bar}/R^2$ as $R^{-1} \to 0$, the fitting curve (1) implies $M_{bar} \propto (v_H)^4$, consistent with the Tully-Fischer relation.

The difference between A_c and A_g (if any) is accounted for as the contribution A_{DM} from *dark matter* (DM): $A_{DM} = A_c - A_g$. However, the centripetal acceleration A_c is given by the fitting function $\mathcal{F}(A_g)$. Thus, the A_{DM} should be given by $\mathcal{F}(A_g) - A_g$, which is determined once A_g is known regardless of DM. This means that the acceleration A_{DM} (attributed to the dark matter) is coupled to the visible mass ρ giving the gravitational acceleration A_g. Then where exactly is the freedom to be attributed to dark matter?

Regarding the sample galaxy NGC3198 (Fig.1), let us try to estimate magnitudes of A_c and A_g from available astronomical data (Venkataramani & Newell 2021). Its rotation curve shows: $V \approx 150\,\mathrm{km{\cdot}s^{-1}}$ at $R \approx 19\,\mathrm{kpc}$ from the galactic center, which implies $A_c^* = V^2/R \approx 4.0 \times 10^{-11}\,\mathrm{m\,s^{-2}}$. Then the fitting curve (1) gives $A_g^* \approx 1.0 \times 10^{-11}\,\mathrm{m\,s^{-2}}$. From these two values, the DM contribution is estimated by the difference:

$$A_{DM}^* = A_c^* - A_g^* \approx 3.0 \times 10^{-11}\,\mathrm{m\,s^{-2}}. \tag{2}$$

One can remark a merit of their analysis. They are using acceleration terms, A_c, A_g and A_{DM}. Hence, their arguments apply to any celestial object in accelerating motion without regard to its magnitude of mass: a star, a gas cloud, or a fluid particle of space-fluid.

g) Invisible field creating visible effect

As one of the possible theories to resolve the current issue, the present paper proposes the *Fluid Gauge Theory* by extending the theory of fluid mechanics in flat space to the general relativity theory in curved space with gravity. The theory reinforces the fluid flow fields with a background (*dark*) gauge field. The new field strengthens the theory with two ways. The gauge field not only ensures the mass conservation of fluid flows, but also assists the flow field with transition of its stress field σ_{jk}, from the *isotropic* pressure $p\delta_{jk}$ prevailing in quiet states of slow motion to *anisotropic* stress field M_{jk} prevailing in turbulent flows. This enables appropriate description for turbulent motions in cosmic space.

It is helpful to remember the case of Kundt-tube experiment (§1.2) to get insight into the present issue. It implies, "*The gauge field within the Kundt-tube is not visible, yet creates visible dust-striations mechanically*". This insight applies analogously to the gravitational potential Φ_g as well: *The gravitational potential Φ_g is not visible, yet its derivatives $\partial_\nu\Phi_g$ create visible dynamical effect.*

h) Composition of the paper

Next section 2 describes the basic fluid system in flat space before extending to the *general relativity* in curved

Global Journal of Science Frontier Research (A) Volume XXIII Issue VIII Version I Year 2023

space. The fluid system is reinforced here by the *fluid gauge theory* equipped with a background (*dark*) gauge field. Extension to relativistic formulation according to the general relativity for curved space under gravity is carried out in the section 3 for *isotropic* pressure field where the stress-energy tensor of fluid motion is derived newly from the fluid Lagrangians. The section 4 explores what the part of the gauge field Lagrangians bring forward, and derives the equation of fluid motion under the *anisotropic* stress field. The dark matter effect of rotating spiral galaxies is investigated in section 5. Last section 6 summarises the outcomes of the present study.[1]

II. Fluid System in Flat Space before Extending to Curved Space

Relativistic formulation of *Fluid Gauge Theory* (*FGT*) is presented in Kambe (2021a) in flat space, which reinforces representation of the stress field within flows by adding rotational nature such as turbulence. This was achieved by extending the isotropic pressure field of Eulerian system to general anisotropic stress fields, according to the general gauge principle (Utiyama 1956).

a) *Lagrangians*

According to the relativistic FGT theory (Kambe 2021a) in flat Lorentzian space, the fluid system is described by the total Lagrangian $\mathcal{L}^{\rm FGT}$ consisting of three components, $\mathcal{L}^{\rm FGT}=\mathcal{L}_{\rm FM}+\mathcal{L}_{\rm int}+\mathcal{L}_{\rm GF}$:

$$\mathcal{L}_{\rm FM}=-c^{-1}(c^2+\bar{\epsilon}(\bar{\rho}))\,\bar{\rho}, \tag{3}$$

$$\mathcal{L}_{\rm int}=c^{-1}j^{\nu}\,a_{\nu}\,, \tag{4}$$

$$\mathcal{L}_{\rm GF}=-(4\mu c)^{-1}f^{\nu\lambda}\,f_{\nu\lambda}, \tag{5}$$

$$f_{\nu\lambda}=\partial_\nu a_\lambda-\partial_\lambda a_\nu,\quad \bar{\rho}\equiv\rho\sqrt{1-\beta^2}, \tag{6}$$

where the *overlined* values denote proper values and $\beta=|\boldsymbol{v}|/c$ (see Appendix A.ii) and the Lagrangian $\mathcal{L}_{\rm GF}$ includes a free parameter μ to be fixed later. The first Lagrangian $\mathcal{L}_{\rm FM}$ describes a perfect fluid in motion with 4-current mass flux $j^\nu=\rho\,v^\nu$ defined by (A2), and the third $\mathcal{L}_{\rm GF}$ describes an action of a background gauge field a_ν so as to ensure the fluid motion to satisfy mass conservation (to be shown later), while the middle $\mathcal{L}_{\rm int}$ describes their mutual interaction between j^ν and the gauge-field a_ν.

[1] Present study was partly presented orally at Physics-2023 held at Los Angeles, USA, 17 - 20 July 2023, and its video at "*STEMrv - Physics*" with the title "*Gauge Theory And Post-Newtonian Gravitational Fields Of General Relativity, With Reference To Dark Matter And Dark Space-Fluid*", by Tsutomu Kambe.

Total action of this system $S^{\rm FGT}$ is defined by

$$S^{\rm FGT}\equiv\int\mathcal{L}^{\rm FGT}{\rm d}\Omega=\int\Big[\mathcal{L}_{\rm FM}+\mathcal{L}_{\rm int}+\mathcal{L}_{\rm GF}\Big]{\rm d}\Omega, \tag{7}$$

where ${\rm d}\Omega\equiv{\rm d}^4x^\nu=c\,{\rm d}t\,{\rm d}^3x$. It is helpful to consider the form of first term $\mathcal{L}_{\rm FM}$ under non-relativistic limit as $\beta\to0$. The expression of $\mathcal{L}_{\rm FM}\,c\,{\rm d}^3x$ per unit mass ($m_1\equiv\rho\,{\rm d}^3x=1$) reduces to the non-relativistic form of $L_{nr}\equiv\frac{1}{2}m_1v^2-\epsilon$ (with v the velocity and ϵ the specific internal energy), neglecting the rest-mass energy $-m_1c^2$ (Kambe 2021a). Hence it is seen that the action $\mathcal{L}_{\rm FM}\,{\rm d}^4x^\nu$ is a *relativistic* version, extended from the classic non-relativistic Lagrangian $L_{nr}\,\rho\,{\rm d}^3x\,{\rm d}t$.

The third $\mathcal{L}_{\rm GF}$ of (5) is the Lagrangian of the (*dark*) gauge field represented in a form satisfying local gauge invariance under variations of the gauge field a_ν (see Kambe (2021b) §II) as well as ensuring current conservation. The tensor $f_{\nu\lambda}$ defined in (6) is called the *field strength tensor*. Its diagonal elements are all vanishing.

It is significant and important to recognize the following. When the gauge field a_ν is represented as $a_\nu=\partial_\nu\Psi$ with a scalar field $\Psi(x^\alpha)$, then $f_{\nu\lambda}$ vanishes identically:

$$f^{(\Psi)}_{\nu\lambda}=\partial_\nu(\partial_\lambda\Psi)-\partial_\lambda(\partial_\nu\Psi)\equiv0. \tag{8}$$

It would not be an exaggeration to say that *Fluid Gauge Theory* has been founded on the basis of this property.

Rewriting the field a_ν as $(\phi,\boldsymbol{a})$, two 3-vectors $\boldsymbol{b}$ and $\boldsymbol{e}$ are defined by using the 3-space notation $\boldsymbol{a}=(a_1,a_2,a_3)$;

$$\boldsymbol{b}\equiv\nabla\times\boldsymbol{a},\qquad \boldsymbol{e}\equiv-\partial_t\boldsymbol{a}-\nabla\phi, \tag{9}$$

where $\boldsymbol{b}$ and $\boldsymbol{e}$ are introduced as a pair of *fluid* Maxwell fields in the fluid system. If the gauge field a_ν is represented as $a_\nu=\partial_\nu\Psi$, all the components $f_{\nu\lambda}$ and $f^{\nu\lambda}$ vanish. Correspondingly, both of $\boldsymbol{b}$ and $\boldsymbol{e}$ vanish.

Next, we are going to deduce equations of motion from the action principle. In addition, the stress field $\sigma(\boldsymbol{x})$ will be used to represent force fields acting on the fluid.

b) *Governing equations*

Let us consider first how the fluid motion is described, and later consider what effect the background (*dark*) field would contribute to the fluid motion.

i. *Equation of fluid motion*

To find the equations of fluid motion, the action principle is applied to $S^{\rm FGT}$, by assuming the gauge field a_ν fixed and vary only the position coordinate x^ν of fluid particles as $x^\nu\to x^\nu+\delta x^\nu$ (for $\nu=1,2,3,$ where the particle is moving with the velocity $v^\nu = \mathrm{D}_t x^\nu$). Since the third Lagrangian $\mathcal{L}_{\rm GF}$ is invariant (no variable to be varied), the action variation is given by

$$\delta \int \Big[\mathcal{L}_{\rm FM}\, \mathrm{d}\Omega + \mathcal{L}_{\rm int}\, \mathrm{d}\Omega\Big], \tag{10}$$

which is required to vanish for arbitrary variation δx^ν of particle position.

Variation of the first term $\mathcal{L}_{\rm FM}\, \mathrm{d}\Omega$ is non-trivial because the term x^ν does not appear in the definition (3) explicitly, but it is included implicitly owing to the fact that the integrand $\mathcal{L}_{\rm FM}\, \mathrm{d}\Omega$ is expressed with proper values only. But one can find its equivalent expression at a moving frame where the fluid is in motion in the real frame of observation, obtained with a Lorentz transformation so that the particle velocity $v^\nu = \mathrm{D}_t x^\nu$ appears explicitly. From (3), such expression is given by

$$\begin{aligned}\mathcal{L}_{\rm FM}\, \mathrm{d}\Omega &= -c^{-1}(c^2 + \bar\epsilon(\bar\rho))\, \bar\rho\ \mathrm{d}x^0\, \mathrm{d}^3x \\ &= -c\,(1 + c^{-2}\bar\epsilon(\bar\rho))\, (\rho \mathrm{d}^3x)\, \mathrm{d}\tau,\end{aligned} \tag{11}$$

with $\bar\rho = \rho\sqrt{1-(|\boldsymbol{v}|/c)^2}$ and $\mathrm{d}\tau = \sqrt{1-(|\boldsymbol{v}|/c)^2}\ \mathrm{d}x^0$. This $\mathrm{d}\tau$ includes the velocity $|\boldsymbol{v}| = |\mathrm{D}_t x^\nu|$, its variation $\delta(\mathrm{d}\tau)$ must be implemented in the variation analysis. Then one may write the variation as

$$\delta[\mathcal{L}_{\rm FM}\, \mathrm{d}\Omega] = \Big[(\delta L_{\rm f})\, \mathrm{d}\tau + L_{\rm f}\, \delta(\mathrm{d}\tau)\Big]\ (\rho \mathrm{d}^3x), \tag{12}$$

where $L_{\rm f} \equiv -c\,(1 + c^{-2}\bar\epsilon(\bar\rho))$. The variation is carried out with keeping the mass element $\Delta m \equiv \rho\, \mathrm{d}^3x$ (within the volume element d^3x) fixed. In regard to the term $\delta(\mathrm{d}\tau)$, we have $\delta(\mathrm{d}\tau^2) = 2\,\mathrm{d}\tau\, \delta\mathrm{d}\tau = -2\eta_{\mu\nu}\ \mathrm{d}x^\mu \delta \mathrm{d}x^\nu$ from (A3). Hence, we obtain the following:

$$\delta \mathrm{d}\tau = -\eta_{\mu\nu} \frac{\mathrm{d}x^\mu}{\mathrm{d}\tau}\, \mathrm{d}\delta x^\nu = -u_\nu\, \mathrm{d}\delta x^\nu. \tag{13}$$

Thus the expression of $\delta[\mathcal{L}_{\rm FM}\, \mathrm{d}\Omega]$ is deduced as

$$-\frac{\Delta m}{c}\left(c^2 \frac{\mathrm{d}}{\mathrm{d}\tau} u_\nu + \frac{1}{\rho}\partial_\nu \bar p\right)\delta x^\nu\, \mathrm{d}\tau, \tag{14}$$

omitting $O(\beta^2)$-terms. Regarding the second Lagrangian term $\mathcal{L}_{\rm int}\, \mathrm{d}\Omega$, its variation is deduced as

$$\delta[\mathcal{L}_{\rm int}\, \mathrm{d}\Omega] = (\Delta m)\, f_{\nu\mu}\, u^\mu\ \delta x^\nu\ \mathrm{d}\tau \tag{15}$$

(see Appendix B.3 of Kambe (2021a)). From (14) and (15), the summation $\delta[\mathcal{L}_{\rm FM}\, \mathrm{d}\Omega] + \delta[\mathcal{L}_{\rm int}\, \mathrm{d}\Omega]$ is given by

$$-c^{-1}\,(\Delta m)\left[c^2 \frac{\mathrm{d}}{\mathrm{d}\tau} u_\nu + \frac{1}{\rho}\partial_\nu \bar p - c\, f_{\nu\mu}\, u^\mu\ \right] \mathrm{d}\tau\, \delta x^\nu \tag{16}$$

with neglecting both higher order terms and vanishing integrals with respect to τ. Requiring $\delta[\mathcal{L}_{\rm FM}\, \mathrm{d}\Omega] + \delta[\mathcal{L}_{\rm int}\, \mathrm{d}\Omega] = 0$ for arbitrary variation δx^ν, one finds

$$c^2 \frac{\mathrm{d}}{\mathrm{d}\tau} u_\nu + \frac{1}{\rho}\partial_\nu \bar p - c\, f_{\nu\mu}\, u^\mu = 0. \tag{17}$$

This is rewritten for $\nu = 1, 2, 3\ (\equiv k)$ as

$$\frac{\mathrm{D}}{\mathrm{D}t} \frac{v_k}{\sqrt{1-\beta^2}} + \frac{1}{\rho}\, \partial_k p - f_{k\nu}\, v^\nu = 0, \tag{18}$$

where $u_k = (v_k/[c\sqrt{1-\beta^2}])$ is used from (A4). Thus, in the non-relativistic limit as $\beta \to 0$, the equation of motion is deduced as follows:

$$\rho\, \mathrm{D}_t\, v_k = -\partial_k p + \rho\, f_{k\nu}\, v^\nu, \quad (k = 1, 2, 3). \tag{19}$$

This is the Euler's equation with the additional term $\rho\, f_{k\nu}\, v^\nu$ on the right hand side. The first term $-\partial_k p$ came from the isotropic pressure stress $\sigma^{\rm I}_{jk} = -p\, \delta_{jk}$ of (41). The second is a new term that came from the an-isotropic stress $\sigma^{\rm A}_{jk}$ to be given below.

ii. *Equations of a_ν (background dark gauge field)*

In order to find the equations governing a_ν from the variation principle, the fluid motion v^ν is kept fixed and only the gauge field a_ν is varied as $a_\nu \to a_\nu + \delta a_\nu$. In this case, the first Lagrangian $\mathcal{L}_{\rm FM}$ is invariant, and the action variation of remaining two is given by $\delta \int \Big[\mathcal{L}_{\rm int}\, \mathrm{d}\Omega + \mathcal{L}_{\rm GF}\, \mathrm{d}\Omega\Big]$, which is required to vanish for arbitrary variation δa_ν.

First, note that $\delta\big(f^{\nu\lambda} f_{\nu\lambda}\big) = 2 f^{\nu\lambda}\, (\delta f_{\nu\lambda})$. Therefore, variation of $c\,(\delta\mathcal{L}_{\rm int} + \delta\mathcal{L}_{\rm GF})$ is given by

$$\left(j^\nu\ - \frac{1}{\mu}\frac{\partial}{\partial x^\lambda} f^{\nu\lambda}\right)\delta a_\nu. \tag{20}$$

From the action principle requiring vanishing of (20) for arbitrary variation δa_ν, we obtain

$$\frac{\partial}{\partial x^\lambda} f^{\nu\lambda} = \mu_{\rm F}\, j^\nu, \qquad j^\nu = (\rho c, \rho \boldsymbol{v}), \tag{21}$$

(Kambe 2021a), where μ of (5) is a control parameter, hence redefined here as $\mu_{\rm F}$, which controls the degree of mutual interaction between the current j^ν and the tensor $f^{\nu\lambda}$ of the background gauge field.

iii. *Equations of a, b and e*

Using the definitions $\boldsymbol{e} = -\partial_t \boldsymbol{a} - \nabla\phi$ and $\boldsymbol{b} = \nabla \times \boldsymbol{a}$ defined in (9), the equation (21) is transformed into a pair of equations analogous to the Maxwell equations of *Electromagnetism*. In fact, with defining $\boldsymbol{d}$ and $\boldsymbol{h}$ by $\boldsymbol{d} = \epsilon \boldsymbol{e}$ and $\boldsymbol{h} = \boldsymbol{b}/\mu_{\rm F}$ with using $\epsilon \equiv 1/(\mu_{\rm F}\, c^2)$, the equation (21) gives a pair of Maxwell equations:

$$-\partial_t(\epsilon \boldsymbol{e}) + \mu_{\rm F}^{-1}\nabla \times \boldsymbol{b} = \boldsymbol{j}, \qquad \nabla\cdot(\epsilon\boldsymbol{e}) = \rho. \qquad (22)$$

Definition (9) leads to another pair:

$$\partial_t \boldsymbol{b} + \nabla \times \boldsymbol{e} = 0, \qquad \nabla\cdot\boldsymbol{b} = 0. \qquad (23)$$

c) *Equation of current conservation*

The equation of current conservation can be derived from Eq.(21), which is directly connected to the gauge-invariant property of the Lagrangian $\mathcal{L}_{\rm GF}$. Applying the divergence operator ∂_ν on (21), one obtains $0 = \partial_\nu\partial_\lambda f^{\nu\lambda} = \mu_{\rm F}\,\partial_\nu j^\nu$. The middle side vanishes because of the anti-symmetry of $f^{\nu\lambda}$ and the symmetry of $\partial_\nu\partial_\lambda$ to interchanging of ν and λ. Hence, total summation leads to the current conservation equation:

$$\partial_\nu j^\nu = 0, \quad \Rightarrow \quad \partial_t \rho + \nabla\cdot(\rho\boldsymbol{v}) = 0. \qquad (24)$$

Thus the third $\mathcal{L}_{\rm GF}$ ensures the *mass conservation*.

Additional remark must be given on the mass conservation. If the gauge field a_ν is represented as $a_\nu = \partial_\nu\Psi$, all the matrix components $f_{\nu\lambda}$ and $f^{\nu\lambda}$ of (3.7) vanish identically. However, even in this case ($a_\nu = \partial_\nu\Psi$), one can deduce the same current conservation, and the system of two Lagrangians $\mathcal{L}_{\rm FM}$ and $\mathcal{L}_{\rm int}$ defines the whole fluid system, since the third Lagrangian vanishes $\mathcal{L}_{GF} \equiv 0$. In fact, firstly, one can show that the variation $\delta\int c\,\mathcal{L}_{\rm int}\,{\rm d}\Omega = \int j^\nu\,\delta a_\nu\,{\rm d}\Omega$ is given by the following:

$$\int j^\nu\,\partial_\nu\delta\Psi\,{\rm d}\Omega = -\int(\partial_\nu j^\nu)\,\delta\Psi\,{\rm d}\Omega.$$

The action principle requires vanishing of this integral for arbitrary variation $\delta\Psi$. Hence we obtain the same current conservation law: $\partial_\nu j^\nu = 0$. Secondly, the total action variation of (10) leads to the equation (19) with $f_{k\nu} = 0$, which is nothing but the Euler equation.

Thus, in the case $a_\nu = \partial_\nu\Psi$, the whole fluid system reduces to the Eulerian system:

$$\rho\,{\rm D}_t\,\boldsymbol{v} = -\nabla p, \qquad \partial_t\rho + \nabla\cdot(\rho\boldsymbol{v}) = 0. \qquad (25)$$

This is the essential point of the *Fluid Gauge Theory.*

d) *Significance of the theory*

The present fluid gauge theory for a perfect fluid represents a broader class of flow fields than the current Eulerian field, by introducing the background field a^ν and covering a wider family of flow fields of a perfect fluid (Kambe, 2020, §5, an inviscid fluid).

In the presence of the gauge field a^ν, the governing equation is given by (19), which can be expressed by an equivalent 3-vector form, as follows:

$$\rho\,{\rm D}_t\boldsymbol{v} = -\nabla\,p + \rho\,\boldsymbol{f}_a, \qquad (26)$$

$$\boldsymbol{f}_a = \boldsymbol{v}\times\boldsymbol{b} + \boldsymbol{e} = \boldsymbol{v}\times\boldsymbol{b} - \nabla\phi - \partial_t\boldsymbol{a}. \qquad (27)$$

Note that this includes the Lorentz-type force $\boldsymbol{f}_a$ in fluid-flow field which is neutral electrically. The role of charge density in the electromagnetism is played by the mass density ρ. Significance of the fluid Lorentz acceleration $\boldsymbol{f}_a$ is interpreted from the following two aspects.

Firstly, as seen in (27), the acceleration $\boldsymbol{f}_a$ is apparently independent of the mass density ρ although the $\boldsymbol{b}$-field is controlled by $\boldsymbol{j} = \rho\boldsymbol{v}$ as seen from (22). The $\boldsymbol{f}_a$ instead depends on the velocity $\boldsymbol{v}$ unlike the gravity acceleration. In addition, it depends on the time derivative $\partial_t\boldsymbol{a}$ and rotational term $\nabla\times\boldsymbol{a}$. Hence the $\boldsymbol{f}_a$ would become significant in turbulent flow fields in which flow fields are time-dependent and rotational. The fluid Lorentz acceleration $\boldsymbol{f}_a$ is considered to be a generalization of the pressure force $-\nabla p$, as seen next.

Secondly, physical meaning of $\boldsymbol{f}_a$ may be given as follows. The force field $\boldsymbol{F}_a \equiv \rho\boldsymbol{f}_a$ is represented by the stress field $M^{\nu k}$. In fact, for spatial components $(i,k = 1,2,3)$, the k-th component of the force $\boldsymbol{F}_a \equiv \rho\boldsymbol{f}_a$ can be written as follows:

$$(\boldsymbol{F}_a)^k = (\rho\boldsymbol{e} + \rho\boldsymbol{v}\times\boldsymbol{b})^k = -\partial_\nu M^{\nu k}, \qquad (28)$$

$$M^{0k} = c\epsilon\,(\boldsymbol{e}\times\boldsymbol{b})_k,\ M^{00} = \tfrac{1}{2}\,\epsilon\,|\boldsymbol{e}|^2 + \tfrac{1}{2}\,\mu_{\rm F}^{-1}\,|\boldsymbol{b}|^2 \equiv w_e,$$

$$M^{ik} = -\epsilon\,e_i e_k - \mu_{\rm F}^{-1}\,b_i b_k + w_e\delta_{ik}, \qquad (29)$$

where $\partial_\nu = (c^{-1}\partial_t, \partial_k)$, and $\mu_{\rm F}$ and $\epsilon = 1/(\mu_{\rm F}\,c^2)$ are parameters of flow fields, The equality $(\rho\boldsymbol{e} + \rho\boldsymbol{v}\times\boldsymbol{b})_k = -\partial_\nu M^{\nu k}$ can be shown by using (22) and (23). The stress tensor M^{ik} of (29) as well as the parameters ϵ and $\mu_{\rm F}$ are analogous to the Maxwell stress tensor of electromagnetism. The term $(-\nabla\,p)^k$ on the right-hand side of (26) can be written as $-\partial_j(p\,\delta^{jk})$, a force from the isotropic pressure stress $-p\,\delta^{jk}$. According to the *present* fluid gauge theory, the state of isotropic pressure stress $p\,\delta^{jk}$ of Eulerian system is extended to the state of combined an-isotropic stress $p\,\delta^{jk} + M^{jk}$.

In the next section III, we try to apply the *Fluid Gauge Theory* to fluid flows under gravity of cosmic space. To that end, formulation of the theory must be extended to such a form appropriate to the general relativity.

III. Fluid Flow in Curved Space with Gravity (I) Isotropic Pressure Field

A new approach of Gravity-space Fluid Dynamics is taken in this section by reformulating the Fluid Gauge Theory, in order being applicable to space-fluid flows in curved space under gravity. This approach aims at capturing how the space-fluid behaves and how the dark matter effect is associated with fluid flows in the galactic space, where the space is curved by the gravity field and abundant neutral gas-clouds are moving under its influence. Neutral hydrogen gas-clouds are free to move around the cosmic space under gravity, behaving as *continuous gaseous fluids*, hence could be described as fluid flows in gravity space. The neutral clouds caught by the galactic disks are moving at hyper orbital-speeds of the order $200 \sim 300$ km$\cdot$ s^{-1}.

Its theoretical frame is formulated according to the variational principle for the Lagrangians consisting of the one for curved empty space built of geometry alone and another for a perfect fluid in the presence of gravity. In the general relativity (Einstein 1915), the Einstein field equation takes the form:

$$\overline{G} = \kappa \overline{T}, \qquad \kappa \equiv 8\pi G/c^4 \tag{30}$$

where $\overline{G}$ and $\overline{T}$ are respectively the Einstein curvature tensor and the stress-energy tensor of a perfect fluid. A constant parameter κ represents connection between the gravitational geometry and the fluid motion where G is the gravity constant and c the light speed. The equation (30) is a simplified symbolic equation. More detailed form will be given explicitly later with (44).

Regarding the stress-energy tensor $\overline{T}$, it is noted that its tensor representation is usually given, not as one derived from Lagrangian, but given either a definition of a perfect fluid, or given as a form deduced by relativistic covariant transformation from the state at rest.

In the present section III, the currently used form of stress-energy tensor $\overline{T}$ is derived from the relativistic FGT-Lagrangian $\mathcal{L}_{\rm FM}$ of a perfect fluid, defined by the equation (3). The present section derives the tensor from $\mathcal{L}_{\rm FM}$, by extending the Lagrangian given relativistically in *flat* space to that in *curved* space. However, the FGT-Lagrangian of a perfect fluid includes another two Lagrangians $\mathcal{L}_{\rm int}$ and $\mathcal{L}_{\rm GF}$ given by (4) and (5).

It must be remarked that the representation of $\overline{T}$ currently used is not sufficient to describe general rotational motions of space-fluids. This is closely associated with the *isotropic* nature of the pressure stress adopted. Those insufficient aspects of Eulerian system were already mentioned in previous section. In particular, the section II,d described its details. The *Fluid Gauge Theory* of §II was proposed to amend the *inadequacy* (insufficiency) of the system covered by the current Eulerian theory. Derivation of the contributions from the remaining two Lagrangians and extension to the general relativity are carried out in the next section IV.

An important feature of the FGT theory is that it takes into account a new component of a gauge-field a_ν which is a *non-gravitational* field. Incorporation of such a non-gravitational field to the gravity field is assured in the framework of general relativity by the *local-flatness theorem* (Schutz 1985) and the Einstein *equivalence principle* (Will 1993). In addition to the well-known gravitational Lagrangian built of metric alone yielding gravitational curved-space, this principle enables the FGT Lagrangians taken into the system. Thus, governing equations of motion are derived for space-fluids in motion under influence of gravity and gauge-field ensuring the mass conservation.

Thus, in the cosmic fluid dynamics, new terms are introduced to the equations of motion, having forms analogous to the electromagnetism but working for neutral fluids. One particular term to be mentioned takes a form analogous to the Lorentz force, $\boldsymbol{v} \times \boldsymbol{b}$, where the fluid magnetic field $\boldsymbol{b}$ is derived from the gauge field a_ν.

The FGT theory for fluid flows has an amazing similarity with the gravito-magnetic field known by the *ETL*-theory (*Einstein-Lense-Thirring*), studied by Pfister (2007, 2012), Mashhoon (2008) and Ruggiero & Tartaglia (2002), recently in particular by Ludwig (2021a,b) and Srivastava et al. (2023). Although both theories predict deviation of orbital motions from the Keplerian, the *ETL*-effect is the frame-dragging, namely a geometrical effect proportional to the small gravity constant G, while the former *FGT*-effect is a dragging by the fluid gauge field a_ν to ensure the fluid continuity condition. Comparing both, it is seen below that the gravitational *ETL*-effect is much smaller (in orders of magnitude) than the fluid-mechanical *FGT*-effect.

Thus, the *Gravity-space Fluid Dynamics* is formulated according to general relativity. In a general non-inertial system of reference with $x^\alpha = (x^0, x^1, x^2, x^3)$ a space-time point and $x^0 = ct$, the square of interval is represented in terms of the metric coefficients $g_{\alpha\beta}$ as

$$\mathrm{d}s^2 = g_{\alpha\beta}\, \mathrm{d}x^\alpha \mathrm{d}x^\beta, \tag{31}$$

a) Hilbert action principle for gravity and space fluid

Let us define the action I by

$$I=\int \mathcal{L}\,\mathrm{d}^4x=\int L\,(-g)^{1/2}\,\mathrm{d}^4x \tag{32}$$

and follow the Hilbert variation principle (Hilbert (1915), Misner et al. (2017)), where $g=\det g_{\alpha\beta}$, and $(-g)^{1/2}\,\mathrm{d}^4x$ is the proper 4-volume (*e.g.* Schutz (1985) §6.2), and $\mathcal{L}\equiv(-g)^{1/2}\,L$ the Lagrangian density.

When one deals with the empty space, the Lagrangian L is built of geometry alone (written as L_{geom}), which is represented by the Hilbert form (Hilbert 1915):

$$L_{\text{geom}}\equiv\frac{1}{2\kappa}\,\mathcal{R},\qquad \kappa\equiv 8\pi G/c^4, \tag{33}$$

where $\mathcal{R}$ is the scalar curvature defined as the trace of the Ricci tensor $\mathcal{R}=R^{\alpha}{}_{\alpha}$. [2]

When the space is not empty but filled with flows of neutral clouds, then the Lagrangian L has an additional term L_{fluid} from the clouds; thus $L=L_{\text{geom}}-L_{\text{fluid}}$, or

$$\mathcal{L}=L_{\text{geom}}\,(-g)^{1/2}-L_{\text{fluid}}\,(-g)^{1/2}, \tag{34}$$

where the term $-L_{\text{fluid}}$ is used instead of L_{fluid} because the term is moved to right-hand side of equation later. If the space fluid term $L_{\text{fluid}}(-g)^{1/2}$ is neglected, the Lagrangian $\mathcal{L}$ is given only by $\mathcal{L}_{\text{geom}}\equiv L_{\text{geom}}\,(-g)^{1/2}=(2\kappa)^{-1}\,\mathcal{R}\,\sqrt{-g}$, and its variation with respect to the metric coefficient $g^{\alpha\beta}$ results in $\delta\mathcal{L}=(2\kappa)^{-1}\,G_{\alpha\beta}\,\delta g^{\alpha\beta}$, where $G_{\alpha\beta}$ is the Einstein curvature tensor. Then the variation principle $\delta\mathcal{L}=0$ requires $G_{\alpha\beta}=0$ for arbitrary variation $\delta g^{\alpha\beta}$, which gives geometrical description of the empty space, namely a Lorentzian manifold of the vacuum solution.

To find the corresponding component from the fluid field L_{fluid}, the variation of L_{fluid} with respect to the metric coefficient $g^{\alpha\beta}$ proves to be useful for generating the stress-energy tensor $T^{(\text{fluid})}_{\alpha\beta}$ of the space-fluid. The stress-energy tensor $T^{(\text{fluid})}_{\alpha\beta}$ gives the source term on the right-hand side of the Einstein field equation (30). From the Hilbert action principle, the Einstein's geometrodynamics is given by

$$G_{\alpha\beta}=\kappa c\;T^{(\text{fluid})}_{\alpha\beta}\qquad(\kappa=8\pi G/c^4). \tag{35}$$

Its detailed representation is given by (44).

[2] $R^{\alpha}{}_{\alpha}=g^{\alpha\nu}R_{\nu\alpha}$, where $R_{\alpha\beta}$ is the Ricci curvature tensor defined by $R^{\nu}{}_{\alpha\nu\beta}$, and $R^{\nu}{}_{\alpha\mu\beta}$ is he Riemann curvature tensor.

b) Variational analysis of the gravity-space fluid

The action principle for the Lagrangian $\mathcal{L}_{\text{geom}}=L_{\text{geom}}(-g)^{1/2}$ is well-known (Landau & Lifshitz (1975), Hilbert (1915), Misner et al. (2017) and Wald (1984)). Hence, only resulting final expression is given here. Variation of $\mathcal{L}$ of (34) with respect to $g^{\alpha\beta}$ is given by :

$$\delta\left(\mathcal{L}\,\mathrm{d}^4x\right)=\frac{1}{2\kappa}\,G_{\alpha\beta}\,\delta g^{\alpha\beta}\;\;(-g)^{1/2}\,\mathrm{d}^4x$$

$$-\left[\frac{\delta L_{\text{fluid}}}{\delta g^{\alpha\beta}}-\tfrac{1}{2}\,g_{\alpha\beta}\,L_{\text{fluid}}\right]\delta g^{\alpha\beta}\;\;(-g)^{1/2}\,\mathrm{d}^4x, \tag{36}$$

(see §21.2 of Misner et al. (2017))[3] ,where $G_{\alpha\beta}$ (*Einstein curvature tensor*) and $\delta(-g)^{1/2}$ are given by

$$G_{\alpha\beta}\equiv R_{\alpha\beta}-\tfrac{1}{2}\,\delta_{\alpha\beta}\mathcal{R}, \tag{37}$$

$$\delta(-g)^{1/2}=-\tfrac{1}{2}\,(-g)^{1/2}\,g_{\alpha\beta}\,\delta g^{\alpha\beta}. \tag{38}$$

In §2, we studied the FGT theory where the Lagrangian $\mathcal{L}^{\text{FGT}}$ was introduced. According to the equation (34), the fluid part $\mathcal{L}_{\text{fluid}}\equiv L_{\text{fluid}}\,(-g)^{1/2}$ is given by $\mathcal{L}^{\text{FGT}}$,

$$\mathcal{L}_{\text{fluid}}=\mathcal{L}^{\text{FGT}}=\mathcal{L}_{\text{FM}}+\mathcal{L}_{\text{int}}+\mathcal{L}_{\text{GF}}. \tag{39}$$

where $\mathcal{L}_{\text{FM}}$, $\mathcal{L}_{\text{int}}$ and $\mathcal{L}_{\text{GF}}$ are defined in (3) $\sim$ (5).

i. *Contribution from* $\mathcal{L}_{\text{FM}}=-c\,\overline{\rho}-c^{-1}\overline{\rho\,h(\rho)}$

Let us start considering the contribution from the first term $\mathcal{L}_{\text{FM}}$ for variation analysis. Owing to the inherent nature of fluid motion, the Lagrangian $\mathcal{L}_{\text{FM}}\,\overline{\mathrm{d}^4x}$ is divided into following two terms:

$$-c\;\overline{\rho\,\mathrm{d}^4x}-c^{-1}\;\overline{\rho\,h}\;\overline{\mathrm{d}^4x}=-c\;\mathcal{M}\;\mathrm{d}\tau-c^{-1}\;\overline{\mathcal{P}}\;\overline{\mathrm{d}^4x}, \tag{40}$$

where the firs term represents the mass-property of the fluid of mass $\mathcal{M}$ and the second term representing a thermodynamic property of continuous medium characterized with an enthalpy $\mathcal{P}$ per unit volume:[4]

[3] In the section §21.2 of Misner et al. (2017), the Palatini method of variation with respect to the Christoffel connection is also carried out. However, it is shown that contribution from those variations vanishes, resulting in vanishing of the covariant derivative of the metric tensor $g_{\alpha\beta}$ in the present formulation.

[4] The second term ρ is taken into account from relativistic point of view. The post-Newtonian formulations (Blenched et al. 1990 Jaranowski et al. 2015) also take the fluid enthalpy $\mathcal{P}=\rho\epsilon+\rho$; in their formulation. In view of the present analysis to be given below, an alternative expression $\mathcal{P}=p+\rho\tilde{\varepsilon}$ would be appropriate, where the term $\tilde{\varepsilon}$ represents not only the thermal energy but a certain internal energy of kinematical origin.

$$\mathcal{P} \equiv \rho h = (\rho\epsilon + p), \tag{41}$$

and $\mathcal{M} \equiv \overline{\rho\, \mathrm{d}^3x}$ is the proper mass within the proper 3-volume $\overline{\mathrm{d}^3x}$:

$$\mathcal{M} \equiv (\rho\sqrt{1-\beta^2})\,(\mathrm{d}^3x/\sqrt{1-\beta^2}) = \rho\,\mathrm{d}^3x,$$

and $\mathrm{d}\tau \equiv \overline{\mathrm{d}x^0} = \sqrt{1-\beta^2}\,\mathrm{d}x^0$ is the proper time.

Finally, the right-hand side of (40) is rewritten as

$$\mathcal{L}_{\mathrm{FM}}\,\overline{\mathrm{d}^4x} = -c\,\mathcal{M}\,\mathrm{d}\tau - c^{-1}\,\overline{\mathcal{P}}\ \ (-g)^{1/2}\,\mathrm{d}^4x. \tag{42}$$

c) Governing equations of the combined system $\mathcal{L}^{geom-FM} \equiv \mathcal{L}_{\mathrm{geom}} - \mathcal{L}_{\mathrm{FM}}$

Let us first examine the case of combined Lagrangian $L^{geo-F} = L_{\mathrm{geom}} - L_{\mathrm{FM}}$, where L_{fluid} is replaced by the first part L_{FM} (rather than the total: $L_{\mathrm{fluid}} = L_{\mathrm{FM}} + L_{\mathrm{int}} + L_{\mathrm{GF}}$). Remaining parts will give new innovative effects which are investigated in the next §IV. The present case deduces the stress-energy tensor well-known in the current cosmological theory. Let us check it here now. From (36), the action principle requires vanishing of the following expression for arbitrary variation of $\delta g^{\alpha\beta}$:

$$\delta\left(\mathcal{L}^{geo-F}\mathrm{d}^4x\right) = \Big[\frac{1}{2\kappa}\Big(R_{\alpha\beta} - \tfrac{1}{2}\,\mathcal{R}\,\delta_{\alpha\beta}\Big)$$

$$-\Big(\frac{\delta L_{\mathrm{FM}}}{\delta g^{\alpha\beta}} - \tfrac{1}{2}\,g_{\alpha\beta}L_{\mathrm{FM}}\Big)\Big]\,\delta g^{\alpha\beta}\,(-g)^{1/2}\,\mathrm{d}^4x. \tag{43}$$

Vanishing of (43) for arbitrary $\delta g^{\alpha\beta}$ leads to

$$G_{\alpha\beta} = 2\kappa\,\Big(\tfrac{1}{2}\,g_{\alpha\beta}L_{\mathrm{FM}} - \frac{\delta L_{\mathrm{FM}}}{\delta g^{\alpha\beta}}\Big) = \kappa\,c\,T_{\alpha\beta}. \tag{44}$$

$$T_{\alpha\beta} \equiv\ \rho\,u_\alpha u_\beta + c^{-2}\,\mathcal{P}\,\Big(u_\alpha u_\beta + g_{\alpha\beta}\Big), \tag{45}$$

where $\kappa c = 8\pi G/c^3$. The left-hand side of (44) is the Einstein tensor $G_{\alpha\beta} = R_{\alpha\beta} - \frac{1}{2}\,\mathcal{R}\,\delta_{\alpha\beta}$, and the tensor $T_{\alpha\beta}$ on the right-hand side is the stress-energy tensor of the perfect fluid motion (*cf.* Misner et al. (2017), Box-5.1, §22.3).

The form of stress-energy tensor $T_{\alpha\beta}$ of (45) is given in standard texts (Misner et al. (2017); Will (1993); Schutz (1985); Wald (1984)). Each text shows $T_{\alpha\beta}$ differently though slightly. However, those have a common feature of the flow field where the pressure stress is *isotropic*. This must be reviewed carefully from physical view-point. One more feature in common is that no action principle is given for its derivation.

The *fluid gauge theory* generalizes the stress field from isotropic to *an-isotropic* stress, improving and strengthening description of flow fields of *rotational* nature or time-dependent rotational turbulent motions. The derivation is based on the action principle.

i. *Cosmological Fluid Dynamics: Equations of motion*

Stress energy tensor of a perfect fuid is given by (45):

$$T_{\alpha\beta} = Q\,u_\alpha u_\beta + c^{-2}\,\mathcal{P}\,g_{\alpha\beta}, \tag{46}$$

where $\mathcal{P} = p + \rho\epsilon$ and $Q \equiv \rho + c^{-2}\mathcal{P}$. Applying the divergence operator ∇^α to the first leg α, we obtain local conservation law of the energy-momentum:

$$\nabla^\alpha T_{\alpha\beta} = \Big[u_\alpha\nabla^\alpha Q + Q\,(\nabla^\alpha u_\alpha)\Big]\,u_\beta$$

$$+Q\,(u_\alpha\nabla^\alpha)u_\beta + c^{-2}\,\nabla_\beta\mathcal{P} = 0. \tag{47}$$

The vanishing of $\nabla^\alpha T_{\alpha\beta}$ is implied by the Bianchi identity (*e.g.* Schutz (1985) §6.6).

(a) *Parallel component* to u^β (Continuity equation) :

Let us first take the component along the 4-velocity u^β of this equation (see (Misner et al. 2017) §22.3):

$$0 = u^\beta\nabla^\alpha T_{\alpha\beta} = -u_\alpha\nabla^\alpha\rho - (\rho + c^{-2}\mathcal{P})\,(\nabla^\alpha u_\alpha). \tag{48}$$

This reduces to the equation of mass conservation (24):

$$\partial_t\rho + \nabla\cdot(\rho\boldsymbol{v}) = 0, \tag{49}$$

by noting that $u_\alpha\nabla^\alpha = u^\alpha\nabla_\alpha = \mathrm{D}_t = \partial_t + \boldsymbol{v}\cdot\nabla$, and $\nabla^\alpha u_\alpha = \nabla_\alpha u^\alpha = \nabla\cdot\boldsymbol{v}$ (see (A6) for $\rho = 1.$), and neglecting the last term $c^{-2}\mathcal{P}$ under the assumption $\beta^2 \ll 1$.

(b) *Orthogonal component* (Equation of motion):

Let us consider the three other components orthogonal to the 4-velocity u_β of $\nabla^\alpha T_{\alpha\beta}\,(=0)$. The following *Orthogonal Projection tensor* $\mathcal{Z}$ is useful:

$$\mathcal{Z} \equiv g^{\mu\beta} + u^\mu u^\beta. \tag{50}$$

In order to pluck them out of $\nabla^\alpha T_{\alpha\beta} = 0$, we take the contraction of $\mathcal{Z}$ with $\nabla^\alpha T_{\alpha\beta} = 0$:

$$0 = \mathcal{Z}\,\nabla^\alpha T_{\alpha\beta}\ =\ (\rho + c^{-2}\mathcal{P})\,(u^\alpha\nabla_\alpha)u^\mu$$

$$+c^{-2}\,\nabla^\mu\mathcal{P} + c^{-2}\,u^\mu(u^\beta\nabla_\beta)\mathcal{P}, \tag{51}$$

where the factor $(u^\alpha \nabla_\alpha) u^\mu$ on the right-hand side becomes $c^{-2} \mathrm{D}_t v^\mu$ with neglecting terms of $O(\beta^2)$. Thus vanishing of the last expression (51) reduces to

$$\rho\, \mathrm{D}_t v^\mu + \nabla^\mu \mathcal{P} = \rho\, (\partial_t + \boldsymbol{v} \cdot \nabla) v^\mu + \nabla^\mu \mathcal{P} = 0, \quad (52)$$

(*cf.* (A6)) with omitting small terms of $O(\beta^2)$. This is the Euler's equation of motion for a perfect fluid.

IV. Fluid Flow In Curved Space By Gravity (II) New Anisotropic Stress Field

In the previous section, the action principle was applied to the composite Lagrangians $\mathcal{L}_{\rm geom} - \mathcal{L}_{\rm FM}$, and the Euler's equation of motion was derived for a perfect fluid from the Bianchi identity. In addition, the Lagrangian $\mathcal{L}_{\rm FM}$ yields the stress-energy tensor $\overline{T}$ which is used currently. However, the action principle was applied to *only one* term of the Lagrangian $\mathcal{L}_{\rm FM}$, not to the total Lagrangian $\mathcal{L}^{\rm FGT}$ of (39) including two more terms: $\mathcal{L}_{\rm int}$ and $\mathcal{L}_{\rm GF}$. This section explores *new mechanism* which these two terms bring forward. Thus, new anisotropic stress field is introduced into the flow field of space-fluids.

Main concern is the stress field within the flow field. In the previous section, it is represented with the term $\mathcal{P}\, g_{\alpha\beta}$ of $T_{\alpha\beta}$ of (46). This results in the last term of (52) for the Gravito-space Fluid Dynamics. In ordinary Eulerian fluid dynamics, this term corresponds to the pressure gradient $\boldsymbol{\nabla} p$.

The FGT theory includes a new component of gauge field $a_\nu(x^\alpha)$. In addition to the gravitational Lagrangian $L_{\rm geom}$ of (33) yielding curved space, the non-gravitational Lagrangians $\mathcal{L}_{\rm int}$ and $\mathcal{L}_{\rm GF}$ are incorporated here according to the *local-flatness theorem* and *equivalence principle* (Schutz (1985); Will (1993); Misner et al. (2017)).

a) Incorporation of gauge field: Equivalence Principle

According to the *local flatness* theorem (Schutz (1985) §6.2), the relativistic equations derived in §II should be valid as well at a locally-flat Lorentz frame in curved gravity space. Equations governing the gauge field a_ν and the field strength tensor ($f^{\nu\lambda} = \partial^\nu a^\lambda - \partial^\lambda a^\nu$) are already given relativistically by (21) in §II b (*ii*) as

$$\frac{\partial}{\partial x^\lambda} f^{\nu\lambda} = \mu_{\rm F}\, j^\nu, \quad \text{equivalently} \quad f^{\nu\lambda}{}_{,\lambda} = \mu_{\rm F}\, j^\nu, \quad (53)$$

where the 4-current $j^\nu \equiv \rho\, v^\nu = (\rho c, \rho \boldsymbol{v})$ plays the source of $f^{\nu\lambda}$, and the constant $\mu_{\rm F}$ on the right-hand side is a *fluid* parameter (introduced in (5)), corresponding to the permeability in the electromagnetism.

The power of the *Equivalence Principle* allows the above equation (53) (which is valid in flat Lorentz frame) is transformed to the form in any other curved frame by the rule of *Commas replaced by Semicolons* (*i.e.* Partial derivatives replaced by Covariant derivatives). Namely we have a replaced system:

$$\widehat{\nabla}_\lambda\, f^{\nu\lambda} = \mu_{\rm F}\, j^\nu, \quad \text{equivalently} \quad f^{\nu\lambda}{}_{;\lambda} = \mu_{\rm F}\, j^\nu, \quad (54)$$

valid in curved gravity space, where the symbol $\widehat{\nabla}_\lambda$ denotes covariant derivative with respect to x^λ.[4]

b) Equation in local Lorentz frame under interaction

To find the equation of motion under interaction with the background (*dark*) gauge field a_ν, we take the composite Lagrangian $\mathcal{L}_{F-int} \equiv \mathcal{L}_{\rm FM} + \mathcal{L}_{\rm int}$ and apply the action principle. First let us take its variation:

$$\delta \mathcal{L}_{F-int} = \delta(\mathcal{L}_{\rm FM}\, \mathrm{d}\Omega) + \delta(\mathcal{L}_{\rm int}\, \mathrm{d}\Omega). \quad (55)$$

The variation $\delta(\mathcal{L}_{\rm FM}\, \mathrm{d}\Omega)$ is given straight-forwardly by

$$-c\, \mathcal{M}\, \delta(\mathrm{d}\tau) - c^{-1} \mathcal{P}\, \overline{\mathrm{d}^3 x}\, \delta(\mathrm{d}\tau) - c^{-1}\, \partial_\nu \mathcal{P}\, \delta x^\nu\, \overline{\mathrm{d}^4 x}, \quad (56)$$

from (40). Before carrying out its variation, the second term $\mathcal{L}_{\rm int}\, \mathrm{d}\Omega = c^{-1} j^\nu\, a_\nu\, \mathrm{d}\Omega$ is rewritten as

$$c^{-1} \rho\, v^\nu\, a_\nu\, \mathrm{d}^3 x\, c\, \mathrm{d}t = (\rho\, \mathrm{d}^3 x)\; a_\nu\, \mathrm{d}x^\nu$$

(with $v^\nu \mathrm{d}t = \mathrm{d}x^\nu$). Carrying out variation of this term demands an insight into deep physical significance of the gauge field a_ν. The following equivalent but twisted re-writings (or transformations) disclose its hidden power. Keeping the mass element $\mathcal{M} = \rho\, \mathrm{d}^3 x$ invariant (fixed) for the variation δ, since $\mathcal{L}_{\rm int}\; \mathrm{d}\Omega = \mathcal{M}\, a_\nu\, \mathrm{d}x^\nu$, we have

$$\delta(\, \mathcal{L}_{\rm int}\; \mathrm{d}\Omega) = \mathcal{M} \Big(a_\nu\, \mathrm{d}(\delta x^\nu) + \delta a_\nu\, \mathrm{d}x^\nu \Big)$$

$$= \mathcal{M} \Big(\mathrm{d}(a_\nu \delta x^\nu) - \mathrm{d}a_\nu \delta x^\nu + \frac{\partial a_\nu}{\partial x^\kappa} \delta x^\kappa\, \mathrm{d}x^\nu \Big) \quad (57)$$

$$= \mathcal{M} \Big(\mathrm{d}(a_\nu \delta x^\nu) - \frac{\partial a_\nu}{\partial x^\kappa} \mathrm{d}x^\kappa \delta x^\nu + \frac{\partial a_\kappa}{\partial x^\nu} \delta x^\nu \mathrm{d}x^\kappa \Big), \quad (58)$$

where the last term of (57), $(\partial a_\nu / \partial x^\kappa) \delta x^\kappa \mathrm{d}x^\nu$, was replaced with its equivalent sum $(\partial a_\kappa / \partial x^\nu) \delta x^\nu\, \mathrm{d}x^\kappa$ in the

[4] $\widehat{\nabla}_\lambda\, f^{\nu\lambda} \equiv f^{\nu\lambda}{}_{;\lambda} = f^{\nu\lambda}{}_{,\lambda} + f^{\alpha\lambda}\, \Gamma^\nu{}_{\alpha\lambda} + f^{\nu\alpha}\, \Gamma^\lambda{}_{\alpha\lambda}$

last expression (58) by interchanging ν and κ. Replacing $\mathrm{d}x^\kappa$ with equivalent $u^\kappa\,\mathrm{d}\tau$, we obtain

$$\delta(\mathcal{L}_{\rm int}\,\mathrm{d}\Omega) = \mathcal{M}\,\mathrm{d}(a_\nu\,\delta x^\nu) + \mathcal{M}\,f_{\nu\kappa}\,u^\kappa\,\delta x^\nu\,\mathrm{d}\tau, \quad (59)$$

where $f_{\kappa\nu} = \partial_\kappa a_\nu - \partial_\nu a_\kappa$.

Returning the $\delta(\mathcal{L}_{\rm FM}\,\mathrm{d}\Omega)$ of (56) again and using $\delta\mathrm{d}\tau = -u_\nu\,\mathrm{d}\delta x^\nu$ of (13), we find $\delta(\mathcal{L}_{\rm FM}\,\mathrm{d}\Omega)$ given by

$$\delta(\mathcal{L}_{\rm FM}\mathrm{d}\Omega) = -c^{-1}\mathcal{M}\left(c^2\frac{\mathrm{d}}{\overline{\mathrm{d}\tau}}u_\alpha + \frac{1}{\rho}\partial_\alpha\mathcal{P}\right)\delta x^\alpha\,\overline{\mathrm{d}\tau}. \quad (60)$$

neglecting higher order terms of $O(\beta^2)$ (see Kambe (2021a) Appendix B.2 for this derivation). Since $u_k = v_k/c$ $(k = 1,2,3)$ and $\overline{\mathrm{d}\tau} = c\,\mathrm{d}t$, the first term $c^2\,(\mathrm{d}/\overline{\mathrm{d}\tau})u_\alpha$ in the parenthesis becomes $(\mathrm{D}/\mathrm{D}t)v_\alpha$.

Finally we find the expression for $\delta\mathcal{L}_{F-int} = \delta(\mathcal{L}_{\rm FM}\,\mathrm{d}\Omega) + \delta(\mathcal{L}_{\rm int}\,\mathrm{d}\Omega)$ given by

$$-\,c^{-1}\,\mathcal{M}\left(c^2\frac{\mathrm{d}}{\overline{\mathrm{d}\tau}}u_\alpha + \frac{1}{\rho}\partial_\alpha\mathcal{P} - c\,f_{\alpha\beta}\,u^\beta\right)\delta x^\alpha\,\overline{\mathrm{d}\tau}. \quad (61)$$

This is required to vanish for arbitrary δx^α. Thus, the action principle leads to

$$c^2\frac{\mathrm{d}}{\overline{\mathrm{d}\tau}}u_\alpha + \frac{1}{\rho}\partial_\alpha\mathcal{P} - c\,f_{\alpha\beta}\,u^\beta = 0. \quad (62)$$

Equivalence Principle allows this equation transformed to the form in curved frame by replacing $\mathrm{d}/\overline{\mathrm{d}\tau}$ with the covariant derivative $\widehat{\nabla}$ with respect to x^0:

$$c^2\,\widehat{\nabla}_0\,u_\alpha + \frac{1}{\rho}\partial_\alpha\mathcal{P} - c\,f_{\alpha\beta}\,u^\beta = 0. \quad (63)$$

omitting higher order terms with respect to small β. In locally flat Lorentz frame of metric $\eta_{\alpha\beta}$ with $v_\alpha = c\,u_\alpha$ (with same approximation), this is rewritten as

$$\rho\,\widehat{\nabla}_t\,v_\alpha = -\partial^\beta(\mathcal{P}\,\eta_{\alpha\beta}) + f_{\alpha\beta}\,j^\beta, \quad j^\beta = \rho\,v^\beta. \quad (64)$$

The first term on the right-hand side describes a force from isotropic stress $\mathcal{P}\,\eta_{\alpha\beta}$ $(\alpha,\beta = 1,2,3)$.

c) New anisotropic stress in local Lorentz frame

The action of the background (dark) gauge field a_ν generates the new term $f_{\alpha\nu}\,j^\nu$ of (64) deduced from the interaction Lagrangina $\mathcal{L}_{\rm int}$. Remarkably, the term $f_{\alpha\nu}\,j^\nu$ can be represented with another equivalent form $-\,\partial^\beta M_{\alpha\beta}$ denoting an-isotropic stress field acting on the fluid field (analogous to the Maxwell stress of electromagnetism). This is shown by using the 4-current j^ν of (53) and the one below it. Substituting $j^\nu = \mu_{\rm F}^{-1}\,\partial_\lambda f^{\nu\lambda}$ from (53), the second term $f_{\alpha\nu}\,j^\nu$ of (64) becomes

$$f_{\alpha\nu}\,j^\nu = \mu_{\rm F}^{-1}\,f_{\alpha\nu}\,\partial_\lambda f^{\nu\lambda} = -\,\partial^\beta M_{\alpha\beta}. \quad (65)$$

where the fluid Maxwell stress $M_{\alpha\beta}$ is defined (for $i,\,k = 1,2,3$) by $M_{00} = \frac{1}{2}\,\epsilon\,|\boldsymbol{e}|^2 + \frac{1}{2}\,\mu_{\rm F}^{-1}\,|\boldsymbol{b}|^2 \equiv w_{\rm e}$, $M_{0k} = M_{0k} = -c\epsilon\,(\boldsymbol{e}\times\boldsymbol{b})_k$, and $M_{ik} = -\epsilon\,e_ie_k - \mu_{\rm F}^{-1}\,b_ib_k + w_{\rm e}\,\delta_{ik}$, with $\mu_{\rm F}$ and $\epsilon = 1/(\mu_{\rm F}\,c^2)$ being parameters of the fow field. One can show the following equality:

$$-\,\partial^\beta M_{k\beta} = (\rho\boldsymbol{e} + \rho\boldsymbol{v}\times\boldsymbol{b})_k\,, \quad (66)$$

which can be shown by using (22) and (23), where $\partial_\lambda = (c^{-1}\partial_t, \partial_k)$ and $\partial^\beta = \eta^{\beta\lambda}\partial_\lambda = (-c^{-1}\partial_t, \partial_k)$,

Using the relation $f_{\alpha\nu}\,j^\nu = -\partial^\beta M_{\alpha\beta}$ of (65) and substituting $-\partial^\beta M_{\alpha\beta}$ into the last term of (64), we obtain

$$\rho\,\widehat{\nabla}_t\,v_\alpha = -\partial^\beta(\mathcal{P}\,\eta_{\alpha\beta}) - \partial^\beta M_{\alpha\beta}, \quad (67)$$

Thus, an aimed equation has been derived in local Lorentz frame with incorporating the an-isotropic stress.

The last (67) implies that the factor $\mathcal{P}\,g_{\alpha\beta}$ in the second term of stress energy tensor (46) is replaced as

$$\mathcal{P}\,g_{\alpha\beta} \;\Rightarrow\; \mathcal{P}\,g_{\alpha\beta} + M_{\alpha\beta}. \quad (68)$$

V. Application to the Dark Matter Effect of Rotating Galaxies

Now let us think how our formulation of the *Gravity-space Fluid Dynamics* can be applied to the *dark matter* effect of rotating spiral galaxies. Concerning the rotating galaxies, we have currently two kinds of cosmological-views, which are now reviewed first.

From observations of celestial objects within a spiral galaxy in rotation, observed data enable to plot their orbital velocities *versus* their distances from the galactic center. The gravitational potential deduced from visible mass distribution of stars and gases within the galaxy, however, is not sufficient to reproduce the observed velocity curve of orbital motion. On the other hand, paradoxically enough, the recent study (McGaugh et al. 2016) proposed a unified law (from statistical analyses of about 200 galaxies) that the rotational motion of a disk galaxy is determined entirely by the visible matter it contains, even if the disk is filled with unknown dark matters. Another study by Sofue (2018) also presented observed data from about 500 galaxies, equivalent to those of McGaugh et al. (2016). These imply a strong connection between the visible baryonic matters and the physics producing the rotational motion.

Present study is taking double-sided approach both dynamically and physically by incorporating a new dynamical field of gauge-field, and attacking the system with a new physics incorporating anisotropic stress fields. This approach is based on the general-relativistic version of the fluid gauge theory extended to the gravitational space, i.e. Gravity-space Fluid Dynamics

a) *Brief description of analysis with the dark field* $\boldsymbol{a}$

Aiming at a simplified analysis, let us take a cylindrical coordinate frame (Z, R, ϕ) and consider a typical galaxy rotating axi-symmetrically. Suppose that a particular disk galaxy is rotating around the Z-axis with its center at $(R, Z) = (0, 0)$ in steady rotation $(\partial_t = 0)$, and assume that it keeps an axisymmetric disk-like form, as often done in observations for analyzing galaxy data. The disk is given by the plane $Z = 0$ and described with the coordinates (R, ϕ). In this circumstance, it is assumed that $\boldsymbol{v} = (0, 0, V(R))$ and $\boldsymbol{a} = (0, 0, A(R))$.

From observed rotation velocity $V(R)$ of a stellar object at the distance R from the galactic center, its centripetal acceleration A_c is given by $A_c = -V^2/R$ (radial acceleration toward the center). The gravitational potential Φ_g can be estimated by the Poisson equation, $\nabla^2\Phi_g = 4\pi G\rho(Z, R)$ once the mass density distribution $\rho(Z, R)$ is given from observation of stars and gas in the galaxy space (G: gravity constant). Using the potential Φ_g found with integration, the gravitational acceleration A_g is given by $A_g = -\partial\Phi_g/\partial R$.

The study of McGaugh et al. (2016) succeeded, from statistics, to extract the fitting curve (1) connecting average values of $|A_c|$ and $|A_g|$. On account of the property $A_c \neq A_g$, the third term $A_{\rm DM}$ is defined by

$$A_c - A_g = A_{\rm DM}, \qquad (69)$$

which is negative. Regarding the average absolute value $|A_{\rm DM}|$, this shows that $|A_{\rm DM}|$ is given in a statistical sense by a monotonic function of $|A_g|$ with using (1). This implies a strong connection between the gravitational acceleration A_g (from visible *baryonic* mass) and the physics generating the observed A_c and the term $A_{\rm DM}$. But, how the term A_{DM} is determined ?

b) *How* A_{DM} *is determined*

Following the scenario of general relativity, the equation of *Gravity-space Fluid Dynamics* (67) has been derived as a weak field form of small $|\boldsymbol{v}|/c$ in the previous section §IV. The second term $-\partial^\beta M_{\alpha\beta}$ on the right-hand side came from the anisotropic stress $M_{\alpha\beta}$. Using (66), it is replaced by the equivalent form of *fluid* Lorentz force. Thus the equation (67) can be written as

$$\rho\,\widehat{\nabla}_t\, v_k = -\partial_k\mathcal{P} + \rho\boldsymbol{e}_k + \rho(\boldsymbol{v}\times\boldsymbol{b})_k\,, \qquad (70)$$

$$\hat{\nabla}_t\boldsymbol{v} \equiv {\rm D}_t\boldsymbol{v} + \nabla\Phi_g, \qquad (71)$$

with α replaced with $k = 1, 2, 3$, where $\hat{\nabla}_t\boldsymbol{v}$ denotes the covariant derivative of the fluid velocity $\boldsymbol{v}$ with respect to time t in the curved space of gravity field Φ_g, and ${\rm D}_t = \partial_t + \boldsymbol{v}\cdot\nabla$ is the material derivative and $\nabla = (\partial_i)$ and $i = 1, 2, 3$. From (9), we have

$$\boldsymbol{e} = -\partial_t\boldsymbol{a} - \nabla\phi_a = -\nabla\phi_a, \qquad (72)$$

since steady rotation $(\partial_t = 0)$ is assumed. The term $\partial_k\mathcal{P}$ on the right-hand side of (70) is expressed as $\rho\,\partial_k h$ in the dissipation-free motion.[5] Substituting the relation $\partial_k\mathcal{P} = \rho\,\partial_k h$ on the right-hand side of (70), it is seen that the density ρ is multiplied to all the terms of (70) and hence can be eliminated from all the terms.

Thus, using (71), the equation (70) reduces to

$${\rm D}_t\boldsymbol{v} + \nabla\hat{\Phi}_g = \boldsymbol{v}\times\boldsymbol{b}, \qquad (73)$$

where $\hat{\Phi}_g \equiv \Phi_g + h + \phi_a$, with the terms ∇h and $\nabla\phi_a$ absorbed to the gravity term $\nabla\Phi_g$ on the left-hand side as negligibly small terms. The fluid-magnetic field $\boldsymbol{b}$ is derived from the *dark* gauge-field $\boldsymbol{a}$ by $\boldsymbol{b} = \nabla\times\boldsymbol{a}$.

The radial component of ${\rm D}_t\boldsymbol{v}$ of (73) is given by $-V^2/R$, assuming steady, $\partial_t = 0$. Then, the radial component of the axisymmetric steady equation of motion (73) can be written on the galactic plane $(Z = 0)$ as

$$-V^2/R + \partial_R\Phi_g = (\boldsymbol{v}\times\boldsymbol{b})_R, \qquad (74)$$

where $\hat{\Phi}_g$ is replace by the main term Φ_g, and

$$\nabla^2\Phi_g = 4\pi G\rho(Z, R), \qquad (75)$$

$$\boldsymbol{b} = \nabla\times\boldsymbol{a}, \qquad \nabla\times\boldsymbol{b} = \mu_{\rm F}\,\rho\,\boldsymbol{v}, \qquad (76)$$

$$(\boldsymbol{v}\times\boldsymbol{b})_R = V\,b_Z = V\,R^{-1}\partial_R(RA). \qquad (77)$$

[5] $\mathcal{P} \equiv \rho h = (\rho\epsilon + p)$ is the *enthalpy* per unit volume defined by (41), where ϵ and $h = \epsilon + p/\rho$ are thermodynamic variables termed the *internal energy* and *enthalpy* per unit mass. In the dissipation-free motion keeping the mass element $\mathcal{M} = \rho\,{\rm d}^3x$ fixed, the entropy s is unchanged, and the variation of ϵ is given by ${\rm d}\epsilon = -p\,{\rm d}\rho^{-1}$. Then, the h-variation is ${\rm d}h = {\rm d}(\epsilon + p/\rho) = \rho^{-1}\,{\rm d}p$. Then, ${\rm d}(\mathcal{P}\,{\rm d}^3x) = \mathcal{M}{\rm d}h$ reduces to ${\rm d}\mathcal{P} = \rho\,{\rm d}h$ per unit volume.

Comparing the two equations (69) and (74), it is seen that both of the right-hand sides should be equated (since $A_c = -V^2/R$ and $A_g = -\partial_R \Phi_g$). Hence, the term A_{DM} is given by $(\boldsymbol{v} \times \boldsymbol{b})_R$ derived from the field $\boldsymbol{a}$.

From the present theory of Gravity-space Fluid Dynamics, the three terms A_c, A_g and $A_{\rm DM}$ of acceleration are estimated at each position R once the observed value of velocity $V(R)$ is given at R. Those values can be plotted in the diagram $[A_c\, vs\, .\, A_g]$ and compressed with the curve (1) given by McGaugh et al. (2016).

One of the advantages of the analysis using the fitting curve is that the radial accelerations, A_c, A_g and A_{DM}, are concerned exclusively and used. Estimate of radial acceleration can be applied to any celestial object in motion without regard to the magnitude of mass, either a star, a gas cloud, or a fluid particle of space-fluid.

In addition, the simplified analysis in the present §V assumes an axisymmetric disk galaxy in rotation with nearly axisymmetric spherical halo surrounding the disk. Hence the orbiting stellar objects consisting of stars, gas clouds and space-fuids are averaged along their circular orbits. The individual motions are averaged and smoothed out to form a circular continuous current flux $J(Z, R) = \rho V$ along the azimuthal direction ϕ.

Thus, we can estimate the three acceleration terms A_c, A_g and A_{DM} from the theory, and compare the values obtained by computation with corresponding data acquired from observations. Agreement of both sets of values was quite excellent.

To show an example, the sample galaxy *NGC3198* (Fig.1) was examined here too, and the three terms A_c, A_g and A_{DM} were estimated at the particular value of radial position $R_* = 19\,\text{kpc}$ where the test calculations were done in §I f). Using the observed velocity $V(R_*) \approx 150\text{km}\cdot\text{s}^{-1}$ as an input initial condition, A_c is given by $V^2/R \approx 4.0 \times 10^{-11}\,\text{m}\,\text{s}^{-2}$. Results of computation were as follows: $A_{DM} \approx 3.0 \times 10^{-11}\,\text{m}\,\text{s}^{-2}$ and $A_g \approx 1.0 \times 10^{-11}\,\text{m}\,\text{s}^{-2}$. These are consistent with those of §I f). Theoretical estimations were carried out at other radial positions. In addition, other several sample galaxies were examined as far as observation data are available. Agreement with the fitting curve (1) was in fact remarkable. Details of the agreement will be reported elsewhere.[6] Getting the agreement, it is essential that the parameter $\mu_{\rm F}$ takes a non-zero value, which is much smaller by $O(10^{-4})$ compared to the vacuum value of the magnetic permeability.

[6] " *Preprint KH-2023*": shown at " *Tsutomu Kambe Researchgate*". Submitted to GJSFR (2023): Kambe and Hashiguchi, "Dark matter effect, and physical mechanism producing orbital hyper-speed in gas-dominated galaxies, studied relativistically .

c) Outcomes of the analysis Innovative

Present theory provides useful numerical data which can be compared with corresponding data of observation of galaxies. Excellent *quantitative* agreement has been found between them. From the comparison, one can extract new findings, which are really innovative.

Firstly, the present approach according to the Gravity-space Fluid Dynamics captures an essential feature of the *dark matter* effect for galaxies with spiral arms. It is most important to recognize that the explicit mathematical expression (74) is just another expression of the equation (69), and in addition, the computations according to (75) $\sim$ (77) generate results consistent with the data of observation. The theory gives the term A_{DM} an explicit expression $(\boldsymbol{v} \times \boldsymbol{b})_R$. Present analysis implies that the approach according to the Gravity-space Fluid Dynamics can capture an essential feature of the *dark matter* effect observed from a number of spiral galaxies.

From a mathematical view-point, an advantage of the present formulation is that the *acceleration* $A_{\rm DM}$ is given a mathematical expression $(\boldsymbol{v} \times \boldsymbol{b})_R$. However, the term $\boldsymbol{b} = \nabla \times \boldsymbol{a}$ depends on the FGT gauge field $\boldsymbol{a}$. By the equation (76). the field $\boldsymbol{a}$ is determined from the equation $\nabla \times (\nabla \times \boldsymbol{a}) = \mu_{\rm F}\, \rho \boldsymbol{v}$, stating that the field $\boldsymbol{a}$ is generated (excited) by the current flux $\rho\, \boldsymbol{v}$. Its degree of excitation is controlled by the parameter $\mu_{\rm F}$ (a fluid permeability).

Secondly, from the FGT theory, the field $\boldsymbol{a}$ is introduced to ensure the mass conservation and simultaneously drive the flow field with general anisotropic stress field, (Kambe, 2020, §5)which is a generalization of the isotropic pressure of Eulerian theory. As mentioned above, the field $\boldsymbol{a}$ depends on the fluid parameter $\mu_{\rm F}$ (a fuid version of the magnetic permeability). Note that in the current (traditional) theory, the system does not include the field $\boldsymbol{a}$. Hence, the parameter $\mu_{\rm F}$ is regarded as zero and there is no driving mechanism to generate the field $\boldsymbol{a}$ in the current theory. Then no agreement is found.

However, the Gravity-space Fluid Dynamics is a newly developed theory, an extended version of the Fluid Gauge Theory (Kambe 2021a) to the general relativity. It is natural that the theory with non-zero value of $\mu_{\rm F}$ gives rise to such a new field, enabling agreement between theory and observation. If it were zero, the agreement would not be obtained.

Present agreement between astronomical observation and theoretical analysis is really notable. In fact, the observational data were found from a number of galaxies, extracted from a set of about two hundreds (McGaugh et al. 2016) and about five hundreds (Sofue 2018).

The agreement tells that a new physics is working by the action of the background gauge field $\boldsymbol{a}$ which is excited by the high-speed current field $\rho \boldsymbol{v}$ of the space fluid. Typical velocities $|\boldsymbol{v}|$ of order $10^2\ km/sec$ are observed at most halos of galaxies. This is in fact the first case where the non-zero value of $\mu_{\rm F}$ is estimated from natural phenomena.

VI. Summary

This is a novel approach to the cosmological issue of the *dark matter* efect observed in spiral galaxies. In cosmic space, it is essential to recognize firstly that gas clouds are abundant and free to move in the galactic and inter-galactic spaces. Motion of a space-cloud is to be viewed as flow of a continuous fluid in gravity space. Second point concerning the cosmic clouds is that the clouds are moving at very high speed over huge spatial scales. Their orbital speed is estimated to be of the order $200 \sim 300$ km$\cdot$ s^{-1} at about 10 kpc from the galactic center, and gas clouds are distributing widely over outer halo parts of galaxies (Tully & Fisher (1977), Sofue & Rubin (2001), McGaugh et al. (2016)).

Dynamical action of such space-fluids must be a new type. Motion and dynamics of such an exotic fluid is investigated by extending *Fluid Dynamics* to that in the frame of *General Relativity*. The fluid flow field to be extended to curved space is reinforced by the *fluid gauge theory* equipped with a background (*dark*) gauge field $\boldsymbol{a}$. The gauge field $\boldsymbol{a}$ firstly ensures the mass conservation of fluid flows. Hence the space fluids carry out their motion as physically acceptable ways. Not only that, the field $\boldsymbol{a}$ assists the flow field with transition of its stress field from the isotropic pressure stress $p\delta_{jk}$ prevailing in quiet states of slow motion to an-isotropic stress field M_{jk} prevailing in high-speed flow states, moving often turbulently.

In order to capture realistic behaviors of such space fluids and their dynamics, adequate equations of motion must be prepared. An atmosphere of gas clouds exists over a galactic disk captured by its gravity. The *Gravity-space Fluid Dynamics* thus developed captures main feature of the dark-matter effect as the action of the gauge field $\boldsymbol{a}$ on the space fluids. Namely, the dark-matter effect is caused dynamically by the background gauge field $\boldsymbol{a}$ acting on the space fluid, not by adding new invisible (dark) matters to increase gravitation.

From the observation side, McGaugh-Lelli-Schombert (2016) found a strong evidence from a number of galaxies that observed data shows existence of a functional correlation between the observed radial acceleration and that predicted by the observed baryon distribution within galaxies, implying that the dark matter contribution is specified by that of the baryons.

Present theory gives an explicit expression $(\boldsymbol{v} \times \boldsymbol{b})_R$ to the acceleration attributed to the dark-matter effect from (74), which is associated with the gauge field $\boldsymbol{a}$ since $\boldsymbol{b} = \nabla \times \boldsymbol{a}$. The gauge field $\boldsymbol{a}$ is determined by the equation, $\nabla \times \boldsymbol{b} = \mu_{\rm F}\, \rho\, \boldsymbol{v}$ from (76), describing that $\boldsymbol{a}$ is excited by the current flux $\rho\, \boldsymbol{v}$ and the degree of excitation controlled by the field parameter $\mu_{\rm F}$. As noted in § V, comparison between astronomical data and the data from the theory implies that the parameter $\mu_{\rm F}$ of the fluid gauge theory must take a non-zero value, owing to which the high magnitude of $|\boldsymbol{v}|$ is reflected significantly to the gauge field $\boldsymbol{a}$.

Comparison between astronomical data and data deduced from the theory shows excellent agreement. It is considered that the present theory describes dynamics of the galactic (*dark*) halo space where there exists sufficient space clouds for the gauge field $\boldsymbol{a}$ to be able act on the space fluids. Thus the galactic inner space is connected continuously to the deep-outer space of NFW dark halo or CDM models, from physical point of view, by the help of the background gauge field $\boldsymbol{a}$ without presence of dark matters.

Acknowledgement: The author would like to express thanks to Prof. Emeritus Yoshiaki Sofue (University of Tokyo) for discussions on galaxies and rotation curves. Thanks are also due to the friend of mine, Masanori Hashiguchi (Guest Scholar, Meiji Institute for Advanced Study of Mathematical Sciences, Meiji University, Tokyo, Japan) for a number of communications on the subject matter of this study. Formatting of the present text is helped by the *Overleaf* for its creation.

Append

A. *Stresses, and Linked 4d-Spacetime*

i. *Stress fields: isotropic and an-isotropic*

Equation of motion of a perfect fluid is written in the style of FGT theory:

$$\rho\, {\rm D}_t v_k = \partial^j \sigma^{\rm I}_{jk}, \quad \sigma^{\rm I}_{jk} = -p\, \delta_{jk}, \quad (j,k = 1,2,3), \qquad \text{(A1)}$$

where ρ is the fluid mass-density, p the pressure field, v_k the k-th component of fluid velocity. ${\rm D}_t \equiv \partial_t + \boldsymbol{v} \cdot \nabla$ is the material derivative, and $\sigma_{jk}(\boldsymbol{x})$ is the stress field at a 3-space point $\boldsymbol{x}$, and $\sigma^{\rm I}_{jk} = -p\, \delta_{jk}$ represents the *isotropic* pressure stress. The *FGT* theory (§II) is formulated according to the *special relativity* of Lorentzian metric $\eta_{\mu\nu} = \eta^{\mu\nu} = {\rm diag}(-1,1,1,1)$ for $\mu, \nu = 0,1,2,3$. The theory aims to combine two types of stress fields: *isotropic* stress $\sigma^{\rm I}_{jk}(x^\nu)$ and *an-isotropic* stress $\sigma^{\rm A}_{jk}(x^\nu)$.

ii. *Glimpse of linked 4d-spacetime, in fluid mechanics*

Physical fields of the FGT theory are described by two sets of 4-vector fields: (*i*) *Fluid current 4-vector* $j^\nu = \rho\, v^\nu$, and (*ii*) *background gauge-field 4-vector* a_ν (precisely one-form a_ν, $\nu = 0,1,2,3$), where

$$j^{\nu} = (\rho c, \rho \boldsymbol{v}) = \rho\, v^{\nu} = c\overline{\rho} u^{\nu}, \quad v^{\nu} = (c, \boldsymbol{v}) = \frac{\mathrm{d}x^{\nu}}{\mathrm{d}t}, \quad \text{(A2)}$$

where $x^{\nu} = (x^0, x^1, x^2, x^3)$ is a space-time point with $x^0 = c\,t$ (t the time and c the light velocity). The over-lined value $\overline{\rho}$ denotes the proper density (*i.e.* the fluid mass density $\overline{\rho} = \rho\sqrt{1-\beta^2}$ in the instantaneously rest-frame where $\beta = 0$, with $\beta \equiv |\boldsymbol{v}|/c$).

The proper time τ, which is defined by

$$\mathrm{d}\tau^2 = -\mathrm{d}s^2 = -\eta_{\nu\mu}\mathrm{d}x^{\mu}\mathrm{d}x^{\nu}, \qquad \text{(A3)}$$

would play an important role in the variation analyses of §4. Here, using the displacement $\mathrm{d}x^{\nu}$ of a fluid particle, its relativistic 4-velocity is defined by $u^{\nu} = \mathrm{d}x^{\nu}/\mathrm{d}\tau$:

$$u^{\nu} = \frac{\mathrm{d}x^{\nu}}{\mathrm{d}\tau} = \Big(\frac{1}{\sqrt{1-\beta^2}},\ \frac{\boldsymbol{v}}{c\sqrt{1-\beta^2}}\Big), \qquad \text{(A4)}$$

$$\mathrm{d}\tau \equiv \sqrt{1-\beta^2}\,\mathrm{d}x^0 = \sqrt{1-\beta^2}\;c\,\mathrm{d}t. \qquad \text{(A5)}$$

Concerning the structure of *Fluid-Mechanics*, the following observation would be instructive. Namely *there exist glimpses of linked structure of* $4d$*-space-time*, which are $\partial_{\nu} j^{\nu}$ and $j^{\nu}\partial_{\nu}$, represented with $4d$ inner products:

$$\partial_{\nu} j^{\nu} = \partial_t \rho + \nabla\cdot(\rho \boldsymbol{v}); \;\; j^{\nu}\partial_{\nu} = \rho\,(\partial_t + \boldsymbol{v}\cdot\nabla) \equiv \rho\,\mathrm{D}_t, \quad \text{(A6)}$$

where $\partial_{\nu} = (c^{-1}\partial_t, \boldsymbol{\nabla})$. The first is the expression of the *continuity equation*, and the second defines the *material derivative* D_t.

References Références Referencias

1. Blanchet, L., Damour, T. & Schϒafer, G. 1990, MNRAS, 242, 289.
2. Einstein, A. 1915, *Preuss. Akad. Wiss. Berlin, Sitzber.* 778.
3. Hilbert, D. 1915, *Nach. Gesel. Wiss. Gottingen, Math.-Phys.* 1915, 395.
4. Jaranowski, P., Mach, P., Malec E. & Pirog, M. 2015, PhRvD, 91, 024039.
5. Kalberla, P.M.W. & Kerp, J. 2009, ARA&A, 47, 27
6. Kambe, T. 2021a, GJSFR., A, 21 (4), 113.
7. Kambe, T. 2021b, GJSFR., A, 21 (4), 1.
8. Kambe, T. 2022, GJSFR. A, 22 (6), 61.
9. Kundt, A., 1866, *Ann. Phys. & Chem,* 127, 497
10. Landau, L.D. & Lifshitz, E.M. 1975, *The Classical Theory of Fields* (Pergamon).
11. Ludwig, G.D. 2021a, *Euro. Phys*. J. C. 81, 186.
12. Ludwig, G.D. 2021b, *Euro. Phys*. J. Plus, 136 (4).
13. Mashhoon, B. 2008, arXiv:gr-qc/0311030 (gr-qc)
14. McGaugh, S.S. 2005, PhRvL, 95, 171302
15. McGaugh, S.S., Lelli, F. & Schombert, J. 2016 PhRvL, 117, 201101; arXiv: 1609.05917v1 [astroph. GA],
16. Misner, C.W., Thorne, K.S. & Wheeler, J.A. 2017, *Gravitation* (Princeton UP).
17. Pfister, H. 2007, Gen. Rel. Grav,, 39, 1735
18. Pfister, H. 2012, Gen. Rel. Grav,, 44:3217?3224
19. Ruggiero, M. L. & Tartaglia, A. 2002, Nuovo Cimento B, 117, 743.
20. Schutz, B.F. 1985, *A first course in general relativity,* Cambr. UP.
21. Sofue, Y. & Rubin, V. 2001, a, 39, 137.
22. Sofue, Y. 2018, PASJ, 70, 31.
23. Srivastava, Y., Immirzi,G., Swain,J., Panella, O. & Pacetti, S. 2023, *Eur. Phys. J. C,* 83:100.
24. Tully, R.B. & Fisher, J.R. 1977, A&A, 54, 661.
25. Utiyama, R. 1956, PhRvD, 101, 1597
26. Venkataramani, S.C. & Newell, A.C. 2021, *Euro. Phys. J.* S.T., 230, 2139.
27. Wald, R.M. 1984, *General Relativity,* Chicago UP.
28. Will, C.M. 1993, *Theory and experiment in gravitational physics,* CUP.
29. Kambe, T. 2020. Fluid Dyn. Res. 52, 1.

This page is intentionally left blank

Global Journal of Science Frontier Research: A
Physics and Space Science
Volume 23 Issue 8 Version 1.0 Year 2023
Type: Double Blind Peer Reviewed Interenational Research Journal
Publisher: Global Journals
Online ISSN: 2249-4626 & Print ISSN: 0975-5896

Dose Variation Profiles of Small Fields with A 10 MV Photon Beam

By Caio Fernando Teixeira Portela & Arnaldo Prata Mourão

Abstract- Radiotherapy is an important treatment form to care of patients with different types of cancer and improvement quality of life. Radiotherapy is a treatment of carcinogenic tumors using ionising radiation and the refinement of techniques in radiotherapy treatments are programmed to salvage of healthy tissues. The small dimensions in modern advanced radiotherapy treatments have employed in differents hospitals. These fields have differents characteristics for non-establishment in the conditions to traditional dosimetry protocols. The obtained profiles permissible to check out disturbances in the exposures, considering the differences in the dosimetry of small fields and the impacts to local dose deposition. In this work, the dose distribution of an X-ray beam was recorded using a solid water phantom. This phantom was irradiated using small fields with 1x1, 2x2, 3x3 and 5x5 cm^2. The 10 MV X-ray beam was generated in a linear accelerator model Synergy Platform from the manufacturer Elekta and radiochromic film sheets were used to record dose profiles inside a solid water phantom.

Keywords: dose profile, radiotherapy, small fields, solid water phantom.

GJSFR-A Classification: LCC: RC271-272

DOSE VARIATION PROFILES OF SMALL FIELDS WITH A 10 MV PHOTON BEAM

Strictly as per the compliance and regulations of:

Open Association of Research Society, USA

Research | Diversity | Ethics

Dose Variation Profiles of Small Fields with A 10 MV Photon Beam

Caio Fernando Teixeira Portela [α] & Arnaldo Prata Mourão [σ]

Abstract- Radiotherapy is an important treatment form to care of patients with different types of cancer and improvement quality of life. Radiotherapy is a treatment of carcinogenic tumors using ionising radiation and the refinement of techniques in radiotherapy treatments are programmed to salvage of healthy tissues. The small dimensions in modern advanced radiotherapy treatments have employed in differents hospitals. These fields have differents characteristics for non-establishment in the conditions to traditional dosimetry protocols. The obtained profiles permissible to check out disturbances in the exposures, considering the differences in the dosimetry of small fields and the impacts to local dose deposition. In this work, the dose distribution of an X-ray beam was recorded using a solid water phantom. This phantom was irradiated using small fields with 1x1, 2x2, 3x3 and 5x5 cm². The 10 MV X-ray beam was generated in a linear accelerator model Synergy Platform from the manufacturer Elekta and radiochromic film sheets were used to record dose profiles inside a solid water phantom. The solid water phantom loaded with radiochromic film was positioned 1 m away from the X-ray beam's focus. The longitudinal profile of absorbed dose obtained presented the maximum dose value at 2.24 cm of depth for both fields, inside the phantom. Smaller field size generated a maximum absorbed dose smaller. The axial dose profiles were recorded at 1 cm depth, and presented a plateau in the axis Y for the four fields. For axial irradiation on the X-axis, the central region is 99.27% in relation to 100% of the relative dose and on the Y-axis, the central region is 99.39% in relation to 100% of the relative dose.

Keywords: dose profile, radiotherapy, small fields, solid water phantom.

I. Introduction

The evolution of the radiotherapy techniques and protocols available for the treatment of cancer have introduced new theoretical and practical standards to ensure the quality and reliability of these techniques. This scope uses techniques that use small X-ray fields or even dynamic fields to achieve their goals and confer advantages over predecessors. SRS is a technique proposed by Lars Leksell based on static X ray fields obtained through the orthovoltage unit. IMRT is a technique that uses tomographic images during the physical planning of cancer patient treatment. This type of treatment modulates the number of photons that cross a given area, modifying the beam's intensity conforming the dose to the target volume that aims to maximize the radioprotection of surrounding tissues [1; 2; 3].

Small fields are being applied in radiotherapy, include IMRT, VMAT, SRS, SRT and SBRT. The small fields are produced by the implementation of collimation tools through Cones and Multileaf Collimators (MLC) or by devices dedicated to this purpose, such as Cyberknifes and Gamma Knives. The influencing factors include finite source size, steep dose gradients, charged particle disequilibrium, detector size and associated volume averaging effects, and changes in energy spectrum and associated dosimetric pa rameters [4; 5; 6; 7].

Conventionally, external-beam machines like linear accel erators with jaws or MLCs are able to produces fields of typical dimensions smaller than 4×4 cm² when being used to deliver therapeutic dose to cancer patients. A small field is understood like a field created by downstream collimation of a flattened or unflatten photon beam and differ from conventional fields in their lateral dimensions, causing penumbra areas on both sides of the field to overlap and make most commonly used detectors large in relation to the size of the radiation field. The technological development in radio therapy, the use of increasingly smaller and/or modulated small fields generated an increase in the uncertainty of the acquisition of dosimetric data. In the literature, incidents caused by errors in the acquisition of these data from the treatment machine related to small fields have been reported [8; 9; 10; 11].

In this work, the dose distribution of an X-ray beam was recorded using a solid water phantom. This phantom was irradiated using small fields with 1x1, 2x2, 3x3 and 5x5 cm². The 10 MV X-ray beam was generated in a linear accelerator model Synergy Platform from the manufacturer Elekta, and radiochromic film sheets were used to record dose profiles inside a solid water phantom. The solid water phantom loaded with radiochromic film was positioned 1 m away from the X-ray beam's focus.

a) *Small Fields in Radiotherapy*

A small field is a field having dimension smaller than the lateral range of the dose-depositing charged particles set into motion post interaction with the incident beam. With the reduction of the field, through

Author: Programa de Pós-graduação em Ciências e Técnicas Nucleares, Departamento de Engenharia Nuclear - Universidade Federal de Minas Gerais - UFMG, Av. Pres. Antônio Carlos 6627, Pampulha, Belo Horizonte, 31270-901, MG, Brazil.
e-mail: caiofernando_fisica@yahoo.com.br

the collimators, they can occlude the radiation source, interfering in the dose at the point where it is desired to measure, not being possible to differentiate between the primary portion of the radiation and the penumbra, because there is an overlap of the penumbra. to the beam. Furthermore, in small fields the range of secondary electrons is large compared to the size of the field. Under such conditions, there is a reduction in the output factor, or beam intensity, as well as an increase in the penumbra dimension, influencing the field size of the beam to be measured. When occur dose distribution inside a planning target volume (PTV) in smaller and irregular beam lets or segments, problems arise namely lateral charged particle disequilibrium, steep dose gradients, partial occlusion of the primary radiation source by the system of collimation, detector-related field perturbations and detector volume averaging effects[12; 13; 14].

Figure 1 shows a geometric demonstration of the composition of the penumbra region. The penumbra composition in conventional fields is shown in the first drawing. In the Figure a small field was shaped by a collimator that secured part of the finite primary photon source in the produce a lower beam output on the beam axis compared to field sizes where the source is not partially blocked. This primary source occlusion is the first challenge for dosimetric studies when the field size is smaller than the size of the primary photon source.

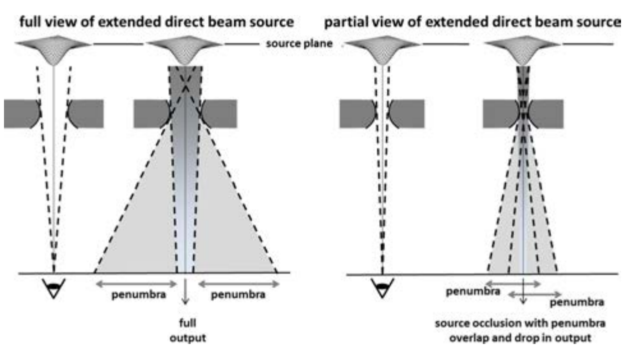

Figure 1: Schematic representation of the source occlusion effect

The greater obstruction of the beam causes a decrease in the homogeneity region, which makes a considerable fraction of the field composed by the beam penumbra itself. In addition to the penumbra issue, the sizing of small fields is influenced by the reach of secondary particles, since the lateral diffusion of charged particles can, according to the energy spectrum, be comparable to the field dimensions itself. [6; 9; 15; 16].

A photon beam is considered small if exists loss of equilibrium of charged particles, partial occlusion of the primary photon from the source by collimating devices or the detector size being large compared to the beam dimensions. The characteristics presented are related to the beam in overlap between field penumbras and detector volume [11; 17].

Another important factor to note is in relation to the definition of the field size. In conventional fields, this is defined as the distance between the points where a given isodose curve, usually 50%, intersects the plane perpendicular to the beam at a specific source-surface distance. One approximation is the width at half height of the beam profile, FWHM, and this approximation may not be true for small fields due to the reduction in beam intensity in its central portion and the overlapping of the penumbra [2; 18].

The problems associated with the use of small fields in radiotherapy are employed in stereotactic radiosurgery (SRS). SRS is a treatment technique which is based on the delivery of single high dose of radiation to small, well-defined intracranial lesions and can be applied for treatment of wide range of indications - from benign diseases to brain metastases. Accuracy of dose calculation and dose delivery are of greatest importance for safe and effective implementation of this technique and therefore the use of stereotactic radiosurgery in a medical center requires special equipment and comprehensive work of a medical physicist. Possible inaccuracies in dose calculation are usually related to the problems of small field dosimetry and calculations in the treatment planning system [5; 9].

II. Methodology and Materials

In this work, a solid water phantom was irradiated in a linear accelerator with a photon beam of 10 MV. Radiochromic films were placed inside the water solid phantom to record the absorbed dose profile variations. The irradiations were carried out in order to obtain the longitudinal dose variation profile (in depth) and the axial dose variation profiles, measured in the phantom at a depth of 1 cm. Irradiations were performed for four different field sizes.

a) Elekta Linear Accelerator

The linear particle accelerator used in experiments is an equipment for irradiations of patients. It is a linear accelerator of electrons, model Synergy Platform, from the manufacturer Elekta, which allows the generation of electron and photon beams. Photon beams can be generated at voltages of 6 and 10 MV. The leak radiation of the head is less than 0.1% of the dose rate in the isocenter, the size of the field in the isocenter ranges from 1×1 to 40×40 cm^2, with multi-leaf collimator (MLC) that has 40 pairs and motorized physical filter with angles from 1^o to 60^o. The motorized physical filter has only the angle of 60^o, in the planning/treatment, changing its inlet and output of the beam. Figure 2 illustrates the position of the solid water phantom charged with a film sheet and placed in the accelerator table at 1 m from the X ray beam's focus.

b) Solid Water Phantom

The solid water phantom used in the tests was built with solid water plates. It was used two plates of 30×30×1 cm³ and a complementary plate of 30×30×2 cm³. These plates responds to radiation beams similarly to water, with an error of 1% and helps in the search for data on dose distribution, as it approximates the absorption and dispersion properties of radiation from muscles and other soft tissues. This material allows better handling as it is solid and widely used in the manufacture of human phantoms [19; 20].

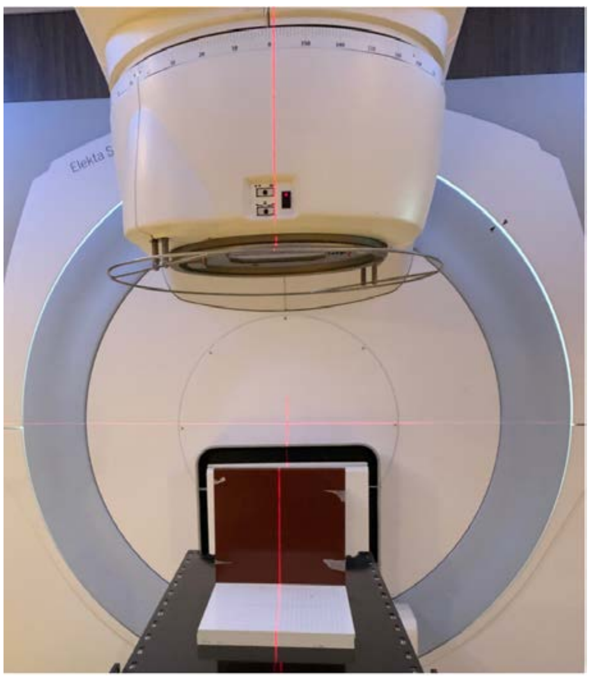

Figure 2: Elekta Linear Accelerator with Water Phantom Solid positioning in the gantry

Figure 3 shows two setups for positioning of the solid water phantom loaded with a film sheet. In the first setup, the phantom is irradiated laterally by the 10MVphoton beam, to record the absorbed dose variations in depth. For this setup the film sheet is loaded along the side edge of the phantom. In the second setup, the phantom is irradiated frontally, to record the dose variatons in the XY axial plane and the film sheet is placed in the center of the plate at a depth of 1,0 cm.

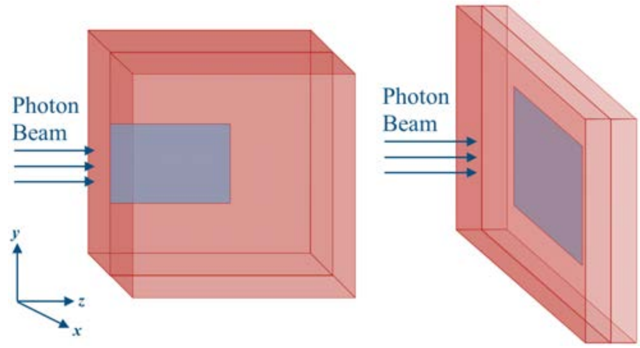

Figure 3: Solid water phantom setups loaded with a sheet of film for irradiation by the 10 MV photon beam, laterally and frontally

c) Radiochromic Films

The film sheets used to record the dose profile were the GAFCHROMIC FILM, model EBT QD+, used in the experiments. This film has a construction characteristic similar to other models of radiochromic films, being a tool for a wide range of doses, equivalent to soft tissues, and can be handled in light rooms. The Gafchromic EBT Dosimetric Films is made by laminating a sensitive layer between two layers of polyester and it is used for measurements of absorbed doses in a range of 0.4 to 40 Gy and have a low dependence on beam energy, making it more suitable for applications in radiotherapy and radiosurgeries.

Radiochromic films when exposed to radiation show a darkening proportional to the dose received as higher is the absorbed dose, as darker they become. The film used has an active layer with 25 μm thickness. The calibration curves of the films are produced to allow the conversion of the darkening values into absorbed dose values. The film, after being irradiated, were stored in a place without humidity and away from sunlight, so that there was no interference in the chemical reactions of diacetylene compounds [21; 22; 23; 24].

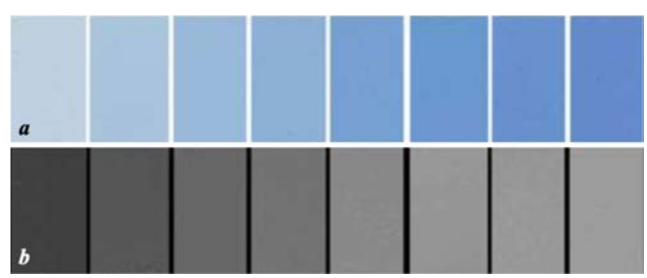

Figure 4: Images of film strips exposed in different absorbed dose values. Images after exposition (a) and images of the red channel after processing (b).

The Figure 4 shows two images of eigth radiochomic film strips. These strips were irradiated with different doses. In Figure 4*a* is possible to observe the change of the strip colors. The first strip, the lightest,

Global Journal of Science Frontier Research (A) Volume XXIII Issue VIII Version I Year 2023

wasn't irradiated and the darkest strip is the highest recorded dose. The Figure 4*b* is the same image as the Figure 4*a*, after being worked on to separate the red channel image from the color image.

d) Radiochromic Films Records

To record the absorbed dose profiles, the phantom loaded with a radiochromic film sheet was positioned in two different configurations (Figure 3), in order to obtain the axial and longitudinal absorbed dose variations, for each field size, when the phantom was irradiated with the photon beam of 10 MV.

In the assembly to obtain the longitudinal dose profiles, the film sheet was positioned between the two plates of solid water and it was irradiated laterally. In the irradiation to obtain the axial dose profiles, the film sheet was positioned inside the plates, in the center of the solid water phantom at a depth of 1.0 cm, being irradiated frontally.

The film sheets were cut for longitudinal and axial irradiations with specific sizes for each field size. Four lateral and four frontal irradiations were performed, one each for field size. The film sheets were cut according with the field size and the photon beam incidency, in the table Table 1 have the sizes of the film sheets used.

Table 1: Film sheet sizes

Field Size (cm^2)	Axial Film Size (cm^2)	Longitudinal Film Size (cm^2)
1×1	4×4	3×12
2×2	5×5	4×12
3×3	6×6	5×12
5×5	8×8	7×12

After irradiation, the film sheets were left to rest for a minimum period of 24 h to stabilize of the reactions and the recorded image. Then, digital images were generated using a scanner device model Scanjet G4050 produced by HP. Digital images of the film sheets were acquired before the irradiation. The images were acquired at a resolution of 300 dpi with the suffix .tiff in color.

The digital images of the film sheets were processed in the image J software using the split tool to separate the Red, Blue and Green (RGB) color channels. In the Figure 5 are the images of the film sheets irradiated frontally and laterally, for the field of 5x5 cm^2.

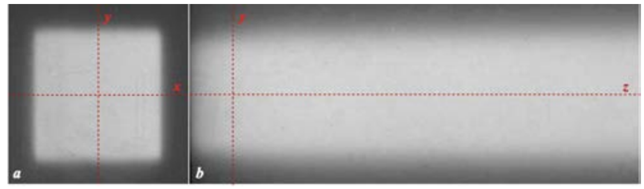

Figure 5: Irradiated radiochromic film sheets placed into the water phantom. color (a) and red channel images (b)

These images are of the red chanel component, separated by the split tool and with the grayscale inversion. Grayscale inversion is required to correlate the lightest color with the higest absorbed dose value. In these images are the positions of the axial (X and Y) and longitudinal Z axes, which were used to generate the absorbed dose profiles.

The image of the red color channel was chosen because the grayscale values in this channel are higher than those presented by the green and blue channels. The highest recorded dose value corresponds to the lightest register that appears in the film image worked on image J software. This will be the highest numerical value in grayscale.

Therefore, the red channel was chosen for the recording of absorbed doses, as it has the highest numerical value and a greater amplitude than the green and blue channels. The graph presented in Figure 6 contains the response curves related to the images of the three channels on the central longitudinal axis (Z).

III. Results

The solid water phantom was irradiated by a 10 MV photon beam. Irradiations were performed with the application of 300 monitor units (MU), which corresponds to a maximum absorbed dose of 2.97 Gy. Axial and longitudinal variations of the relative absorbed dose were obtained for the field sizes of 1×1 cm^2, 2×2 cm^2, 3×3 cm^2 and 5×5 cm^2, with the phantom surface placed at 1.0 m from the source.

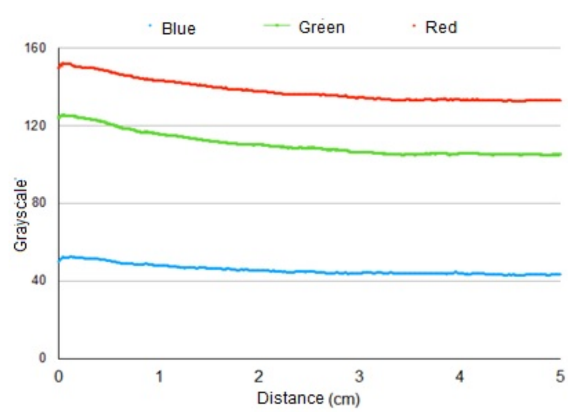

Figure 6: Intensity of the darkening response of an irradiated film strip, per RGB channel

a) Longitudinal Dose Profile

The variations of the relative absorbed dose in depth are shown in Figure 7. The curves show the longitudinal variations for the four field sizes. The absorbed dose starts in zero and increases to the maximum value (peak).This graph shows the position where the film sheets were placed to acquire the axial curves in the XY plane, at a depth of 1 cm.

Considering the field sizes, the average peak value occurs at a distance of 1.89±0,09 cm. At this point, the relative absorbed dose ranged from 100% for the 5×5 cm² field to 69.23% for the 1×1 cm² field. In all positions, the absorbed dose values were higher for the 5×5 cm² field and lower for the smaller field sizes.

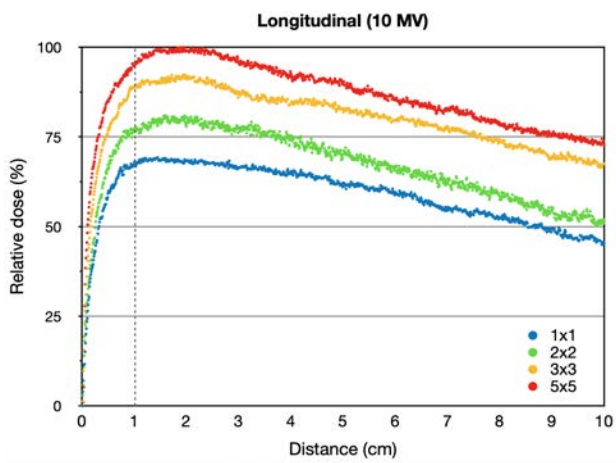

Figure 7: Relative absorbed dose variations at depth of different field sizes in the solid water phantom using a 10 MV photon beam

From the zero point to the distance of 1.89 cm the absorbed dose increase from zero to the maximum value (build-up region). After this point the values going decrecsing with the deep.

At 1.0 cm depth, the relative absorbed dose varied from 95.16% to 67.28% for the fields of 5×5 cm² and 1×1 cm², respectivly. At 10.0 cm depth, the variation of relative absorbed dose was from 73.70% to 45.27% for the fields of 5×5 cm² and 1×1 cm², respectivly. The Table 2 presents results of relative absorbed dose of some points to the lateral irradiation of the solid water phantom.

Table 2: Relative absorbed dose values for longitudinal irradiation

Field size (cm²)	Relative absorbed dose (%)		
	1 cm deep	Peak	10 cm deep
5×5	95.16	100.00	73.70
3×3	89.00	92.31	67.25
2×2	76.62	80.95	51.39
1×1	67.28	69.23	45.27

Observing the longitudinal curves and comparing the values of Table 2, the dose values of the smaller fields were smaller across the observed distance. This reduction in the dose values is more expressive for the fields of 1×1 and 2×2 cm². Considering the peak values, there was a dose reduction of 30.77%, 19.05% and 7.59%, for fields 1×1, 2×2 and 3×3 cm², respectively.

b) Axial Dose Profiles

Figure 8 shows the relative absorbed dose variations for the frontal irradiation of the solid water phantom to the X axis, using field sizes of 1×1, 2×2, 3×3 and 5×5 cm². These profiles were recorded at a depth of 1 cm in the phantom.

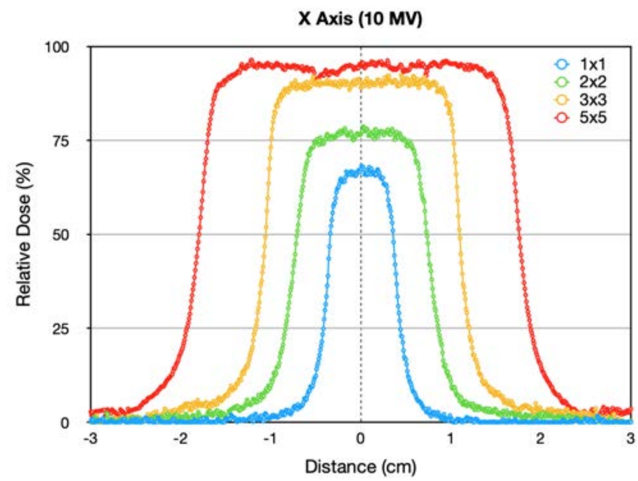

Figure 8: Relative absorbed dose variations for different field sizes measured on the X axis at 1 cm depth, in the solid water simulator irradiated with a 10 MV photon beam

The curves have a plateau region where is the highest dose values. The average dose in the plateau regions varied from 93.87% to 65.90% for the field sizes of 5×5 and 1×1 cm², respectivly. The measurement point (1.0 cm) is in the buildup region, before the peak point (1.89 cm). Therefore, the recorded values are just below the values in the peak point.

Table 3 shows the average values of relative absorbed dose and standard deviation, for each field size. These values were selected considering the central area of the curves and the distance of the values used varied according to the plateau size. The maximum relative dose values found at these selected distances are displayed.

Table 3: Relative absorbed dose values in the plateau region for the X axis

Field size (cm²)	Plateau (cm)	Relative absorbed dose (%)	
		average	maximum
5×5	3.0	93.87±1.94*	96.42
3×3	2.0	89.19±3.09	92.34
2×2	1.5	75.01±3.22	78.68
1×1	0.5	65.90±1.35	68.19

*Standard deviation

The absorbed dose values in the plateaus were smaller for the smaller fields, with some oscillations in the plateau, mainly in the 5×5 cm². The biggest absorbed dose reductions in this region happened in the two smaller fields of 1×1 and 2×2 cm², about 29.80% and 20.09%, repectivly.

Figure 9 shows the relative absorbed dose variations in the frontal irradiation of the solid water phantom to the Y axis, using field sizes of 1×1, 2×2, 3×3 and 5×5 cm². These profiles were recorded at a depth of 1 cm in the solid water phantom.

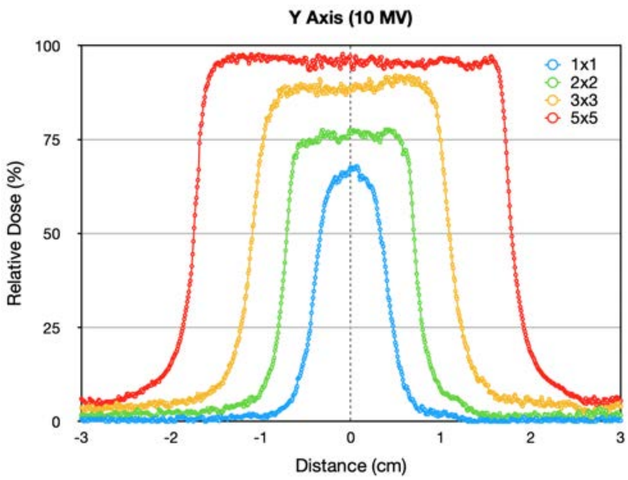

Figure 9: Relative absorbed dose variations for different field sizes measured on the Y axis at 1 cm depth, in the solid water simulator irradiated with a 10 MV photon beam

The average dose in plateau regions varied from 95, 62% to 64,79% for the field sizes of 5×5 and 1×1 cm², respectivly. As the measurement point (1.0 cm) is before peak point (1.89 cm) and the recorded relative absorbed doses for each field size are just below the values in the peak point.

Table 4 shows the average values of relative absorbed dose and standard deviation, for each field size. The plateau size considered for the calculations varied from 3 to 0.5 cm according to the field size. The maximum relative dose values found for these selected distances are displayed. The maximum value of field 5×5 cm² reached to 97.73% and smaller fields had smaller relative absorbed dose values.

Table 4: Relative absorbed dose values in the plateau region for the Y axis

Field size (cm²)	Plateau (cm)	Relative absorbed dose (%)	
		average	maximum
5×5	3.0	95.62±1.32*	97.73
3×3	2.0	87.70±3.80	92.02
2×2	1.5	75.08±2.35	77.61
1×1	0.5	64.79±1.91	67.84

*Standard deviation

Comparing the axial curves in the X and Y axes, they are similar, and the differences are greater for the field of 1×1 cm² where, in the Y axis, the base is larger and the top more arrow, possibly caused by the influence of the position that these collimators are in relation to the photon source.

c) *Isodose Curves*

The isodose curves are used to represent the absorbed dose variations in a plane. The absorbed dose distribution is represented by curves generated by points where the dose values are equal. Isodose curves are regular absorbed dose intervals drawn as depth dose distribution maps and can be expressed as a percentage of the absorbed dose at a reference point. [2; 18; 25].

The Figure 10 shows isodose curves for the field sizes of 1×1, 2×2, 3×3 and 5×5 cm² measured at 1 cm depth in the frontal irradiation of the solid water phantom. The film area shown in the figure for each field size is 6x6 cm². In these curves it is posible to observe the square caracteristic of the field shape and the differences in the size of the irradiated area.

The color scale starts in dark blue and ends in red, corresponding to the variation of the relative absorbed dose from zero to 100% in this XY plane, which is 1 cm deep. It should be noted that the maximum dose that occurs in this plane corresponds to 97.3% of the peak dose (100%) that occurs in the 5×5 field size. The maximum absorbed dose occurs at a deeper region of the solid water phantom.

In the central area of the images, absorbed doses close to the maximum dose in this XY plane (100%) are recorded in red and orange, for field sizes of 5×5 and 3×3 cm². In the 2×2 cm² field size, the central region is colored yellow, corresponding to absorved doses close to 80% of the maximum absorbed dose in this plane XY and in the 1×1 cm² field size the central region is colored green, corresponding to doses close to 65% of the maximum absorbed dose in this plane, according to the color scale variations

Comparing the isodose curves with the axial curves, it's possible to observe the variation found in the axial curves of the X and Y axes occurs in the isodose curves. In these curves it is possible to observe the entire the dose distribution in the axial plane XY and the irradiation field limits.

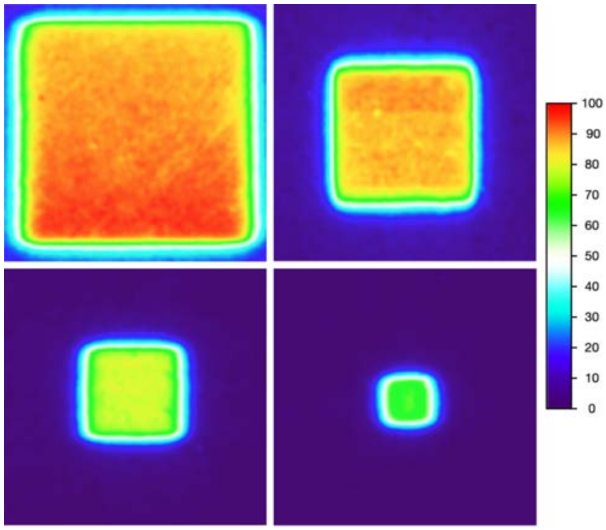

Figure 10: Isodose curves at 1.0 cm deep for fields 1×1, 2×2, 3×3 and 5×5 cm² in a Solid Water Phantom using 10 MV photon beam

IV. Conclusion

In this work, a solid water phantom was irradiated by a photon beam generated with a 10MVvoltage from a Linear Accelerator. The phantom was irradiated in four different field sizes, including small field sizes. The water phantom was irradiated with 3 MU, corresponding to 2,97 Gy in the maximum dose value.

Absorbed dose measurements were performed using radiochromic film sheets inside the solidwater phantom. These films recorded the absorbed dose variation profile in depth and in a specific axial plane at 1 cm depth.

It was observed variations in the behavior of the dose deposition in depth, where all the values of the small fields were smaller. As smaller was the field size, as smaller was the absorbed dose.

Highlights

Dose Variation Profiles of Small Fields with a 10 MV Photon Beam

- Behavior of absorbed dose of small fields in radiotherapy.
- Experimental data showed differences in depth doses for different sizes of small fields.
- The use of Radiochromic films to dose evaluation in differents fields in radiotherapy.

References Références Referencias

1. P. Mourão and F. A. de Oliveira, *Fundamentos de radiologia e imagem*. Difusão Editora, 2018.
2. F. M. Khan, *The physics of radiation therapy*. Lippincott Williams & Wilkins, 2010.
3. P. Charles, S. Crowe, T. Kairn, R. Knight, B. Hill, J. Kenny, C. Lang ton, and J. Trapp, "The influence of monte carlo source parameters on detector design and dose perturbation in small field dosimetry," in *Journal of Physics: Conference Series*, vol. 489, p. 012006, IOP Publishing, 2014.
4. S. Lam, D. Bradley, and M. U. Khandaker, "Small-field radiother apy photon beam output evaluation: detectors reviewed," *Radiation Physics and Chemistry*, vol. 178, p. 108950, 2021.
5. R. G. Leão Jr, R. V. Sousa, A. H. Oliveira, H. L. L. Silva, and A. P. Mourão, "Validação de um modelo computacional de acelerador linear varian clinac 2100 utilizando o código egsnrc para utilização em dosimetria de pequenos campos.," *Brazilian Journal of Radiation Sciences*, vol. 6, no. 1, 2018.
6. I. J. Das, G. X. Ding, and A. Ahnesjö, "Small fields: nonequilibrium radiation dosimetry," *Medical physics*, vol. 35, no. 1, pp. 206–215, 2008.
7. M. K. Tyler, P. Z. Liu, C. Lee, D. R. McKenzie, and N. Suchowerska, "Small field detector correction factors: effects of the flattening filter for elekta and varian linear accelerators," *Journal of Applied Clinical Medical Physics*, vol. 17, no. 3, pp. 223–235, 2016.
8. L. Furnari, "Controle de qualidade em radioterapia," *Revista Brasileira de Física Médica*, vol. 3, no. 1, pp. 77–90, 2009.
9. R. G. L. Júnior, "Avaliação das perturbações físicas de feixes de raios x em pequenos campos estáticos: uma abordagem teórica pelo método de monte carlo," 2018.
10. E. Sham, J. Seuntjens, S. Devic, and E. B. Podgorsak, "Influence of focal spot on characteristics of very small diameter radiosurgical beams," *Medical physics*, vol. 35, no. 7Part1, pp. 3317–3330, 2008.
11. IAEA, "Technical report series no. 483 "dosimetry of small static fields used in external beam radiotherapy an international code of practice for reference and relative dose determination," 2017.
12. X. Chen, E. S. Paulson, E. Ahunbay, A. Sanli, S. Klawikowski, and X. A. Li, "Measurement validation of treatment planning for a mrlinac," *Journal of Applied Clinical Medical Physics*, vol. 20, no. 7, pp. 28–38, 2019.
13. S. Webb, *Intensity-modulated radiation therapy*. CRC Press, 2015.
14. M. A. Mia, M. S. Rahman, S. Purohit, S. M. Kabir, and A. K. Meaze, "Analysis of percentage depth dose for 6 and 15 mv photon energies of medical linear accelerator with cc13 ionization chamber," *NUCLEAR SCIENCE AND APPLICATIONS*, vol. 28, no. 1&2, 2019.
15. Y. Tayalati, S. Didi, M. Zerfaoui, and A. Moussaa, "Monte carlo simulation of 6mv elekta synergy platform linac photon beam using gate/geant4," *arXiv preprint arXiv:1309.0758*, 2013.
16. M. Aspradakis, J. Byrne, H. Pamans, J. Conway, K. Rosser, J. War rington, *et al.*, "Small field mv

photon dosimetry. ipem report 103," *York, UK: IPEM*, 2010.
17. B. Mijnheer, *Clinical 3D dosimetry in modern radiation therapy*. CRC Press, 2017.
18. L. A. Scaff, "Física da radioterapia," 1997.
19. C. Constantinou, F. Attix, and B. R. Paliwal, "A solid water phantom material for radiotherapy x-ray and γ-ray beam calibrations," *Medical physics*, vol. 9, no. 3, pp. 436–441, 1982.
20. M. A. Gargett, A. R. Briggs, and J. T. Booth, "Water equivalence of a solid phantom material for radiation dosimetry applications," *Physics and imaging in radiation oncology*, vol. 14, pp. 43–47, 2020.
21. S. Devic, "Radiochromic film dosimetry: past, present, and future," *Physica medica*, vol. 27, no. 3, pp. 122–134, 2011.
22. S. Devic, N. Tomic, and D. Lewis, "Reference radiochromic film dosimetry: review of technical aspects," *Physica Medica*, vol. 32, no. 4, pp. 541–556, 2016.
23. A. Niroomand-Rad, C. R. Blackwell, B. M. Coursey, K. P. Gall, J. M. Galvin, W. L. McLaughlin, A. S. Meigooni, R. Nath, J. E. Rodgers, and C. G. Soares, "Radiochromic film dosimetry: recommendations of aapm radiation therapy committee task group 55," *Medical physics*, vol. 25, no. 11, pp. 2093–2115, 1998.
24. S. Aldelaijan, F. Alzorkany, B. Moftah, I. Buzurovic, J. Seuntjens, N. Tomic, and S. Devic, "Use of a control film piece in radiochromic film dosimetry," *Physica Medica*, vol. 32, no. 1, pp. 202–207, 2016.
25. M. C. B. T. Adad, G. Hoff, E. E. Streck, and R. Lykawka, "Curvas de isodose no ar em uma sala de mamografia," *Radiologia Brasileira*, vol. 41, pp. 255–258, 2008.

Global Journals Guidelines Handbook 2023

www.GlobalJournals.org

Memberships

FELLOWS/ASSOCIATES OF SCIENCE FRONTIER RESEARCH COUNCIL

FSFRC/ASFRC MEMBERSHIPS

Introduction

FSFRC/ASFRC is the most prestigious membership of Global Journals accredited by Open Association of Research Society, U.S.A (OARS). The credentials of Fellow and Associate designations signify that the researcher has gained the knowledge of the fundamental and high-level concepts, and is a subject matter expert, proficient in an expertise course covering the professional code of conduct, and follows recognized standards of practice. The credentials are designated only to the researchers, scientists, and professionals that have been selected by a rigorous process by our Editorial Board and Management Board.

Associates of FSFRC/ASFRC are scientists and researchers from around the world are working on projects/researches that have huge potentials. Members support Global Journals' mission to advance technology for humanity and the profession.

FSFRC

FELLOW OF SCIENCE FRONTIER RESEARCH COUNCIL

FELLOW OF SCIENCE FRONTIER RESEARCH COUNCIL is the most prestigious membership of Global Journals. It is an award and membership granted to individuals that the Open Association of Research Society judges to have made a 'substantial contribution to the improvement of computer science, technology, and electronics engineering.

The primary objective is to recognize the leaders in research and scientific fields of the current era with a global perspective and to create a channel between them and other researchers for better exposure and knowledge sharing. Members are most eminent scientists, engineers, and technologists from all across the world. Fellows are elected for life through a peer review process on the basis of excellence in the respective domain. There is no limit on the number of new nominations made in any year. Each year, the Open Association of Research Society elect up to 12 new Fellow Members.

Benefit

To the Institution

Get letter of appreciation

Global Journals sends a letter of appreciation of author to the Dean or CEO of the University or Company of which author is a part, signed by editor in chief or chief author.

Exclusive Network

Get access to a closed network

A FSFRC member gets access to a closed network of Tier 1 researchers and scientists with direct communication channel through our website. Fellows can reach out to other members or researchers directly. They should also be open to reaching out by other.

Career | Credibility | Exclusive | Reputation

Certificate

Receive a print ed copy of a certificate

Fellows receive a printed copy of a certificate signed by our Chief Author that may be used for academic purposes and a personal recommendation letter to the dean of member's university.

Career | Credibility | Exclusive | Reputation

Designation

Get honored title of membership

Fellows can use the honored title of membership. The “FSFRC” is an honored title which is accorded to a person’s name viz. Dr. John E. Hall, Ph.D., FSFRC or William Walldroff, M.S., FSFRC.

Career | Credibility | Exclusive | Reputation

Recognition on the Platform

Better visibility and citation

All the Fellow members of FSFRC get a badge of "Leading Member of Global Journals" on the Research Community that distinguishes them from others. Additionally, the profile is also partially maintained by our team for better visibility and citation. All fellows get a dedicated page on the website with their biography.

Career | Credibility | Reputation

Future Work

Get discounts on the future publications

Fellows receive discounts on future publications with Global Journals up to 60%. Through our recommendation programs, members also receive discounts on publications made with OARS affiliated organizations.

Career Financial

GJ Internal Account

Unlimited forward of Emails

Fellows get secure and fast GJ work emails with unlimited forward of emails that they may use them as their primary email. For example, john [AT] globaljournals [DOT] org.

Career Credibility Reputation

Premium Tools

Access to all the premium tools

To take future researches to the zenith, fellows and associates receive access to all the premium tools that Global Journals have to offer along with the partnership with some of the best marketing leading tools out there.

Financial

Conferences & Events

Organize seminar/conference

Fellows are authorized to organize symposium/seminar/conference on behalf of Global Journal Incorporation (USA). They can also participate in the same organized by another institution as representative of Global Journal. In both the cases, it is mandatory for him to discuss with us and obtain our consent. Additionally, they get free research conferences (and others) alerts.

Career Credibility Financial

Early Invitations

Early invitations to all the symposiums, seminars, conferences

All fellows receive the early invitations to all the symposiums, seminars, conferences and webinars hosted by Global Journals in their subject.

Exclusive

Publishing Articles & Books

Earn 60% of sales proceeds

Fellows can publish articles (limited) without any fees. Also, they can earn up to 60% of sales proceeds from the sale of reference/review books/literature/ publishing of research paper. The FSFRC member can decide its price and we can help in making the right decision.

Exclusive Financial

Reviewers

Get a remuneration of 15% of author fees

Fellow members are eligible to join as a paid peer reviewer at Global Journals Incorporation (USA) and can get a remuneration of 15% of author fees, taken from the author of a respective paper.

Financial

Access to Editorial Board

Become a member of the Editorial Board

Fellows may join as a member of the Editorial Board of Global Journals Incorporation (USA) after successful completion of three years as Fellow and as Peer Reviewer. Additionally, Fellows get a chance to nominate other members for Editorial Board.

Career Credibility Exclusive Reputation

And Much More

Get access to scientific museums and observatories across the globe

All members get access to 5 selected scientific museums and observatories across the globe. All researches published with Global Journals will be kept under deep archival facilities across regions for future protections and disaster recovery. They get 10 GB free secure cloud access for storing research files.

ASFRC

ASSOCIATE OF SCIENCE FRONTIER RESEARCH COUNCIL

ASSOCIATE OF SCIENCE FRONTIER RESEARCH COUNCIL is the membership of Global Journals awarded to individuals that the Open Association of Research Society judges to have made a 'substantial contribution to the improvement of computer science, technology, and electronics engineering.

> The primary objective is to recognize the leaders in research and scientific fields of the current era with a global perspective and to create a channel between them and other researchers for better exposure and knowledge sharing. Members are most eminent scientists, engineers, and technologists from all across the world. Associate membership can later be promoted to Fellow Membership. Associates are elected for life through a peer review process on the basis of excellence in the respective domain. There is no limit on the number of new nominations made in any year. Each year, the Open Association of Research Society elect up to 12 new Associate Members.

Benefit

To the Institution

Get letter of appreciation

Global Journals sends a letter of appreciation of author to the Dean or CEO of the University or Company of which author is a part, signed by editor in chief or chief author.

Exclusive Network

Get access to a closed network

A ASFRC member gets access to a closed network of Tier 1 researchers and scientists with direct communication channel through our website. Associates can reach out to other members or researchers directly. They should also be open to reaching out by other.

Career | Credibility | Exclusive | Reputation

Certificate

Receive a print ed copy of a certificate

Associates receive a printed copy of a certificate signed by our Chief Author that may be used for academic purposes and a personal recommendation letter to the dean of member's university.

Career | Credibility | Exclusive | Reputation

Designation

Get honored title of membership

Associates can use the honored title of membership. The “ASFRC” is an honored title which is accorded to a person’s name viz. Dr. John E. Hall, Ph.D., ASFRC or William Walldroff, M.S., ASFRC.

Career | Credibility | Exclusive | Reputation

Recognition on the Platform

Better visibility and citation

All the Associate members of ASFRC get a badge of "Leading Member of Global Journals" on the Research Community that distinguishes them from others. Additionally, the profile is also partially maintained by our team for better visibility and citation. All associates get a dedicated page on the website with their biography.

Career | Credibility | Reputation

Future Work

Get discounts on the future publications

Associates receive discounts on the future publications with Global Journals up to 60%. Through our recommendation programs, members also receive discounts on publications made with OARS affiliated organizations.

Career Financial

GJ Internal Account

Unlimited forward of Emails

Associates get secure and fast GJ work emails with unlimited forward of emails that they may use them as their primary email. For example,
john [AT] globaljournals [DOT] org.

Career Credibility Reputation

Premium Tools

Access to all the premium tools

To take future researches to the zenith, fellows receive access to almost all the premium tools that Global Journals have to offer along with the partnership with some of the best marketing leading tools out there.

Financial

Conferences & Events

Organize seminar/conference

Associates are authorized to organize symposium/seminar/conference on behalf of Global Journal Incorporation (USA). They can also participate in the same organized by another institution as representative of Global Journal. In both the cases, it is mandatory for him to discuss with us and obtain our consent. Additionally, they get free research conferences (and others) alerts.

Career Credibility Financial

Early Invitations

Early invitations to all the symposiums, seminars, conferences

All associates receive the early invitations to all the symposiums, seminars, conferences and webinars hosted by Global Journals in their subject.

Exclusive

Publishing Articles & Books

Earn 30-40% of sales proceeds

Associates can publish articles (limited) without any fees. Also, they can earn up to 30-40% of sales proceeds from the sale of reference/review books/literature/publishing of research paper.

Exclusive Financial

Reviewers

Get a remuneration of 15% of author fees

Associate members are eligible to join as a paid peer reviewer at Global Journals Incorporation (USA) and can get a remuneration of 15% of author fees, taken from the author of a respective paper.

Financial

And Much More

Get access to scientific museums and observatories across the globe

All members get access to 2 selected scientific museums and observatories across the globe. All researches published with Global Journals will be kept under deep archival facilities across regions for future protections and disaster recovery. They get 5 GB free secure cloud access for storing research files.

Associate	Fellow	Research Group	Basic
$4800 **lifetime designation**	$6800 **lifetime designation**	$12500.00 **organizational**	APC **per article**
Certificate, LoR and Momento 2 discounted publishing/year **Gradation** of Research 10 research contacts/day **1 GB** Cloud Storage **GJ** Community Access	**Certificate,** LoR and Momento **Unlimited** discounted publishing/year **Gradation** of Research **Unlimited** research contacts/day **5 GB** Cloud Storage **Online Presense** Assistance **GJ** Community Access	**Certificates,** LoRs and Momentos **Unlimited** free publishing/year **Gradation** of Research **Unlimited** research contacts/day **Unlimited** Cloud Storage **Online Presense** Assistance **GJ** Community Access	**GJ** Community Access

Preferred Author Guidelines

We accept the manuscript submissions in any standard (generic) format.

We typeset manuscripts using advanced typesetting tools like Adobe In Design, CorelDraw, TeXnicCenter, and TeXStudio. We usually recommend authors submit their research using any standard format they are comfortable with, and let Global Journals do the rest.

Alternatively, you can download our basic template from https://globaljournals.org/Template.zip

Authors should submit their complete paper/article, including text illustrations, graphics, conclusions, artwork, and tables. Authors who are not able to submit manuscript using the form above can email the manuscript department at submit@globaljournals.org or get in touch with chiefeditor@globaljournals.org if they wish to send the abstract before submission.

Before and during Submission

Authors must ensure the information provided during the submission of a paper is authentic. Please go through the following checklist before submitting:

1. Authors must go through the complete author guideline and understand and *agree to Global Journals' ethics and code of conduct,* along with author responsibilities.
2. Authors must accept the privacy policy, terms, and conditions of Global Journals.
3. Ensure corresponding author's email address and postal address are accurate and reachable.
4. Manuscript to be submitted must include keywords, an abstract, a paper title, co-author(s') names and details (email address, name, phone number, and institution), figures and illustrations in vector format including appropriate captions, tables, including titles and footnotes, a conclusion, results, acknowledgments and references.
5. Authors should submit paper in a ZIP archive if any supplementary files are required along with the paper.
6. Proper permissions must be acquired for the use of any copyrighted material.
7. Manuscript submitted *must not have been submitted or published elsewhere* and all authors must be aware of the submission.

Declaration of Conflicts of Interest

It is required for authors to declare all financial, institutional, and personal relationships with other individuals and organizations that could influence (bias) their research.

Policy on Plagiarism

Plagiarism is not acceptable in Global Journals submissions at all.

Plagiarized content will not be considered for publication. We reserve the right to inform authors' institutions about plagiarism detected either before or after publication. If plagiarism is identified, we will follow COPE guidelines:

Authors are solely responsible for all the plagiarism that is found. The author must not fabricate, falsify or plagiarize existing research data. The following, if copied, will be considered plagiarism:

- Words (language)
- Ideas
- Findings
- Writings
- Diagrams
- Graphs
- Illustrations
- Lectures

- Printed material
- Graphic representations
- Computer programs
- Electronic material
- Any other original work

Authorship Policies

Global Journals follows the definition of authorship set up by the Open Association of Research Society, USA. According to its guidelines, authorship criteria must be based on:

1. Substantial contributions to the conception and acquisition of data, analysis, and interpretation of findings.
2. Drafting the paper and revising it critically regarding important academic content.
3. Final approval of the version of the paper to be published.

Changes in Authorship

The corresponding author should mention the name and complete details of all co-authors during submission and in manuscript. We support addition, rearrangement, manipulation, and deletions in authors list till the early view publication of the journal. We expect that corresponding author will notify all co-authors of submission. We follow COPE guidelines for changes in authorship.

Copyright

During submission of the manuscript, the author is confirming an exclusive license agreement with Global Journals which gives Global Journals the authority to reproduce, reuse, and republish authors' research. We also believe in flexible copyright terms where copyright may remain with authors/employers/institutions as well. Contact your editor after acceptance to choose your copyright policy. You may follow this form for copyright transfers.

Appealing Decisions

Unless specified in the notification, the Editorial Board's decision on publication of the paper is final and cannot be appealed before making the major change in the manuscript.

Acknowledgments

Contributors to the research other than authors credited should be mentioned in Acknowledgments. The source of funding for the research can be included. Suppliers of resources may be mentioned along with their addresses.

Declaration of funding sources

Global Journals is in partnership with various universities, laboratories, and other institutions worldwide in the research domain. Authors are requested to disclose their source of funding during every stage of their research, such as making analysis, performing laboratory operations, computing data, and using institutional resources, from writing an article to its submission. This will also help authors to get reimbursements by requesting an open access publication letter from Global Journals and submitting to the respective funding source.

Preparing your Manuscript

Authors can submit papers and articles in an acceptable file format: MS Word (doc, docx), LaTeX (.tex, .zip or .rar including all of your files), Adobe PDF (.pdf), rich text format (.rtf), simple text document (.txt), Open Document Text (.odt), and Apple Pages (.pages). Our professional layout editors will format the entire paper according to our official guidelines. This is one of the highlights of publishing with Global Journals—authors should not be concerned about the formatting of their paper. Global Journals accepts articles and manuscripts in every major language, be it Spanish, Chinese, Japanese, Portuguese, Russian, French, German, Dutch, Italian, Greek, or any other national language, but the title, subtitle, and abstract should be in English. This will facilitate indexing and the pre-peer review process.

The following is the official style and template developed for publication of a research paper. Authors are not required to follow this style during the submission of the paper. It is just for reference purposes.

Manuscript Style Instruction (Optional)

- Microsoft Word Document Setting Instructions.
- Font type of all text should be Swis721 Lt BT.
- Page size: 8.27" x 11'", left margin: 0.65, right margin: 0.65, bottom margin: 0.75.
- Paper title should be in one column of font size 24.
- Author name in font size of 11 in one column.
- Abstract: font size 9 with the word "Abstract" in bold italics.
- Main text: font size 10 with two justified columns.
- Two columns with equal column width of 3.38 and spacing of 0.2.
- First character must be three lines drop-capped.
- The paragraph before spacing of 1 pt and after of 0 pt.
- Line spacing of 1 pt.
- Large images must be in one column.
- The names of first main headings (Heading 1) must be in Roman font, capital letters, and font size of 10.
- The names of second main headings (Heading 2) must not include numbers and must be in italics with a font size of 10.

Structure and Format of Manuscript

The recommended size of an original research paper is under 15,000 words and review papers under 7,000 words. Research articles should be less than 10,000 words. Research papers are usually longer than review papers. Review papers are reports of significant research (typically less than 7,000 words, including tables, figures, and references)

A research paper must include:

a) A title which should be relevant to the theme of the paper.
b) A summary, known as an abstract (less than 150 words), containing the major results and conclusions.
c) Up to 10 keywords that precisely identify the paper's subject, purpose, and focus.
d) An introduction, giving fundamental background objectives.
e) Resources and techniques with sufficient complete experimental details (wherever possible by reference) to permit repetition, sources of information must be given, and numerical methods must be specified by reference.
f) Results which should be presented concisely by well-designed tables and figures.
g) Suitable statistical data should also be given.
h) All data must have been gathered with attention to numerical detail in the planning stage.

Design has been recognized to be essential to experiments for a considerable time, and the editor has decided that any paper that appears not to have adequate numerical treatments of the data will be returned unrefereed.

i) Discussion should cover implications and consequences and not just recapitulate the results; conclusions should also be summarized.
j) There should be brief acknowledgments.
k) There ought to be references in the conventional format. Global Journals recommends APA format.

Authors should carefully consider the preparation of papers to ensure that they communicate effectively. Papers are much more likely to be accepted if they are carefully designed and laid out, contain few or no errors, are summarizing, and follow instructions. They will also be published with much fewer delays than those that require much technical and editorial correction.

The Editorial Board reserves the right to make literary corrections and suggestions to improve brevity.

Format Structure

It is necessary that authors take care in submitting a manuscript that is written in simple language and adheres to published guidelines.

All manuscripts submitted to Global Journals should include:

Title

The title page must carry an informative title that reflects the content, a running title (less than 45 characters together with spaces), names of the authors and co-authors, and the place(s) where the work was carried out.

Author details

The full postal address of any related author(s) must be specified.

Abstract

The abstract is the foundation of the research paper. It should be clear and concise and must contain the objective of the paper and inferences drawn. It is advised to not include big mathematical equations or complicated jargon.

Many researchers searching for information online will use search engines such as Google, Yahoo or others. By optimizing your paper for search engines, you will amplify the chance of someone finding it. In turn, this will make it more likely to be viewed and cited in further works. Global Journals has compiled these guidelines to facilitate you to maximize the web-friendliness of the most public part of your paper.

Keywords

A major lynchpin of research work for the writing of research papers is the keyword search, which one will employ to find both library and internet resources. Up to eleven keywords or very brief phrases have to be given to help data retrieval, mining, and indexing.

One must be persistent and creative in using keywords. An effective keyword search requires a strategy: planning of a list of possible keywords and phrases to try.

Choice of the main keywords is the first tool of writing a research paper. Research paper writing is an art. Keyword search should be as strategic as possible.

One should start brainstorming lists of potential keywords before even beginning searching. Think about the most important concepts related to research work. Ask, "What words would a source have to include to be truly valuable in a research paper?" Then consider synonyms for the important words.

It may take the discovery of only one important paper to steer in the right keyword direction because, in most databases, the keywords under which a research paper is abstracted are listed with the paper.

Numerical Methods

Numerical methods used should be transparent and, where appropriate, supported by references.

Abbreviations

Authors must list all the abbreviations used in the paper at the end of the paper or in a separate table before using them.

Formulas and equations

Authors are advised to submit any mathematical equation using either MathJax, KaTeX, or LaTeX, or in a very high-quality image.

Tables, Figures, and Figure Legends

Tables: Tables should be cautiously designed, uncrowned, and include only essential data. Each must have an Arabic number, e.g., Table 4, a self-explanatory caption, and be on a separate sheet. Authors must submit tables in an editable format and not as images. References to these tables (if any) must be mentioned accurately.

Figures

Figures are supposed to be submitted as separate files. Always include a citation in the text for each figure using Arabic numbers, e.g., Fig. 4. Artwork must be submitted online in vector electronic form or by emailing it.

Preparation of Eletronic Figures for Publication

Although low-quality images are sufficient for review purposes, print publication requires high-quality images to prevent the final product being blurred or fuzzy. Submit (possibly by e-mail) EPS (line art) or TIFF (halftone/ photographs) files only. MS PowerPoint and Word Graphics are unsuitable for printed pictures. Avoid using pixel-oriented software. Scans (TIFF only) should have a resolution of at least 350 dpi (halftone) or 700 to 1100 dpi (line drawings). Please give the data for figures in black and white or submit a Color Work Agreement form. EPS files must be saved with fonts embedded (and with a TIFF preview, if possible).

For scanned images, the scanning resolution at final image size ought to be as follows to ensure good reproduction: line art: >650 dpi; halftones (including gel photographs): >350 dpi; figures containing both halftone and line images: >650 dpi.

Color charges: Authors are advised to pay the full cost for the reproduction of their color artwork. Hence, please note that if there is color artwork in your manuscript when it is accepted for publication, we would require you to complete and return a Color Work Agreement form before your paper can be published. Also, you can email your editor to remove the color fee after acceptance of the paper.

Tips for Writing a Good Quality Science Frontier Research Paper

Techniques for writing a good quality Science Frontier Research paper:

1. Choosing the topic: In most cases, the topic is selected by the interests of the author, but it can also be suggested by the guides. You can have several topics, and then judge which you are most comfortable with. This may be done by asking several questions of yourself, like "Will I be able to carry out a search in this area? Will I find all necessary resources to accomplish the search? Will I be able to find all information in this field area?" If the answer to this type of question is "yes," then you ought to choose that topic. In most cases, you may have to conduct surveys and visit several places. Also, you might have to do a lot of work to find all the rises and falls of the various data on that subject. Sometimes, detailed information plays a vital role, instead of short information. Evaluators are human: The first thing to remember is that evaluators are also human beings. They are not only meant for rejecting a paper. They are here to evaluate your paper. So present your best aspect.

2. Think like evaluators: If you are in confusion or getting demotivated because your paper may not be accepted by the evaluators, then think, and try to evaluate your paper like an evaluator. Try to understand what an evaluator wants in your research paper, and you will automatically have your answer. Make blueprints of paper: The outline is the plan or framework that will help you to arrange your thoughts. It will make your paper logical. But remember that all points of your outline must be related to the topic you have chosen.

3. Ask your guides: If you are having any difficulty with your research, then do not hesitate to share your difficulty with your guide (if you have one). They will surely help you out and resolve your doubts. If you can't clarify what exactly you require for your work, then ask your supervisor to help you with an alternative. He or she might also provide you with a list of essential readings.

4. Use of computer is recommended: As you are doing research in the field of science frontier then this point is quite obvious. Use right software: Always use good quality software packages. If you are not capable of judging good software, then you can lose the quality of your paper unknowingly. There are various programs available to help you which you can get through the internet.

5. Use the internet for help: An excellent start for your paper is using Google. It is a wondrous search engine, where you can have your doubts resolved. You may also read some answers for the frequent question of how to write your research paper or find a model research paper. You can download books from the internet. If you have all the required books, place importance on reading, selecting, and analyzing the specified information. Then sketch out your research paper. Use big pictures: You may use encyclopedias like Wikipedia to get pictures with the best resolution. At Global Journals, you should strictly follow here.

6. Bookmarks are useful: When you read any book or magazine, you generally use bookmarks, right? It is a good habit which helps to not lose your continuity. You should always use bookmarks while searching on the internet also, which will make your search easier.

7. Revise what you wrote: When you write anything, always read it, summarize it, and then finalize it.

8. Make every effort: Make every effort to mention what you are going to write in your paper. That means always have a good start. Try to mention everything in the introduction—what is the need for a particular research paper. Polish your work with good writing skills and always give an evaluator what he wants. Make backups: When you are going to do any important thing like making a research paper, you should always have backup copies of it either on your computer or on paper. This protects you from losing any portion of your important data.

9. Produce good diagrams of your own: Always try to include good charts or diagrams in your paper to improve quality. Using several unnecessary diagrams will degrade the quality of your paper by creating a hodgepodge. So always try to include diagrams which were made by you to improve the readability of your paper. Use of direct quotes: When you do research relevant to literature, history, or current affairs, then use of quotes becomes essential, but if the study is relevant to science, use of quotes is not preferable.

10. Use proper verb tense: Use proper verb tenses in your paper. Use past tense to present those events that have happened. Use present tense to indicate events that are going on. Use future tense to indicate events that will happen in the future. Use of wrong tenses will confuse the evaluator. Avoid sentences that are incomplete.

11. Pick a good study spot: Always try to pick a spot for your research which is quiet. Not every spot is good for studying.

12. Know what you know: Always try to know what you know by making objectives, otherwise you will be confused and unable to achieve your target.

13. Use good grammar: Always use good grammar and words that will have a positive impact on the evaluator; use of good vocabulary does not mean using tough words which the evaluator has to find in a dictionary. Do not fragment sentences. Eliminate one-word sentences. Do not ever use a big word when a smaller one would suffice.

Verbs have to be in agreement with their subjects. In a research paper, do not start sentences with conjunctions or finish them with prepositions. When writing formally, it is advisable to never split an infinitive because someone will (wrongly) complain. Avoid clichés like a disease. Always shun irritating alliteration. Use language which is simple and straightforward. Put together a neat summary.

14. Arrangement of information: Each section of the main body should start with an opening sentence, and there should be a changeover at the end of the section. Give only valid and powerful arguments for your topic. You may also maintain your arguments with records.

15. Never start at the last minute: Always allow enough time for research work. Leaving everything to the last minute will degrade your paper and spoil your work.

16. Multitasking in research is not good: Doing several things at the same time is a bad habit in the case of research activity. Research is an area where everything has a particular time slot. Divide your research work into parts, and do a particular part in a particular time slot.

17. Never copy others' work: Never copy others' work and give it your name because if the evaluator has seen it anywhere, you will be in trouble. Take proper rest and food: No matter how many hours you spend on your research activity, if you are not taking care of your health, then all your efforts will have been in vain. For quality research, take proper rest and food.

18. Go to seminars: Attend seminars if the topic is relevant to your research area. Utilize all your resources.

19. Refresh your mind after intervals: Try to give your mind a rest by listening to soft music or sleeping in intervals. This will also improve your memory. Acquire colleagues: Always try to acquire colleagues. No matter how sharp you are, if you acquire colleagues, they can give you ideas which will be helpful to your research.

20. Think technically: Always think technically. If anything happens, search for its reasons, benefits, and demerits. Think and then print: When you go to print your paper, check that tables are not split, headings are not detached from their descriptions, and page sequence is maintained.

21. Adding unnecessary information: Do not add unnecessary information like "I have used MS Excel to draw graphs." Irrelevant and inappropriate material is superfluous. Foreign terminology and phrases are not apropos. One should never take a broad view. Analogy is like feathers on a snake. Use words properly, regardless of how others use them. Remove quotations. Puns are for kids, not grunt readers. Never oversimplify: When adding material to your research paper, never go for oversimplification; this will definitely irritate the evaluator. Be specific. Never use rhythmic redundancies. Contractions shouldn't be used in a research paper. Comparisons are as terrible as clichés. Give up ampersands, abbreviations, and so on. Remove commas that are not necessary. Parenthetical words should be between brackets or commas. Understatement is always the best way to put forward earth-shaking thoughts. Give a detailed literary review.

22. Report concluded results: Use concluded results. From raw data, filter the results, and then conclude your studies based on measurements and observations taken. An appropriate number of decimal places should be used. Parenthetical remarks are prohibited here. Proofread carefully at the final stage. At the end, give an outline to your arguments. Spot perspectives of further study of the subject. Justify your conclusion at the bottom sufficiently, which will probably include examples.

23. Upon conclusion: Once you have concluded your research, the next most important step is to present your findings. Presentation is extremely important as it is the definite medium though which your research is going to be in print for the rest of the crowd. Care should be taken to categorize your thoughts well and present them in a logical and neat manner. A good quality research paper format is essential because it serves to highlight your research paper and bring to light all necessary aspects of your research.

Informal Guidelines of Research Paper Writing

Key points to remember:

- Submit all work in its final form.
- Write your paper in the form which is presented in the guidelines using the template.
- Please note the criteria peer reviewers will use for grading the final paper.

Final points:

One purpose of organizing a research paper is to let people interpret your efforts selectively. The journal requires the following sections, submitted in the order listed, with each section starting on a new page:

The introduction: This will be compiled from reference matter and reflect the design processes or outline of basis that directed you to make a study. As you carry out the process of study, the method and process section will be constructed like that. The results segment will show related statistics in nearly sequential order and direct reviewers to similar intellectual paths throughout the data that you gathered to carry out your study.

The discussion section:

This will provide understanding of the data and projections as to the implications of the results. The use of good quality references throughout the paper will give the effort trustworthiness by representing an alertness to prior workings.

Writing a research paper is not an easy job, no matter how trouble-free the actual research or concept. Practice, excellent preparation, and controlled record-keeping are the only means to make straightforward progression.

General style:

Specific editorial column necessities for compliance of a manuscript will always take over from directions in these general guidelines.

To make a paper clear: Adhere to recommended page limits.

Mistakes to avoid:

- Insertion of a title at the foot of a page with subsequent text on the next page.
- Separating a table, chart, or figure—confine each to a single page.
- Submitting a manuscript with pages out of sequence.
- In every section of your document, use standard writing style, including articles ("a" and "the").
- Keep paying attention to the topic of the paper.
- Use paragraphs to split each significant point (excluding the abstract).
- Align the primary line of each section.
- Present your points in sound order.
- Use present tense to report well-accepted matters.
- Use past tense to describe specific results.
- Do not use familiar wording; don't address the reviewer directly. Don't use slang or superlatives.
- Avoid use of extra pictures—include only those figures essential to presenting results.

Title page:

Choose a revealing title. It should be short and include the name(s) and address(es) of all authors. It should not have acronyms or abbreviations or exceed two printed lines.

Abstract: This summary should be two hundred words or less. It should clearly and briefly explain the key findings reported in the manuscript and must have precise statistics. It should not have acronyms or abbreviations. It should be logical in itself. Do not cite references at this point.

An abstract is a brief, distinct paragraph summary of finished work or work in development. In a minute or less, a reviewer can be taught the foundation behind the study, common approaches to the problem, relevant results, and significant conclusions or new questions.

Write your summary when your paper is completed because how can you write the summary of anything which is not yet written? Wealth of terminology is very essential in abstract. Use comprehensive sentences, and do not sacrifice readability for brevity; you can maintain it succinctly by phrasing sentences so that they provide more than a lone rationale. The author can at this moment go straight to shortening the outcome. Sum up the study with the subsequent elements in any summary. Try to limit the initial two items to no more than one line each.

Reason for writing the article—theory, overall issue, purpose.

- Fundamental goal.
- To-the-point depiction of the research.
- Consequences, including definite statistics—if the consequences are quantitative in nature, account for this; results of any numerical analysis should be reported. Significant conclusions or questions that emerge from the research.

Approach:

- o Single section and succinct.
- o An outline of the job done is always written in past tense.
- o Concentrate on shortening results—limit background information to a verdict or two.
- o Exact spelling, clarity of sentences and phrases, and appropriate reporting of quantities (proper units, important statistics) are just as significant in an abstract as they are anywhere else.

Introduction:

The introduction should "introduce" the manuscript. The reviewer should be presented with sufficient background information to be capable of comprehending and calculating the purpose of your study without having to refer to other works. The basis for the study should be offered. Give the most important references, but avoid making a comprehensive appraisal of the topic. Describe the problem visibly. If the problem is not acknowledged in a logical, reasonable way, the reviewer will give no attention to your results. Speak in common terms about techniques used to explain the problem, if needed, but do not present any particulars about the protocols here.

The following approach can create a valuable beginning:

- Explain the value (significance) of the study.
- Defend the model—why did you employ this particular system or method? What is its compensation? Remark upon its appropriateness from an abstract point of view as well as pointing out sensible reasons for using it.
- Present a justification. State your particular theory(-ies) or aim(s), and describe the logic that led you to choose them.
- Briefly explain the study's tentative purpose and how it meets the declared objectives.

Approach:

Use past tense except for when referring to recognized facts. After all, the manuscript will be submitted after the entire job is done. Sort out your thoughts; manufacture one key point for every section. If you make the four points listed above, you will need at least four paragraphs. Present surrounding information only when it is necessary to support a situation. The reviewer does not desire to read everything you know about a topic. Shape the theory specifically—do not take a broad view.

As always, give awareness to spelling, simplicity, and correctness of sentences and phrases.

Procedures (methods and materials):

This part is supposed to be the easiest to carve if you have good skills. A soundly written procedures segment allows a capable scientist to replicate your results. Present precise information about your supplies. The suppliers and clarity of reagents can be helpful bits of information. Present methods in sequential order, but linked methodologies can be grouped as a segment. Be concise when relating the protocols. Attempt to give the least amount of information that would permit another capable scientist to replicate your outcome, but be cautious that vital information is integrated. The use of subheadings is suggested and ought to be synchronized with the results section.

When a technique is used that has been well-described in another section, mention the specific item describing the way, but draw the basic principle while stating the situation. The purpose is to show all particular resources and broad procedures so that another person may use some or all of the methods in one more study or referee the scientific value of your work. It is not to be a step-by-step report of the whole thing you did, nor is a methods section a set of orders.

Materials:

Materials may be reported in part of a section or else they may be recognized along with your measures.

Methods:

- Report the method and not the particulars of each process that engaged the same methodology.
- Describe the method entirely.
- To be succinct, present methods under headings dedicated to specific dealings or groups of measures.
- Simplify—detail how procedures were completed, not how they were performed on a particular day.
- If well-known procedures were used, account for the procedure by name, possibly with a reference, and that's all.

Approach:

It is embarrassing to use vigorous voice when documenting methods without using first person, which would focus the reviewer's interest on the researcher rather than the job. As a result, when writing up the methods, most authors use third person passive voice.

Use standard style in this and every other part of the paper—avoid familiar lists, and use full sentences.

What to keep away from:

- Resources and methods are not a set of information.
- Skip all descriptive information and surroundings—save it for the argument.
- Leave out information that is immaterial to a third party.

Results:

The principle of a results segment is to present and demonstrate your conclusion. Create this part as entirely objective details of the outcome, and save all understanding for the discussion.

The page length of this segment is set by the sum and types of data to be reported. Use statistics and tables, if suitable, to present consequences most efficiently.

You must clearly differentiate material which would usually be incorporated in a study editorial from any unprocessed data or additional appendix matter that would not be available. In fact, such matters should not be submitted at all except if requested by the instructor.

Content:

- Sum up your conclusions in text and demonstrate them, if suitable, with figures and tables.
- In the manuscript, explain each of your consequences, and point the reader to remarks that are most appropriate.
- Present a background, such as by describing the question that was addressed by creation of an exacting study.
- Explain results of control experiments and give remarks that are not accessible in a prescribed figure or table, if appropriate.
- Examine your data, then prepare the analyzed (transformed) data in the form of a figure (graph), table, or manuscript.

What to stay away from:

- Do not discuss or infer your outcome, report surrounding information, or try to explain anything.
- Do not include raw data or intermediate calculations in a research manuscript.
- Do not present similar data more than once.
- A manuscript should complement any figures or tables, not duplicate information.
- Never confuse figures with tables—there is a difference.

Approach:

As always, use past tense when you submit your results, and put the whole thing in a reasonable order.

Put figures and tables, appropriately numbered, in order at the end of the report.

If you desire, you may place your figures and tables properly within the text of your results section.

Figures and tables:

If you put figures and tables at the end of some details, make certain that they are visibly distinguished from any attached appendix materials, such as raw facts. Whatever the position, each table must be titled, numbered one after the other, and include a heading. All figures and tables must be divided from the text.

Discussion:

The discussion is expected to be the trickiest segment to write. A lot of papers submitted to the journal are discarded based on problems with the discussion. There is no rule for how long an argument should be.

Position your understanding of the outcome visibly to lead the reviewer through your conclusions, and then finish the paper with a summing up of the implications of the study. The purpose here is to offer an understanding of your results and support all of your conclusions, using facts from your research and generally accepted information, if suitable. The implication of results should be fully described.

Infer your data in the conversation in suitable depth. This means that when you clarify an observable fact, you must explain mechanisms that may account for the observation. If your results vary from your prospect, make clear why that may have happened. If your results agree, then explain the theory that the proof supported. It is never suitable to just state that the data approved the prospect, and let it drop at that. Make a decision as to whether each premise is supported or discarded or if you cannot make a conclusion with assurance. Do not just dismiss a study or part of a study as "uncertain."

Research papers are not acknowledged if the work is imperfect. Draw what conclusions you can based upon the results that you have, and take care of the study as a finished work.

- You may propose future guidelines, such as how an experiment might be personalized to accomplish a new idea.
- Give details of all of your remarks as much as possible, focusing on mechanisms.
- Make a decision as to whether the tentative design sufficiently addressed the theory and whether or not it was correctly restricted. Try to present substitute explanations if they are sensible alternatives.
- One piece of research will not counter an overall question, so maintain the large picture in mind. Where do you go next? The best studies unlock new avenues of study. What questions remain?
- Recommendations for detailed papers will offer supplementary suggestions.

Approach:

When you refer to information, differentiate data generated by your own studies from other available information. Present work done by specific persons (including you) in past tense.

Describe generally acknowledged facts and main beliefs in present tense.

The Administration Rules

Administration Rules to Be Strictly Followed before Submitting Your Research Paper to Global Journals Inc.

Please read the following rules and regulations carefully before submitting your research paper to Global Journals Inc. to avoid rejection.

Segment draft and final research paper: You have to strictly follow the template of a research paper, failing which your paper may get rejected. You are expected to write each part of the paper wholly on your own. The peer reviewers need to identify your own perspective of the concepts in your own terms. Please do not extract straight from any other source, and do not rephrase someone else's analysis. Do not allow anyone else to proofread your manuscript.

Written material: You may discuss this with your guides and key sources. Do not copy anyone else's paper, even if this is only imitation, otherwise it will be rejected on the grounds of plagiarism, which is illegal. Various methods to avoid plagiarism are strictly applied by us to every paper, and, if found guilty, you may be blacklisted, which could affect your career adversely. To guard yourself and others from possible illegal use, please do not permit anyone to use or even read your paper and file.

CRITERION FOR GRADING A RESEARCH PAPER (COMPILATION) BY GLOBAL JOURNALS

Please note that following table is only a Grading of "Paper Compilation" and not on "Performed/Stated Research" whose grading solely depends on Individual Assigned Peer Reviewer and Editorial Board Member. These can be available only on request and after decision of Paper. This report will be the property of Global Journals.

Topics	**Grades**		
	A-B	**C-D**	**E-F**
Abstract	Clear and concise with appropriate content, Correct format. 200 words or below	Unclear summary and no specific data, Incorrect form Above 200 words	No specific data with ambiguous information Above 250 words
Introduction	Containing all background details with clear goal and appropriate details, flow specification, no grammar and spelling mistake, well organized sentence and paragraph, reference cited	Unclear and confusing data, appropriate format, grammar and spelling errors with unorganized matter	Out of place depth and content, hazy format
Methods and Procedures	Clear and to the point with well arranged paragraph, precision and accuracy of facts and figures, well organized subheads	Difficult to comprehend with embarrassed text, too much explanation but completed	Incorrect and unorganized structure with hazy meaning
Result	Well organized, Clear and specific, Correct units with precision, correct data, well structuring of paragraph, no grammar and spelling mistake	Complete and embarrassed text, difficult to comprehend	Irregular format with wrong facts and figures
Discussion	Well organized, meaningful specification, sound conclusion, logical and concise explanation, highly structured paragraph reference cited	Wordy, unclear conclusion, spurious	Conclusion is not cited, unorganized, difficult to comprehend
References	Complete and correct format, well organized	Beside the point, Incomplete	Wrong format and structuring

Index

save our planet

Global Journal of Science Frontier Research

Visit us on the Web at www.GlobalJournals.org | www.JournalofScience.org
or email us at helpdesk@globaljournals.org

ISSN 9755896